NON DARCY FLOW IN POROUS MEDIA AND ITS APPLICATIONS TO TRANSIENT PROBLEMS

(VOLUME II)

A Thesis Submitted
In Partial Fulfilment of the Requirements
for the Degree of
DOCTOR OF PHILOSOPHY

By
PUNYABRATA BASAK

to the

DEPARTMENT OF CIVIL ENGINEERING
INDIAN INSTITUTE OF TECHNOLOGY KANPUR
JULY 1975

APPENDIX - A

NON DARCY FLOW - A PERSPECTIVE

INTRODUCTION

INTRODUCTION

Non Darcy Flow and its Importance

The flow of water which follows the famous Darcy's law (1856) expressed as

$$v = ki \quad . \quad . \quad . \quad . \quad . \quad (1)$$

where v = Superficial flow velocity

i = Hydraulic Gradient

k = Constant of Proportionality called coefficient of permeability.

is called the Darcian flow, while the flow not expressible by above eqn. (1) can be designated as non Darcy flow.

Darcy's law has made a tremendous impact on the understanding of the movement of water in solids and porous media. Darcy's law when combined with the equation of continuity leads to heat conduction or diffusion type equations which are mathematically solvable for various boundary conditions. Any refinement in the Darcy's equation either may result in an unsolvable nonlinear differential equation or make the boundary conditions difficult for mathematical treatment. But the mathematical difficulties have not deterred a study of non Darcy flow behaviour.

It is to be noted here that Darcy (1856) established his experimental law under the following six conditions.

1. Medium size sand
2. The sand bed was stable; that is there was no structural or particle orientation changes during flow, and movement of fines was negligible.
3. The sands tested were of inert type i.e., there was no surface force to affect the permeant.
4. The flow was under isothermal condition
5. The testing was conducted over medium range of gradients
6. The flow was under steady state condition.

If one's testing conditions are different from Darcy's, deviations from Darcy's law might be expected.

Consequences of non Darcy behaviour are of potential interest in several disciplines. Drainage and water movement in clay soils are of primary importance to soil sciencee, Hydrology and Soil Engineering. Consolidation of clay deposits caused by water migration is of utmost interest and fundamental importance to Soil Mechanics. The consideration of non Darcy flow during consolidation may perhaps remove many descripencies. Between observed and predicted results based on present Darcian theory. The existence of threshold gradient has also important implications in consolidation of

saturated clays and for water sealing properties of clays (Swartzendruber 1968). Non Darcy behaviour will also drastically affect the flow through unsaturated soils which is of primary importance to agriculture and hydrology.

Some of the applications of non Darcy flow in practical problems which have been solved by different authors may be mentioned here. Hansbo (1960), Elnagger et al (1971) and Parlange (1973) dealt with the consolidation of soils depicting non Darcy flow behaviour. Bondarenko (1968) calculated the drainage spacing for soils showing the phenomenon of initial gradient. Swartzendruber (1968) gave the head distribution in an acquifier having non Darcian behaviour. Slepicka (1961a) studied the discharge from wells placed in a non Darcian aquifer.

Non Darcy flow of water through soils is generally observed under two circumstances and they are

(1) Flow at high gradients - the main cause of deviations being inertial effects.

(2) Flow at low gradients - the main cause of deviations here is due to the predominance of soil-water interaction at the molecular level and the associated effects. These are explained later in detail.

Darcy's law is generally observed to be perfectly valid for intermediate range of gradients. In this report, the non Darcy flow which is observed only at the low gradients, is discussed unless mentioned otherwise.

Chapter 1

CAUSES OF NON-DARCIAN BEHAVIOUR

There are several hypotheses used to explain the non Darcian flow in the laminar region and these can be grouped under the following six heads

(1) Non Newtonian liquid viscosity hypothesis

(2) Bingham Plastic fluid and "Quasi-Crysta--lline" Water structure hypothesis

(3) Electro kinetic coupling hypothesis

(4) Wall force hypothesis

(5) Domain structure hypothesis

(6) Transient particle arrangement hypothesis

A brief description of each of the above hypotheses will be given below.

(1) Non Newtonian Liquid viscosity hypothesis:

Under this hypothesis non Darcian flow is supposed to originate from non Newtonian liquid viscosity caused by modified water structure induced by clay water interaction. Low (1961) first developed this hypothesis and later it was extensively used by different authors to explain their experimental data.

(Swartzendruber, 1962a, 1962b, 1966, 1967; Kutilek 1964, 1965, 1967a, 1967b, 1969 and 1971; Kutilek and Salingerova 1966, 1967; Karadi & Nagy 1961). Von Engelhardt and Tunn (1955), Lutz and Kemper (1959), Hansbo (1960), Hadas (1964) and Thames (1966) also explained their experimentally observed non Darcian behaviour on the basis of increased viscosity due to surface activity of soil minerals. Kutiliek (1964 & 1967) proposed that some part of water in a clay-water system behaves as a Newtonian fluid whereas the other part behaves as non-Newtonian liquid. A detailed discussion about the changed viscosity and density of water in a clay-water system is given later in this report. Experimental results of each of the above mentioned researchers are also given in a separate chapter.

(2) Bingham Plastic fluid and "Quasi crystalline" water structure hypothesis

Bondarenko (1968), Churyev and Gorokhov (1970), Nerpin and Deryagin (1969), Miller and Low (1963) and many others believe that water in capillaries has the properties of Bingham body. Nerpin or Deryagin and Bondarenko measured the yield shear stress of capillary

water of the order of 10^{-2} to 10^{-3} dynes/cm^2, and hence, according to them initiation of flow in narrow capillaries of soils needs certain hydraulic gradient and thereby violating Darcy's Law at low gradients. Bondarenko and others attributed this property of capillary water to the hydrogen bonding and quasi-crystalline water structure in the capillaries.

(3) Electrokinetic Coupling Hypothesis:-

Electrokinetic coupling is the interaction that occurs between viscous and electrical flows in membrane materials such as clays (Abramson, 1936, Overbreek 1952). When a liquid is forced through clay, by a hydraulic gradient, the coupling gives rise to an induced streaming potential that causes an electro-osmotic flow opposite to the flow caused by hydraulic gradient (Swartzendruber 1966, 1967) resulting thereby in a reduction in the flow rate as predicted from any theory based on Darcy's law (e.g. Poiseulle's law or Kozeny Carman's equation) Swartzendruber (1967) gave the velocity-gradient relationship as

$$v = ki - Ci_e \quad . \quad . \quad . \quad . \quad . \quad (2)$$

$$\text{or} \qquad v = (k - C\,E/k)i \quad . \quad . \quad . \quad . \quad (3)$$

where $i = \frac{h}{L}$ = hydraulic gradient

$i_e = \frac{E}{L}$ = streaming potential gradient,

E is the streaming potential across the sample of length L.

If E/h is assumed as constant (Abramson 1934, Overbreek 1952), v is still found to be directly proportional to hydraulic gradient i,e Darcian flow is observed but Bull and Gortner (1932) and Swartzendruber (1966) found that E/h decreases with 'h', and hence, with hydraulic gradient, thereby making the flow non Darcy. Henniker (1952) also observed a retardation in flow at low gradients and he also used streaming potential to explain it. Olsen (1960) calculated the effect of electrokinetic coupling on the flow rate in percent and he found that the coupling influence is negligibly small (less than 1%).

(4) Wall force hypothesis:

Taking hints from Martin (1960), Klausner and Kraft (1965a, 1965b, 1966a and 1966b) proposed a capillary model with a force F normal to the surface (resulting from the electrical field from the crystalline structure of soil minerals) and hypothesised that this

force F brings a shear force which increases as the solid particles is approached. With some theoretical deduction they were able to show that the existence of the wall force can give rise to the non linear velocity gradient relationship. For their analysis Klausner and Kraft assumed that there is no variation of viscosity and density of pore fluid. So the entire non Darcy effect is assumed to be due to existence of wall forces alone.

(5) Domain Structure Hypothesis:

Michaels (1959) and Quirk (1959) suggested that the primary particles in a clay mass may be arranged in groups such as aggregates, packets or domains, and that the total porosity may be distributed among inter and intra group components. If such grouping arrangement of particles exists in clays, the flow channels surrounding particle groups probably will be considerably larger than those passing through the groups and between the individual particles. If this sort of domain or cluster structure is accepted then the Kozeny-Carman's permeability equation based on parallel capillary tube model and Darcy's law will be completely invalid. The failure of Kozeny-Carman's

equation might mean the failure of parallel capillary tube model and might warrant a better model.

Following the domain structure or cluster concept Olsen (1961) derived a flow rate equation which reads as

$$\frac{q_{NDS}}{q_{Kozeny}} = N^{2/3} \frac{(1 - \frac{e_c}{e_T})^3}{(1 + e_c)^{4/3}} \quad \ldots\ldots(4)$$

where q_{NDS} = Flow rate for soil with domain or cluster structure

$$q_{Kozeny} = \frac{1}{K_o S^2} \frac{\gamma}{\mu} \frac{e^3}{1 + e} i A \quad \ldots\ldots(5)$$

where e = void ratio, K_o = shape factor, S = specific surface, γ and μ are viscosity and density of liquid, and A is area of flow.

Parameters in equation (4) are explained in Figs. 1 and 2.

Using eqn. (4) Olsen calculated the values of discrepency ratio $(\frac{q_{NDS}}{q_{Kozeny}})$ for different porosities with a definite cluster geometry (Fig. 3).

Compared to Kozeny-Carman's equation Olsen's

V_v = Total void volume
V_s = Total solids
V_c = Volume of cluster voids
V_p = Volumes of voids betn.clusters
e_t = Total void ratio = V_v/V_s
e_c = Cluster void ratio = V_c/V_s
N = Number of particles per cluster

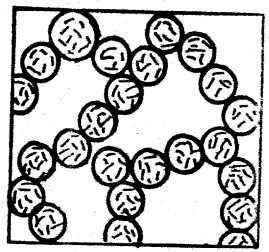

Figs.1,2 & 3 are after Olsen (1961)

FIG.1 : Cluster Model

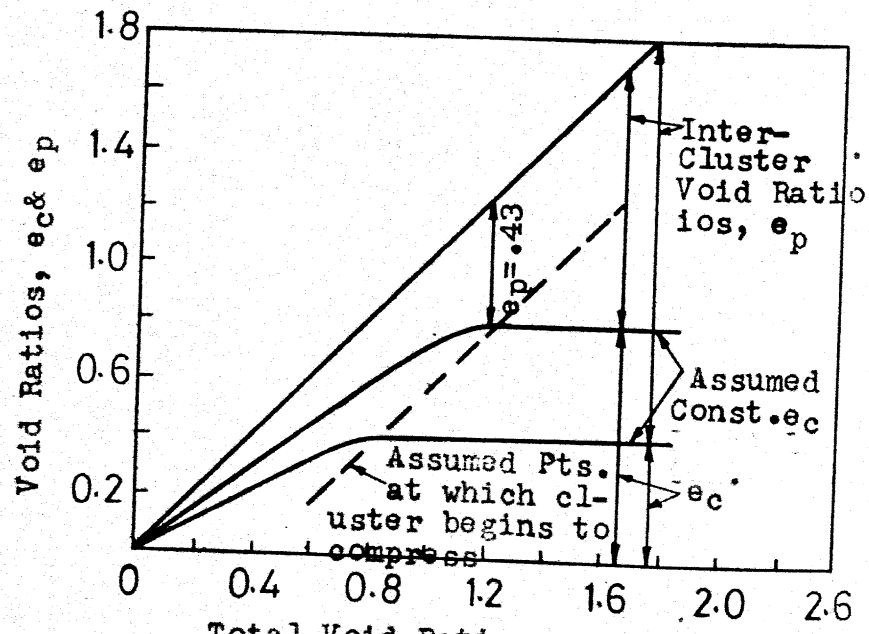

Fig.2: Assumed Relationships Betn.The Total, Cluster and Inter-Cluster Void Ratios

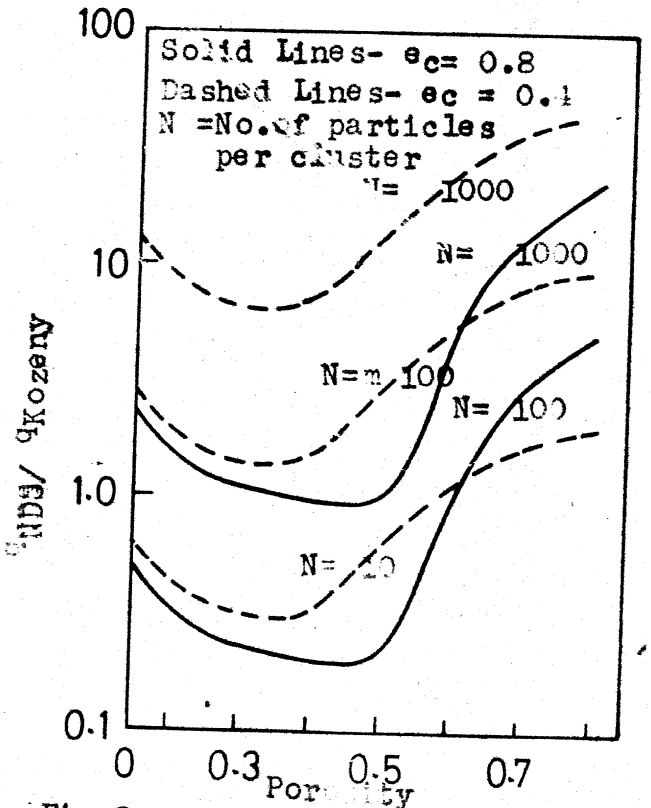

Fig.3 : Possible Discrepencies For Systems of Clusters

equation (eqn. 4) may give better result for flocculated and aggregated soils and might explain some of the "apparent" deviations from Darcy's law.

(6) Transient Particle Arrangement Hypothesis:

Michaels and Lin (1954), Martin (1960), Olsen (1960, 1961), Swartzendruber (1962b), Miller and Low (1963), Zaslavski (1964), Blackmore and Marshall (1965), Mitchell and Younger (1967), Marshall (1968), Gairon (1968), Miller, Overman and Perverly (1969), Kutilek (1969) and Novak (1970) suggest that the particle re-orientation or the change of the geometric arrangement of particles in the soil sample (i.e., fabric or structural change) is the most important effect in non Darcy flow.

Michaels and Lin's (1954) data (quoted in Martin 1960) demonstrate that clay fabric alone can alter the permeability at a given void ratio by 1000 percent. It is possible that the application of hydraulic gradient to a structure or fabric sensitive clay will change its fabric appreciably (void ratio may or may not remain same during this process) giving rise to an observed non Darcy behaviour Martin (1960) explained Von Engelhardt and Tunn's (1955) non Darcy data in terms

of reversible void plugging or movements of fines from one part of the sample to the other parts and concluded that mejor cause of non Darsian behaviour is the aggregation or dispersion of fines.

Olsen (1960, 1961) derived a relation between flow rates and orientation of particles in a soil mass and his equation reads as

$$\frac{q_{NDPO}}{q_{Kozeny}} = \frac{2}{\left[1 + \frac{\frac{1}{2}\left\{\sqrt{(1+\frac{1}{R})^2 + \frac{4e}{R}} - \frac{1}{R}\right\}}{\left\{\sqrt{(1+\frac{1}{R})^2 + \frac{4e}{R}} + (1-\frac{1}{R})\right\}}\right]^2 \sin^2\theta} \qquad ..(6)$$

where q_{NDPO} = Flow rate for a particular orientation of particles

q_{Kozeny} = Flow rate given by Kozeny-Carman's equation,

Other parameters of the equation (6) are explained in Fig. 4.

The discrepancy ratio $(= \frac{q_{NDPO}}{q_{Kozeny}})$ is calculated for different particle orientations and is shown in Fig. 5. As seen from this fig., at the same porosity or void ratio, as the particle orientation changes (due to the application of hydraulic gradient) the flow velocity changes giving rise to an apparent non Darcy.

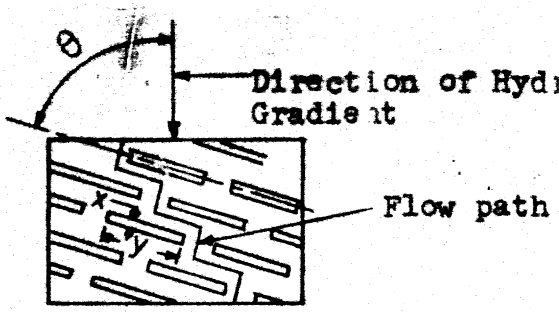

Fig.4 : Model & Parameters of tortuous flow paths

G = Average degree of particle orientation

T = Tortuousity-flow path length per unit distance along the hyd.grad.vector

R = Particle axial ratio = X/Y

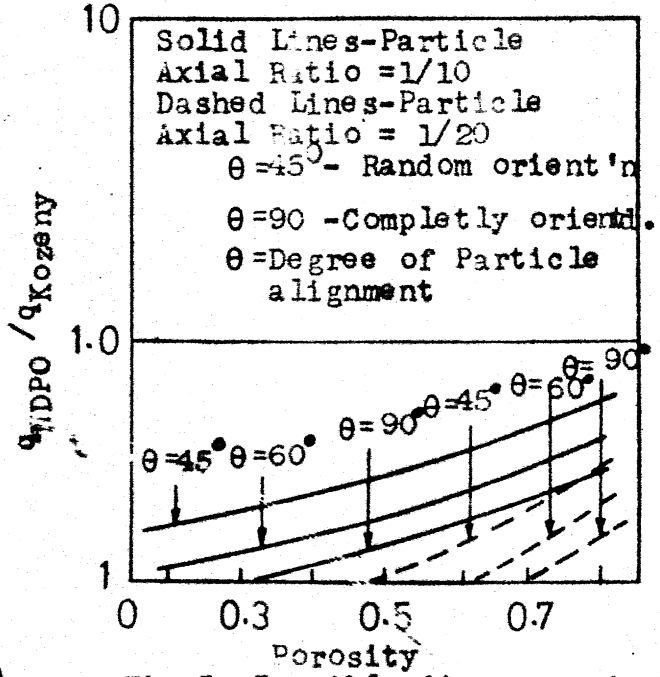

Fig.5: Possible discrepencies due to tortuous flow paths

Figs.4 & 5 are after Olsen (1961)

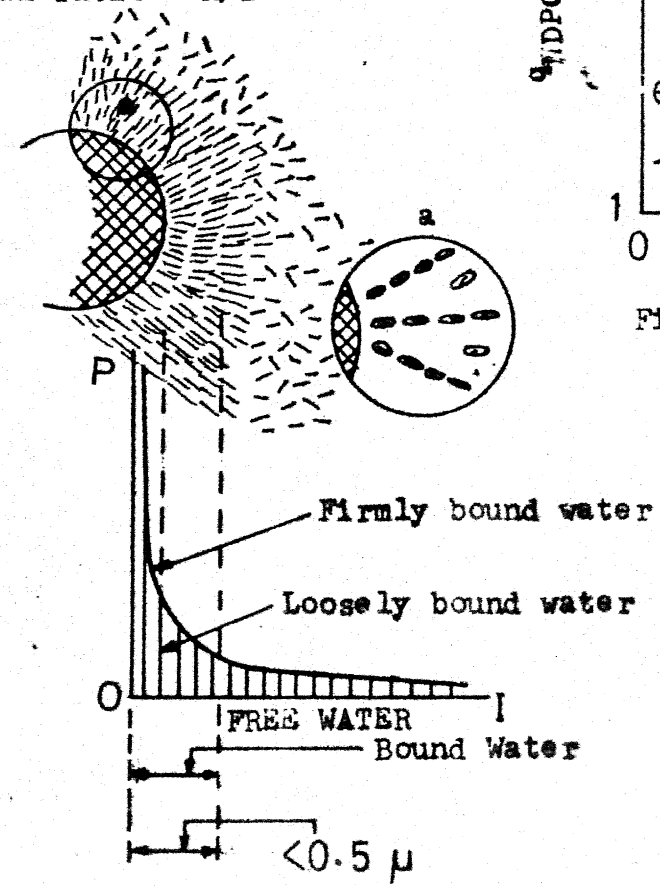

Fig.6: The Electromolecular Field Surrounding the Soil Particle (After Citovics, 1951)

behaviour.

Swartzendruber (1962a and 1962b) hinted that if with increasing gradient the particles orient themselves in such a way that effective cross section of flow area changes then one would expect a non Darcy behaviour.

Miller and Low (1963) considered the rearrangement of particles during their flow experiments, to be parallel to the flow path and the velocity-gradient relation was no more linear as the tortuosity decreases.

Zaslavski (1964) found that shift of particles cause hydraulic conductivity (slope of v-i curve) to be time and gradient dependent.

Blackmore & Marshall (1965) have shown that in a bentonite suspension the shift of particles causes a gradual decrease in spacing, the change being continuous and dependent upon applied hydraulic gradient and velocity.

Mitchell and Younger (1967) observed that the behaviour of compacted specimens was such as to indicate that particle migration as the more likely cause for non Darcy flow.

Marshall (1968) found that, when water flows through a bed of unstable material, the hydraulic conductivity and hence velocity gradient relationship can be affected by detachment of particles or by change of the volume of the material.

Gairon (1968), (quoted in Kutilek 1969) conducted experiments with bentonite clay pastes and according to his results the flow was less than proportional, at least at low concentration and be explains these deviations from the proportional Darcian flow mainly by the displacement of particles within the column of clay paste.

Miller, Overman and Peverly (1969) observed that not only simple movement but also bending and flexing of particles or breaking of edge to surface bonds, to permit particle reorientation along the flow path may cause non Darcy flow.

Kutilek (1969) analytically demonstrated the dependence of hydraulic conductivity and hence velocity-gradient relationship, upon the hydraulic gradient in suspension of platy particles.

Novak (1970) explained his nonlinear velocity gradient relation for bentonite in terms of shifting of the position of bentonite particles conforming to the velocity and direction of flow.

CHAPTER 2

BOUND WATER AND ITS ROLE IN NON DARCY BEHAVIOUR:

The discussion here is devided into two parts

PART A consists of

(1) A perspective view of water in clay-water system and its role in the abnormal flow through clays

(2) Models describing the nature of bonded water

PART B consists of a discussion about

(1) viscosity

(2) density

and (3) thickness of bound water with special reference to its role on the observed non-Darcy behaviour.

PART A

(1) A perspective view of water in the clay-water system and its role in the abnormal flow through clays.

Karadi and Nagy (1961) and Williamson (1951) gave an excellent picture of the state of water in the

clay-water system. Water consists of polar molecules formed by a negatively charged oxygen ions and positively charged hydrogen ions. As the dielectric constants of water and of the mineral particle differ appreciably from each other, an electric field having surplus energy develops on the surface of the mineral particle, and as a consequence, water molecules become polarized and dipoles of the water become oriented. These oriented dipoles stick to the mineral particle surface. The range of electromolecular forces is around 0.25 to 0.5 μ and their magnitude sharply decreases with increasing distance from the surface of the soil particle. The magnitude of this force on the soil particle surface may attain a value of 10,000 kg/sq cm, but at a distance of 0.5 μ it is neglegible. Citovics (1951) schematically presented this situation (Fig. 6). As explained in the fig. the fluid of thickness 0.1 to 0.15 μ around the soil particle adheres to it with a large force and hence it is called firmely bonded or adsorbed water. Beyond this layer the electromolecular forces decrease appreciably, and the water molecules are loosely bonded, sometimes reffered to as liosorbed water. This loosely bound water may exist up to an appreciable distance

and in fact the range of void ratios found in soils for engineering use are such that there is a very good probability that allmost all the water there, is bound (loosely or strongly). In support, Grim (1952) writes that in a concentrated clay-water system as in a plastic clay mass, the nature of the adsorbed water is of extreme importance in determining its properties because all or almost all of the water is non liquid. Macey (1940, 1942) also supports Grim's idea. Lutz and Kemper (1959) observed the same feature with Na-clays. From vapour pressure data Shereshefsky (1928) as quoted by Lutz and Kemper (1959) observed that the wall surface of a small capillary exerts an appreciable influence on the water molecules, even at a distance of 10,000 Å or about 3000 water molecule diameters. After a survey of the existing literature Romanov (1968) summarized the pecularities of bound water as follows.

(1) Bound water does not freeze even at very low temperatures, as low as - 78°C (Bouyancas 1917 and Rode 1952)

(2) It's density and viscosity are different from those of free water,

(3) It's specific heat is less than unity, about 0.76 cal/gm. i.e., closely approaching that of ice (Andeanov 1949)

(4) Films of adsorbed water possess shear elasticity i.e., [illegible] approach the mechanical properties of solid.

(5) Although it is a non conductor, its dielectric constant is smaller than that of free water (Dumanskii & Chapek 1934) and it is incapable of containing solutes (Dumanskii & Dumanskaya 1934).

Martin (1960) also presented an excellent review on the different aspects of adsorbed water in clay.

Macey (1940, 1942 and 1948) determined the change in permeability with water content for saturated clays. He found that observed permeability values were much smaller than the calculated values from equation (5). Macey observed that better agreement between the experimental and calculated values was obtainable by assuming that a very thick layer of bound water exists on the clay surface.

Michaels and Lin (1954) conducted experiments on kaolinite bed and their results (fig. 7) show that the permeability decreases with increasing polarity of the permeant. The plots indicate that the Kozeny-Carman equation is obeyed over a considerable void ratio range

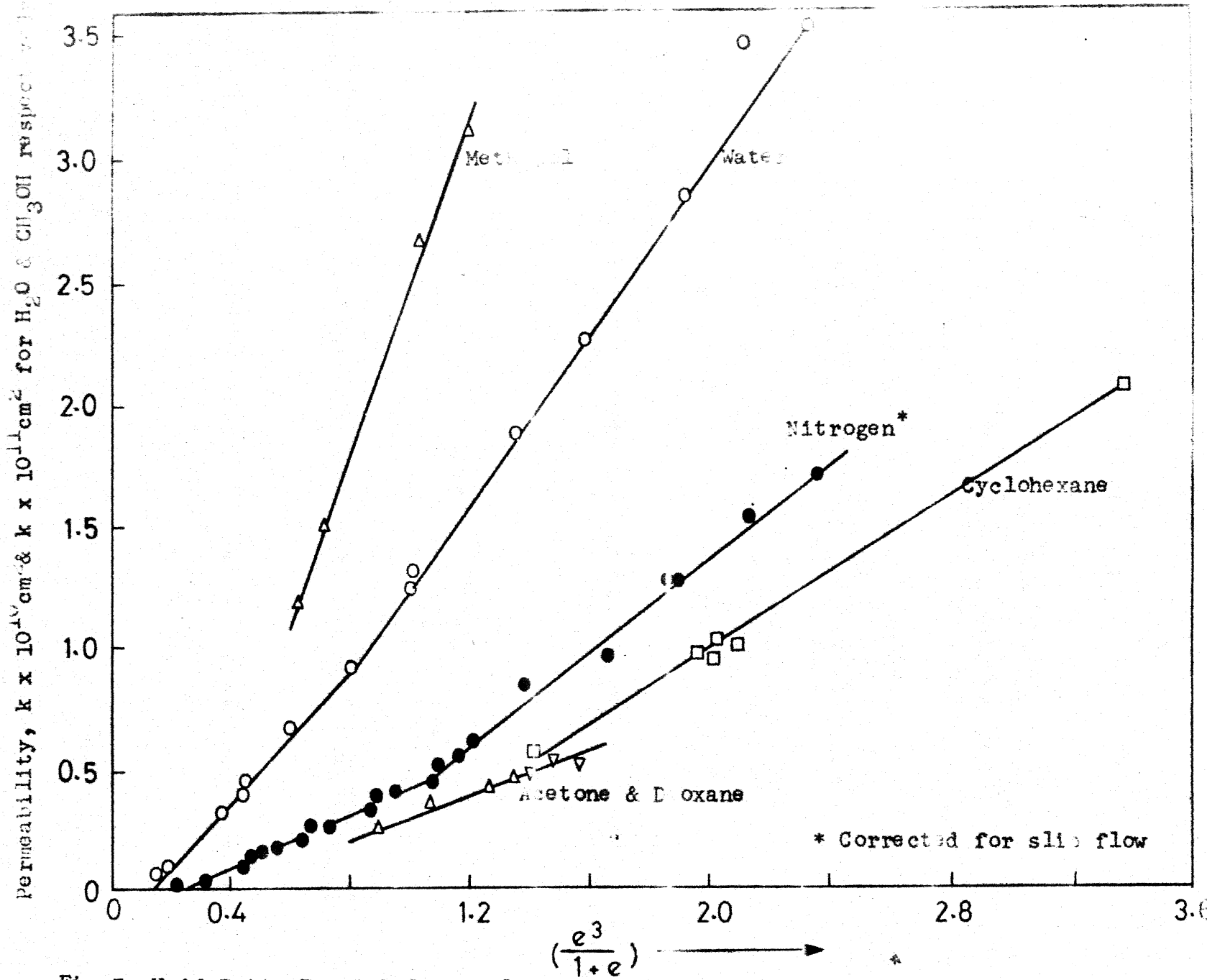

Fig.7: Void Ratio-Permeability Relationship for Various Fluids (After Michaels & Lin, 1954)

for all the permeants. However, deviations from Kozeny-Carman relation occur for all permeants at low gradients and none of the curves pass through the origin.

(1) Abnormal fluid properties (e.g., increased viscosity, changed density etc.) contribute less than 30 percent towards the total resistance to fluid flow through kaolinite beds.

(2) Clay fabric changes during permeation with some permeants playing a predominant role in the non-Darcy behaviour at low gradients.

(2) Models describing the nature of adsorbed water:

Precise nature and structure of bound-water is not yet known, but it is generally agreed that some form of organization of the water molecules exists in the water immediately adsorbed on the clay mineral surfaces. (Grim, 1962).

At present there are three models available for adsorbed water structure and they are

(1) "Ice like" or "Solid" structure proposed by Rosenqvist (1959)

(2) Hexagonal net structure proposed by Hendricks and Jefferson (1938)

or (3) Two dimensional fluid model proposed by Martin (1960)

Each of the theories is briefly described below.

Rosenqvist's "Ice like" or "Solid" structure hypothesis presumes that the water molecules are not rigidly fixed into a well ordered lattice but there is more "order" than in normal liquid water. One may infer that each bond is stronger than in normal liquid water due to the polarization of the clay surface. Presumably, this water would resist both normal and shear stresses to a larger degree than normal water.

Hendricks and Jefferson's Hexagonal net structure hypothesis states that the hydrates of the silicate minerals in montmorillonite, contain layers of water molecules joined into a hexagonal net. Further they explain the stability of the hexagonal net by the attraction between hydrogen atoms of water molecules and neighboring oxygen ions of the silicate layers, or oxygen atoms of other water molecules in the net.

The two dimensional fluid model proposed by Martin (1960) recognizes a stronger bond in adsorbed water than normal water. Martin visualised the water to be more tightly bonded laterally than normally, resulting in the ability to withstand large normal stresses but

not any shear stresses. Michaels (1961) supported Martin's two dimensional fluid model.

PART - B

(1) Viscosity of Water in Clay-Water System:-

A good amount of quantitative and qualitative data is available for the viscosity of loosely bound or strongly bound adsorbed water in clay water system. All the research workers agree that a water structure, which varies in extent with particle arrangement and the adsorbed cationic species, exists at the surface of clay particles and this gives a high viscosity to the adsorbed water.

Rosenqvist (1961) observed that the viscosity of clay water increases with decreasing distance from the mineral surface. He indirectly determined the coefficient of viscosity from the coefficient of self diffusion data for different moisture contents and the results show an exponential increase of average viscosity with decreasing moisture content as reproduced in fig. 8. It is seen that an average viscosity of 24 centipoise is obtained at 30% water content and 153 centipoise at 10% water content in contrast to the viscosity of 1 centipoise of ordinary water not acted by any surface

forces. Kemper, Maasland and Porter (1964) estimated viscosity of water adjacent to sodium and calcium saturated bentonite surfaces from diffusion rates of deuterium hydroxide in oriented clay pastes at several moisture contents. Their data indicates around 60% reduction of mobility (inverse of viscosity) in water which is more than three molecular layers from clay solid surface.

Low (1960) calculated the viscosity of water in the clay water system from the activation energy data, using the relation

$$\mu = B \epsilon^{E/RT} \qquad \ldots\ldots\ldots (7)$$

where μ = coefficient of viscosity

B = an empirical const.

ϵ = exponential

E = activation energy

R = Molar gas constant

T = absolute temperature

Low estimated the activation energy E from permeability tests in conjunction with equation

$$\log Q = \log \left(\frac{K}{B} Ai\right) - \frac{E}{RT} \qquad \ldots\ldots\ldots (8)$$

where K = Intrinsic permeability = $\frac{k\mu}{\gamma}$

Q = Flow rate

A = Area of flow

i = hydraulic gradient.

Equation (8) is obtained from eqn. (7) and Darcy's law ($Q = K Ai$). Equation (8) suggests that the plot of log Q vs $\frac{1}{T}$ permits computation of activation energy (if the pressure gradient is kept constant). Low's data indicates that the activation energy for viscous flow in the clay-water system is approximately 13% larger than the activation energy for viscous flow of pure water which clearly indicates a very high viscosity for water in the clay-water systems. Under similar conditions, however, Rosenqvist (1959) observed a 250 percent increase. Like Rosenqvist (1960, 1961), Olsen (1960) also concluded that viscosity decreases exponentially with distance from the clay particle. One of the main reason why existing theories of hydraulic conductivity (like Kozeny Carman's equation) do not give correct results in case of surface active soils is perhaps the existing equations do not take this increased viscosity and its variation into account. Carman (1939) and Macay (1942) concluded that existing theories of water flow through porous media can not be applied to clays or surface active soils without assuming that part of the water which is immobile to have high viscosity.

To study the effect of this increased viscosity of strongly and loosely bound water on the flow rate or permeability, Olsen (1960, 1961) presented a capillary model consisting of infinitely viscous liquid of thickness 't' clinging around the pore wall, and beyond the distance 't' from the wall the liquid is assumed to have constant viscosity equal to the bulk liquid value. This assumption simply means that the influence of high viscosity on flow rates is equivalent to a reduction in the pore size by a thickness 't'. Olsen (1960) says, that a more reasonable concept of abnormal viscosity probably would be one in which viscosity decreases exponentially with distance from a clay particle surface. Nevertheless, the use of simpler rigid film concept in this analysis can be justified on the grounds that both concepts lead to similar violations of Poiseuille's law. Using rigid film concept, Olsen derived the following flow rate equation

$$\frac{q_{NDHV}}{q_{Kozony}} = 1 + \frac{3}{2}(S_o t)\left(\frac{1-n}{n}\right)\left[\frac{n^3}{1-n^2}\cdot\frac{1}{K_o\ T^2\ S_o^2}\right] \qquad (9)$$

where q_{NDHV} = Flow rate when there is a rigid film of infinite viscous layer around clay particle

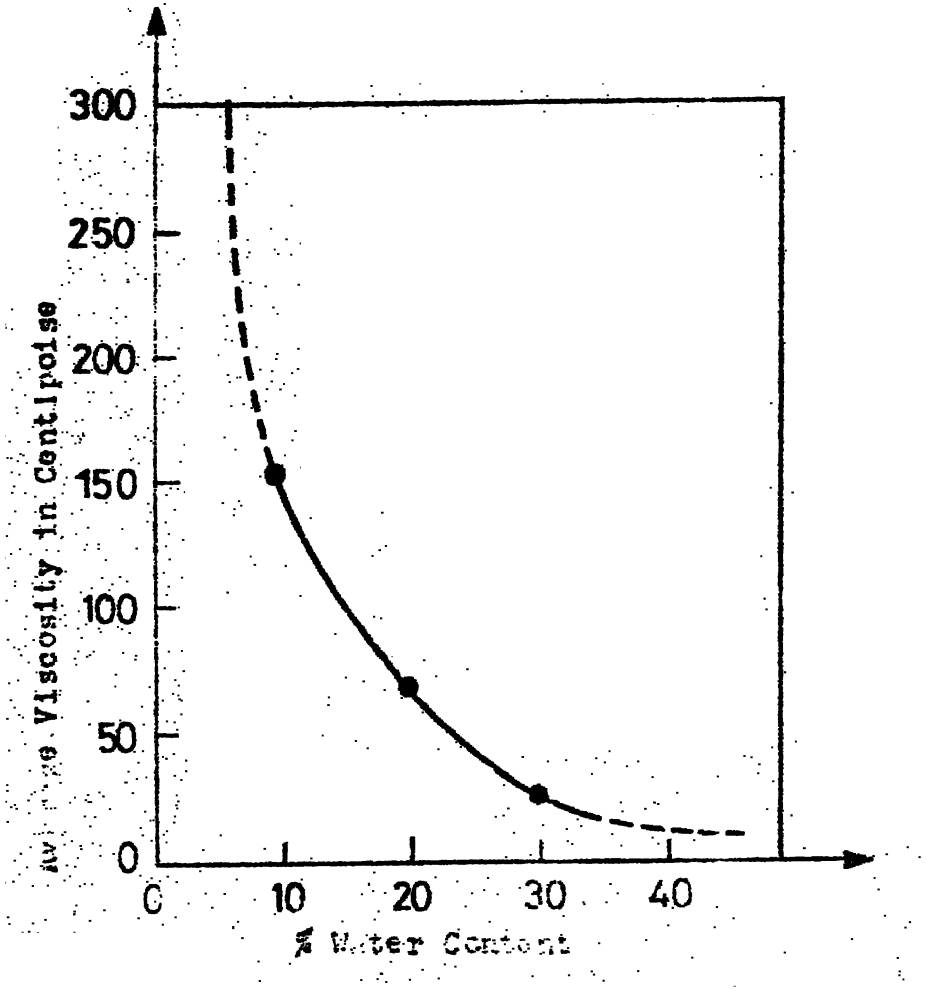
300
250
200
150
100
50
0
0
10
20
30
40
% Water Content

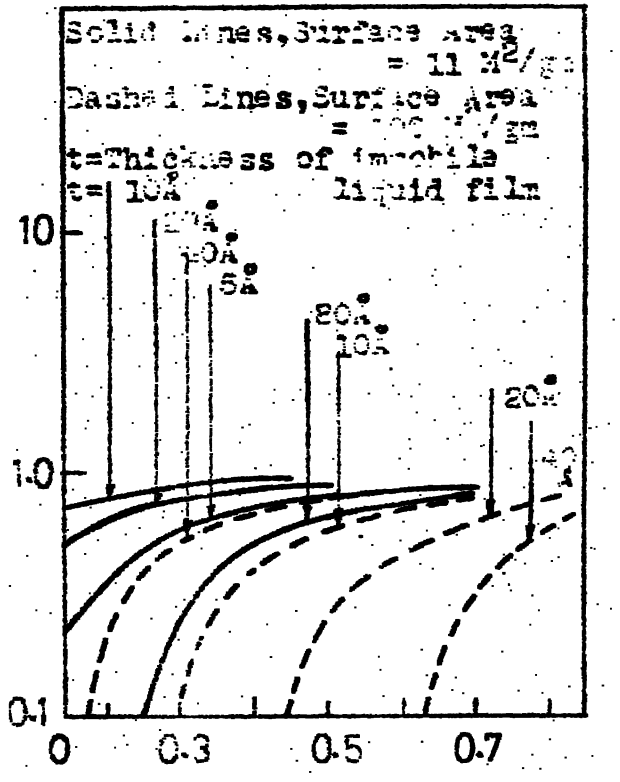
Solid Lines, Surface Area
= 11 M²/gm
Dashed Lines, Surface Area
t=Thickness of
liquid film
t= 10Å
5Å
10
1.0
0.1
0
0.3
0.5
0.7

q_{Kozeny} = Flow rate for Kozeny Carman's equation with constant viscosity of pore water

S_o = Specific surface per unit volume of particles

t = Thickness of rigid film

n = Porosity

T = Tortuosity factor $\approx \sqrt{2}$

K_o = Pore shape factor ≈ 2.5

Equation (9) gives the estimated possible discrepencies due to high viscosity in water of clay-water system. Eqn. (9) is plotted and is shown in fig. (9). For interpretation of this fig. the assumption needed is that 't' remains constant in the entire flow process. Equation (9) & fig. (9) show that for particular thickness 't', as porosity increases discrepency ratio (= q_{NDHV}/q_{Kozeny}) approaches unity but at lower porosities, actual flow rate (q_{NDHV}) is much smaller than predicted by Kozeny-Carman's equation (q_{Kozeny}).

Blackmore (1969) experimentally confirmed the effect of adsorbed water film thickness and its viscosity on the hydraulic conductivity of bentonite and kaolinite.

(2) Density of Adsorbed or Bound Water:-

Realising the importance of role of bound water in the physical properties of clay water system, several investigators tried to find the density of bound water.

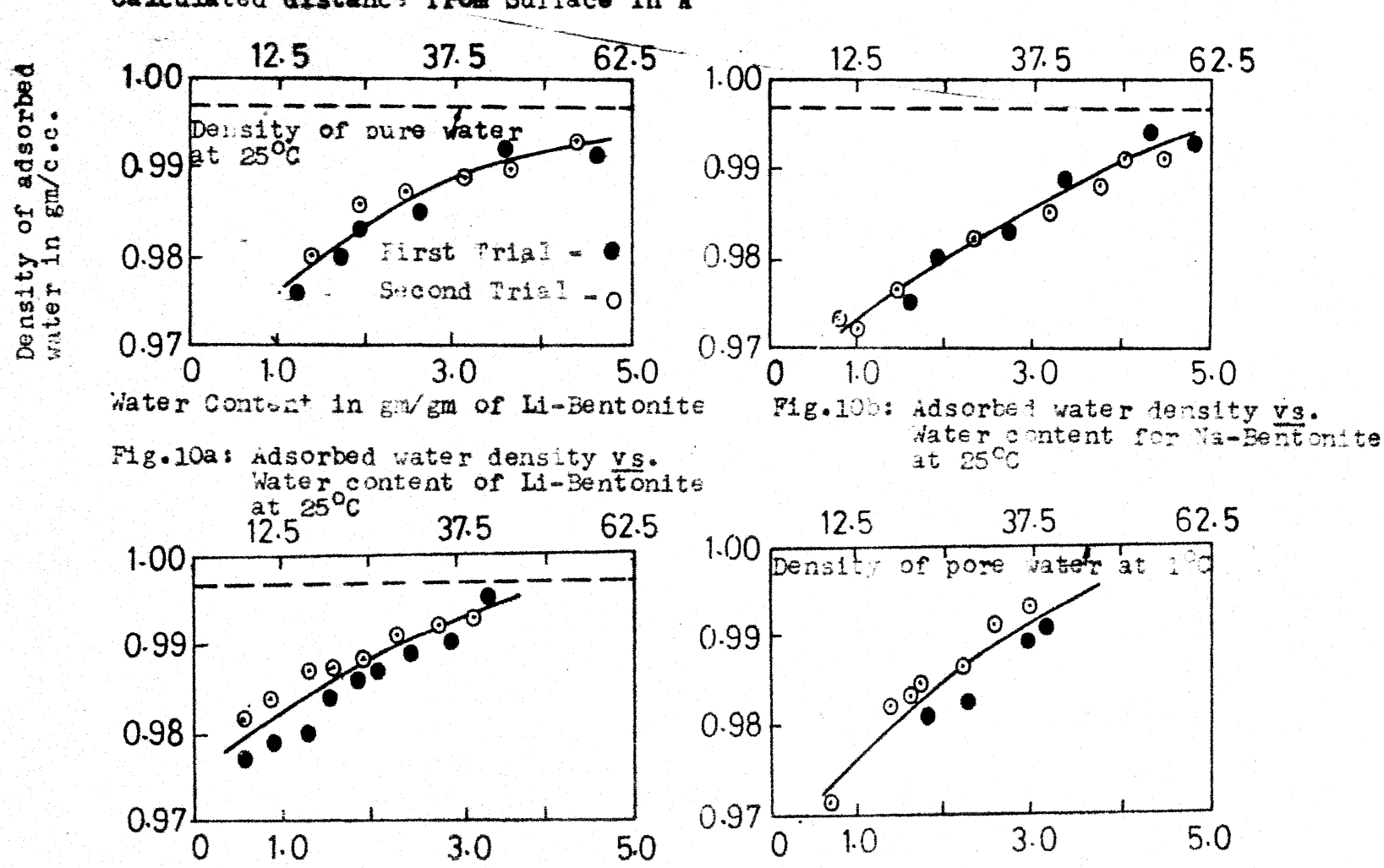

Fig.10a: Adsorbed water density vs. Water content of Li-Bentonite at 25°C

Fig.10b: Adsorbed water density vs. Water content for Na-Bentonite at 25°C

Fig.10c: Adsorbed water density vs. Water content of Na-Bentonite at 25°C

Fig.10d: Adsorbed water density vs. Water content of Li-Bentonite at 1°C

Fig.10 : ADSORBED WATER DENSITY VS WATER CONTENT
(After Anderson & Low, 1958)

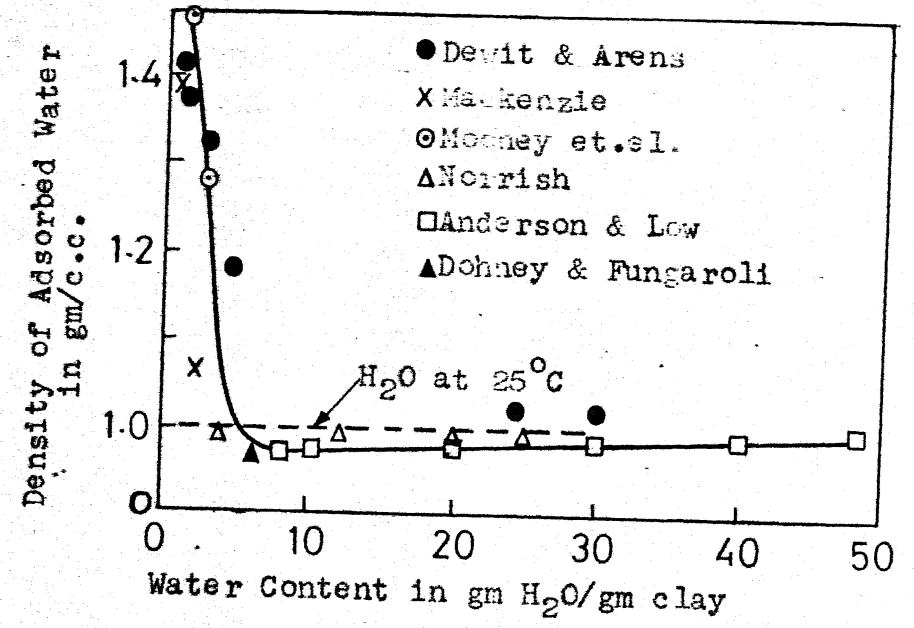

Fig.11 : Summary of Adsorbed Water Density Data for Na-Montmorillonite clay (Modified From Martin,1962)

(After Dohney & Fungaroli,1970)

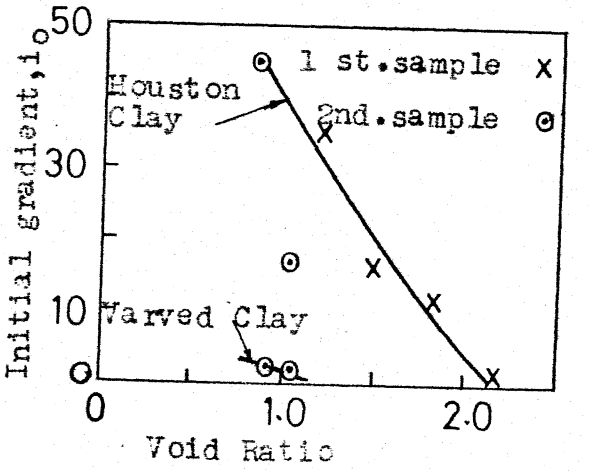

Fig.12: Summary of experimental results plotted as i_o against e

(After Li,1963)

Although there is quantitative difference between the values of density of adsorbed water found by various authors but qualitatively it is observed by Norrish (1954), Anderson & Low (1958), Cirahan (1962) and Dohney and Fungaroli (1972) that density of water in clay-water systems above 5% water content is less than 1.0 gm/cc (minimum value quoted is 0.97 gm/cc) and as the water content increases beyond that the density gradually approaches to 1.0 gm/cc (density of free water). Experiments performed by Dewit and Arens (1950), Mackenzie (1958), Mooney et al (1951) indicate that below 5% water content the density sharply increases beyond 1.00 gm/cc and reaches a peak value of 1.4 gm/cc indicating thereby an increase of density as one approaches the clay surface. The results of Anderson & Low (1958) are shown in fig. 10 and table 1. Density data for Dewit and Arens (1950), Norrish (1954) and Mooney et el (1951) are shown in tables 2 & 3. For better perspective view about the density data covering a wider water content range, Dohney & Fungaroli (1972) plotted the results of all research workers including themselves and is shown in fig. 11.

Buchanan (1964) observed an increase in the density of water (from an average of 0.98 to an average of 1.13 gm/cc) in a consolidating soil at the end of consolidation.

The increase of density with the reduction of water (or closeness of the soil particle) is attributed to the fact that more and more saturating water falls within the surface forces of the solid minerals and thereby making the water more and more abnormal compared to the free water.

Kutilek (1964a, 1962) observed that the density of adsorbed water is lower than 1 and is influenced by the surface properties of the minerals and by the exchangeable cations. He further states that water density is higher on the Montomorillonites than kaolinites because monovalent cations cause higher density than bivalent cations.

(3) Thickness of Bound Water:

The thickness of adsorbed or bound water is of vital importance in the quantification of total probable discharge from surface active soils under hydraulic gradients. According to Grim (1953) many attempts have been made to estimate the thickness of adsorbed water with definite non liquid characteristics without very good agreement among the values suggested. Houwink (1937) arrived at a value of 25A°. Grim & Cuthbert (1945) suggested the thickness of strongly adsorbed water to be 7.5A° to 10A° with gradual transition to liquid water. Jaeger (1938) and Spiel (1940) concluded that the thickness of adsorbed water at optimum

TABLE 1

DENSITY OF ADSORBED WATER AT 25°C

(Data from Anderson & Low (1958) and Low and Anderson (1958b)) Quoted in Martin (1960)

Water content (gm H_2O/gm clay)	Adsorbed water density (gm/ml)		
	Na	Li	K
0.60	-	-	0.980
0.78	0.9715	-	-
1.00	0.9731	-	0.983
1.214	-	0.977	-
2.00	0.980	0.984	0.988
3.00	0.986	0.989	0.993
3.35	-	-	0.994
4.00	0.991	0.992	-
4.61	-	0.993	-
4.80	0.995	-	-
6.70	0.9971	0.9971	0.9971

TABLE 2

ADSORBED WATER DENSITY ON CLAY

(Dewit & Arens (1950), Quoted in Martin (1960))

Mineral	Relative Humidity (percent)	Water content (mg/g)	Density of Adsorbed water (g/cm^3)
Montmorillonite	25	116	1.41
	50	165	1.37
	75	284	1.32
	100	460	1.16
	-	2440	1.02
	-	3010	1.02
Kaolinite	25	4	1.68
	50	8	1.12
	75	9	1.03
	100	65	0.99
Illite	25	30	1.36
	50	49	1.17
	75	69	1.08
	100	188	1.04
	-	1038	1.00

TABLE 3

DENSITY OF ADSORBED WATER CALCULATED FROM X'RAY DATA

(Data from Mooney, Keenan & Wood (1951) and Norrish (1959) Quoted in Martin (1960))

Author	Experimental Data		Calculated adsorbed water density (gm/ml)
	d_{100} (A)	Water content (gH_2O/g clay)	
Money et al	9.8	0	-
	12.4	0.10	-
	12.4	0.15	1.46
	15.4	0.20	-
	15.4	0.28	1.27
Norrish	9.5	0	-
	19.0	0.37	0.986
	40.0	1.19	0.986
	61.0	2.0	0.986
	73.5	2.5	0.99

plasticity of kaolinite is of the order of several hundred angstroms. Rutgers (1954) suggested a value of 16 to 100A°. Lutzor & Kemper (1959) calculated the thickness of water adsorbed on Wyoming Bentonite surface from the pressure memlrave data for different equillibrium pressures and the results are shown in table 4. Norton & Johnson (1944) reported the thickness associated with kaolinite particles ranged from 290A° to 13A° with increase of pressure. Williamson (1951) reported a thickness as high as 1000A° which means allmost all the water in the natural soils within the working void ratio range is bound water (loosely or strongly). This is also supported by Grim (1952).

TABLE 4

Thickness of water layer on surfaces of clay particles (Wyoming Bentonite)

(After Lutz & Kemper (1959))

System	Thickness* of water films at 5 equillibrium pressures				
	0.54 Atm.	1.70 Atm.	3.0 Atm.	6.0 Atm.	12.0 Atm.
	Å	Å	Å	Å	Å
Na-Saturated clay in water	66.0	35.9	25.0	15.1	9.4
Na-Saturated clay in 0.03 N NaCl	61.5	33.3	24.2	15.5	8.5
Na-Saturated clay in 1.0 N NaCl	46.2	24.1	16.0	10.3	6.8
Ca-Saturated clay in water	40.5	20.4	14.8	9.6	7.1
Ca-Saturated clay in 0.01 N. $CaCl_2$	35.8	18.9	14.4	10.6	7.3
K-Saturated clay in water	68.2	36.6	24.5	14.3	8.6

* Calculated on the basis of 800 m^2 of surface/gm. of clay, and 10 $Å^2$ as the packing area for a single water molecule.

Chapter 3

EXPERIMENTAL AND THEORETICAL NON DARCY VELOCITY GRADIENT RELATIONSHIPS

Various authors have suggested several empirical velocity gradient relationships based on their experimental results. There are also a few theoretical solutions available which are predominantly based on capillary tube model. Kutilek (1969) suggested several v-i relationships based on non Newtonian flow. The types and names of equations will be given first and their discussion will follow. The chapter is devided into 4 Parts as given below

'A': EMPIRICAL EQUATIONS AVAILABLE

'B': THEORETICAL SOLUTIONS AVAILABLE

'C': SOLUTIONS BASED ON NON NEWTONIAN FLUID FLOW

'D': SHAPES OF EXPERIMENTALLY OBSERVED VELOCITY-GRADIENT CURVES.

PART A.

EMPIRICAL EQUATIONS AVAILABLE

The following is a list of empirical equations reported in literature.

(1) Puzyrevskaya's equation (1931)

$$v = K(i - i_o) \quad \ldots\ldots \quad (10)$$

(2) Valarovich and Tchuraev's Equation (1964)

$$v = Ai + \frac{C}{i^3} - B \quad \ldots\ldots \quad (11)$$

(3) Izbashe's Equation (1931)

$$v = Ki^n \quad \ldots\ldots \quad (12)$$

(4) Slepicka's Equation (1961)

$$v = \alpha\left(\frac{n}{\alpha}\right)^{f-1} K^f i^f \quad \ldots\ldots \quad (13)$$

(5) Swartzendruber's Equation (1962a, 1962b)

i) $$v = M\left[i - I(1 - \epsilon^{-i/I})\right] \quad \ldots\ldots \quad (14)$$

ii) $$v = B\left[1 - J(1 - \epsilon^{-Ci})\right] \quad \ldots\ldots \quad (15)$$

and

(6) Kutilek's Equation (1965)

$$v = M\left[\frac{1}{B}\log\left(A + e^{Bi}\right) - I_o\right] \quad \ldots\ldots \quad (16)$$

(1) Puzyrevskaya's equation:

Puzerevskaya (1931) first proposed the equation of the form

$$v = K(i - i_o) \quad \ldots\ldots \quad 10$$

where i_o = Threshold gradient below which there is no flow.

Li (1963) found that for Houston and varved clay. Threshold gradient decreases approximately linearly with increasing void ratio and his results are shown in fig. 12. Kondon (1967) also observed that the threshold gradient increases with decreasing porosity and increasing specific surface and he explained his results on the basis of rheological properties of water in thin slits and narrow capillaries. Bondarenko (1968) concluded that liquids with H-bonds behave as Bingham material and have a definite threshold gradient due to certain yield stress of the pore water. About the validity of equation (10) Valarovich and Tchuraev (1964) suggest that the equation gives correct result only when one works with large pressure gradients and materials with uniform pore radii.

(2) Valarovich and Tchuraev's Equation.

Based on experimental results, Valarovich and Tchuraev (1964) forwarded an equation of the form

$$v = Ai + \frac{C}{i^3} - B \qquad \ldots\ldots \quad (11)$$

where A, B and C are constants which depend on the pore radii, the type of pore distribution, the porosity of the sample and the rheological properties of the fluid.

This equation is identical with Nerpin's Bingham body equation to be discussed later.

(3) Izbash's Equation:

For the non linear portion in the laminar region, Izbash (1931) proposed the equation of the form

$$v = Ki^n \quad \ldots\ldots \quad (12)$$

where $n > 1$ depending on soil properties.

Hansbo (1960) supported the same equation and claimed that his data and Silfverberg's (1949) data fit well in the above equation for the values of 'n' in between 1 to 1.5. Dudgeon (1966) found the value of n to be 1.12 to 1.25.

(4) Slepicka's Equation:

From dimensional analysis and experimental results, Slepicka (1961) proposed an equation of the form

$$v = \alpha\left(\frac{h}{\sigma}\right)^{f-1} K^f i^f \quad \ldots\ldots \quad (13)$$

or $$v = K_f\, i^f \quad \ldots\ldots \quad (13a)$$

where $K_f = \alpha\left(\frac{h}{\sigma}\right)^{f-1} K^f$

= general coefficient of filtration

η = Dynamic coefficient of viscosity

σ = Surface tension (contact tension of solid liquid interface.)

α = A factor.

Depending on the values of f in equation (13) or (13a), the flow regime can be devided into prelinear regime, linear regime and post linear regime as explained in fig. (13).

Slepicka observed an experimental linear relation between the value of f in the prelinear regime (our main concern) and Darcy's K (slope of v-i curve in the linear regime) in log scale as shown in fig. 14. Slepicka also found a linear plot between critical gradient i_1 (as defined in fig. 13) and Darcy's K. The result is shown in fig. 15. As seen from fig. 14, the value of f (which is nothing but 'n' in Izbash's eqn. Eq. 12) varies between 1.3 to 2.3 depending on Darcy's K value.

(5) Swartzendruber's Equation

From the experimental v-i curves Swartzendruber (1962a) proposed the equation

$$v = M\left[i - I(1 - \epsilon^{-i/I}\right] \quad \ldots\ldots \quad (14)$$

where M and I are constants. I is the 'i' intercept obtained when linear part of equation (14) is extended as explained in fig. 16.

I is the measure of departure from Darcy's law.

The fit of the equation (14) for the experimental data of Hansbo (1960), Von Engelhardt and Tunn (1955) and Lutz & Kemper (1959) are shown in fig. 17, 18 and 19.

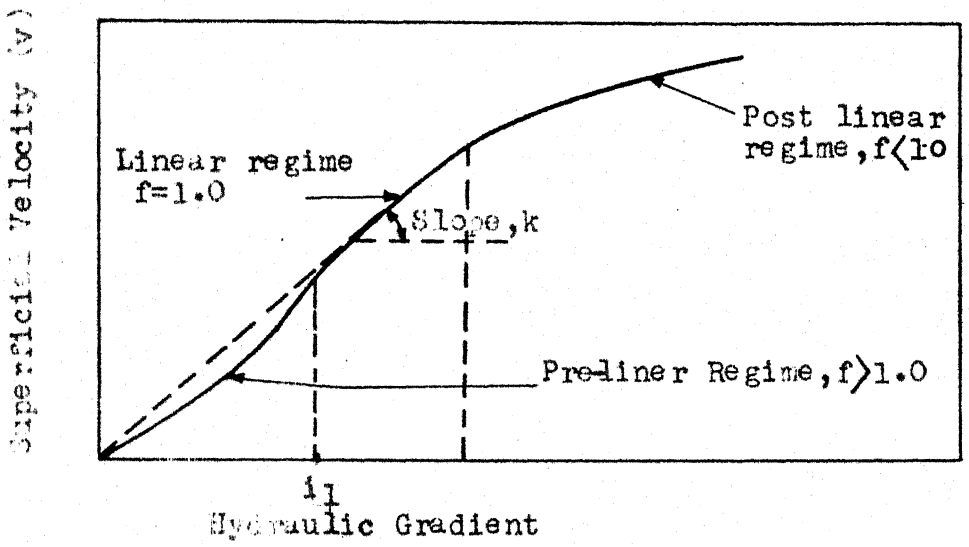

Fig.13: Velocity Gradient Relationship as proposed by Slepicka,1961

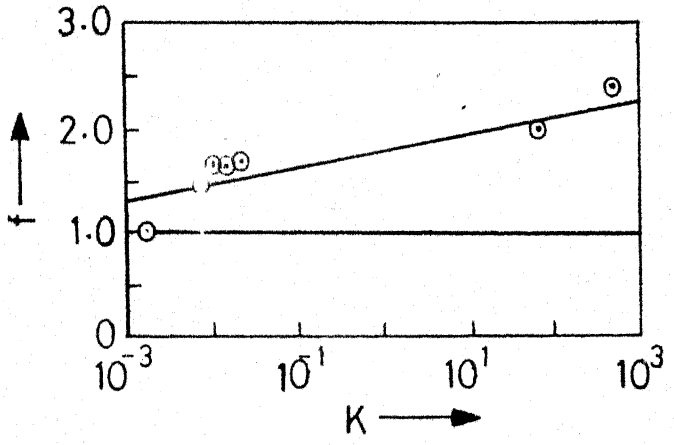

Fig.14: Relation between f & k (Pre-linear) (After Slepicka,1961)

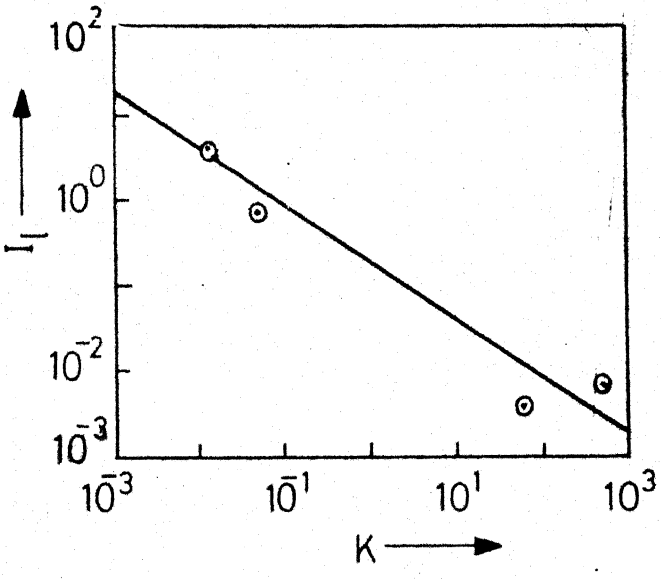

Fig.15: Relationship between i_1 & k (After Slepicka,1961)

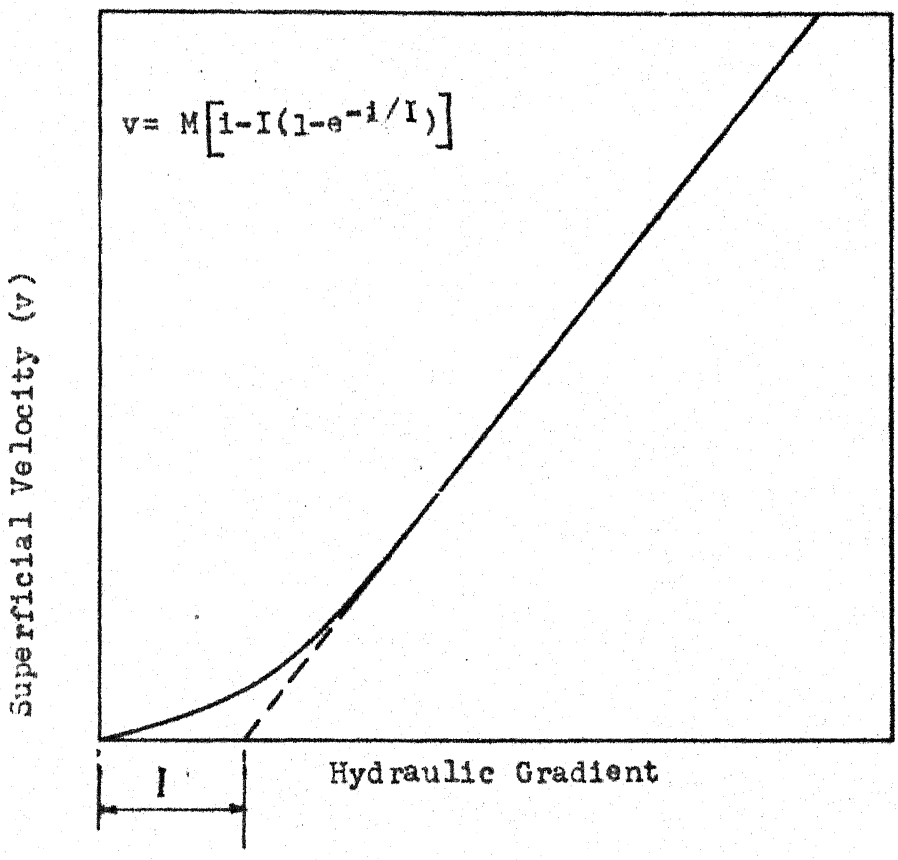

Fig.16: Velocity Gradient Relationship as proposed by Swartzendruber (1962 a)

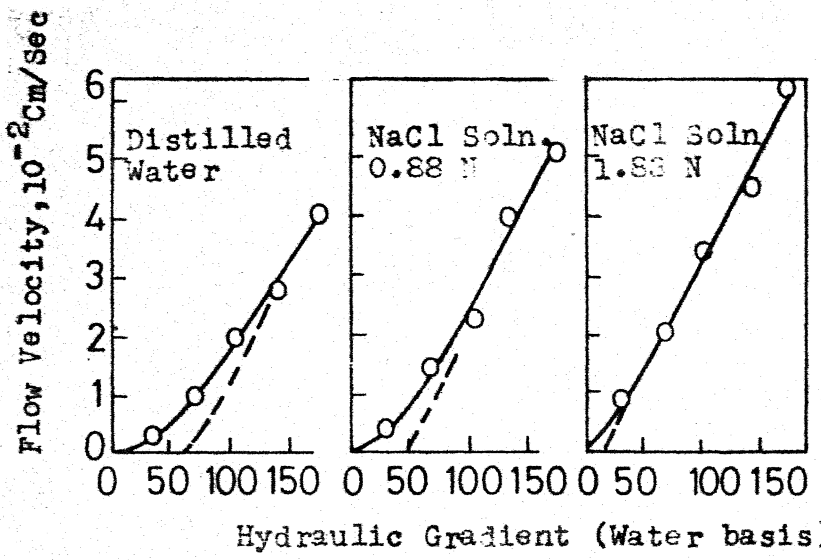

Fig.17 : Typical fit of the data of Von Engelhardt & Tunn (1955) for sand stone sample No.15L, using eqn.14

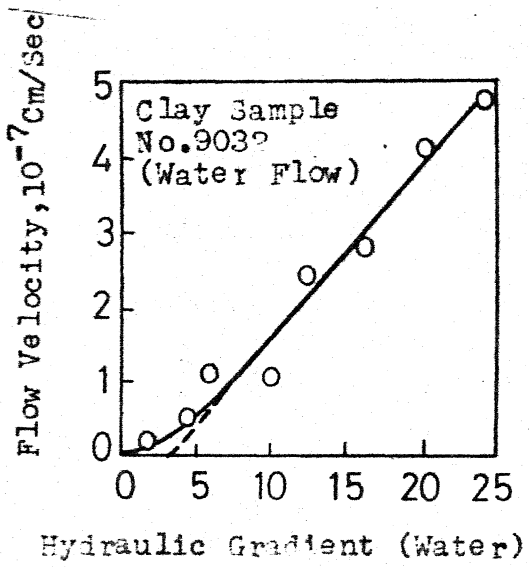

Fig.18 : Typical fit of the data of Hansbo (1960) using eqn.14

Figs.17,18 & 19 are after Swartzendruber (1962 a)

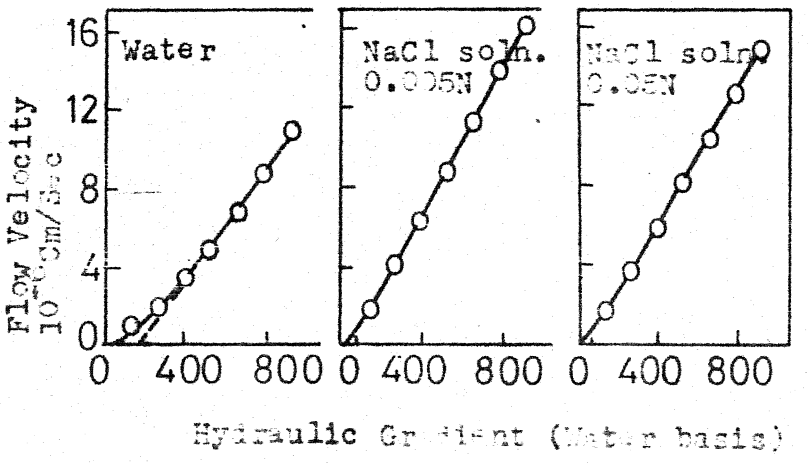

Fig.19: Typical Fit of the data of Lutz & Kemper (1959) for Na-sat. Bladen clay, using eqn.14

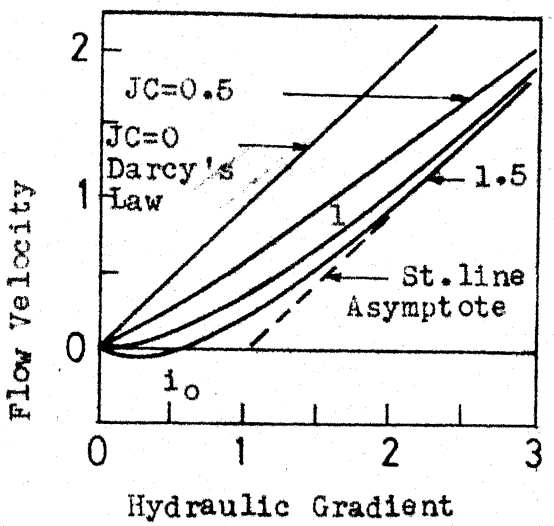

Fig.20 : Plots of equation 15 with B=1 & J=1

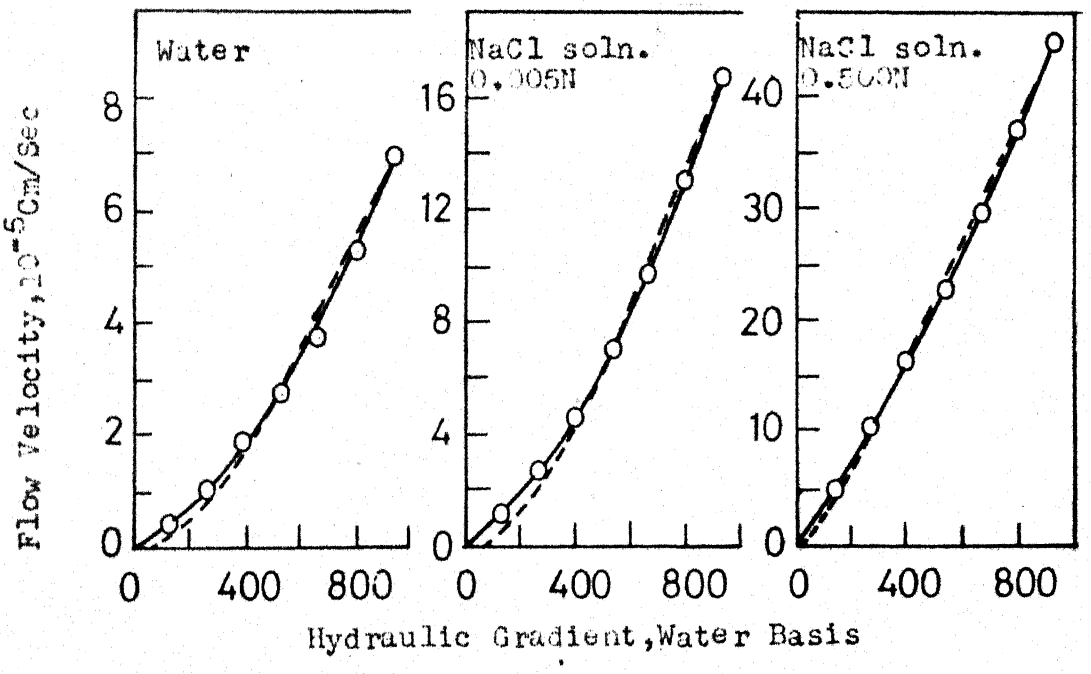

Fig.21: Data for Na-sat.Utah Bentonite (Lutz & Kemper,1959) as fitted by eqn.15 (Solid line) and eqn.14 (Broken lines)

After Swartzendruber,1962 b

Later, Swartzendruber (1962b) improved equation (14) by bringing one more parameter and his equation reads as

$$v = B\left[i - J(1 - \epsilon^{-Ci})\right] \qquad \ldots\ldots \quad (15)$$

where B, J and C are constants.

Equation (15) is plotted in fig. 20. The term J^2C is a measure of non Darcian behaviour.

Swartzendruber claims that equation (15) fits better with the experimental results than equation (14) mainly because in Eq. 14 the slope of the v-i curve at i = 0, is always zero, regardless of the magnitude of I, (except when I = 0). A comparison of equation (14) and (15) for Lutz and Kemper's (1959) data is shown in fig. 21.

(6) Kutilek's Equation

Assuming a higher viscosity of pore water near clay surface and based on experimental results Kutilek (1964) proposed the equation

$$v = M\left[\frac{1}{B}\log\left(A + e^{Bi}\right) - I_o\right] \qquad \ldots\ldots \quad (16)$$

where $B = \dfrac{\log \frac{M}{M'}}{I_o}$

$A = \dfrac{M}{M'} - 1$

M = hydraulic conductance

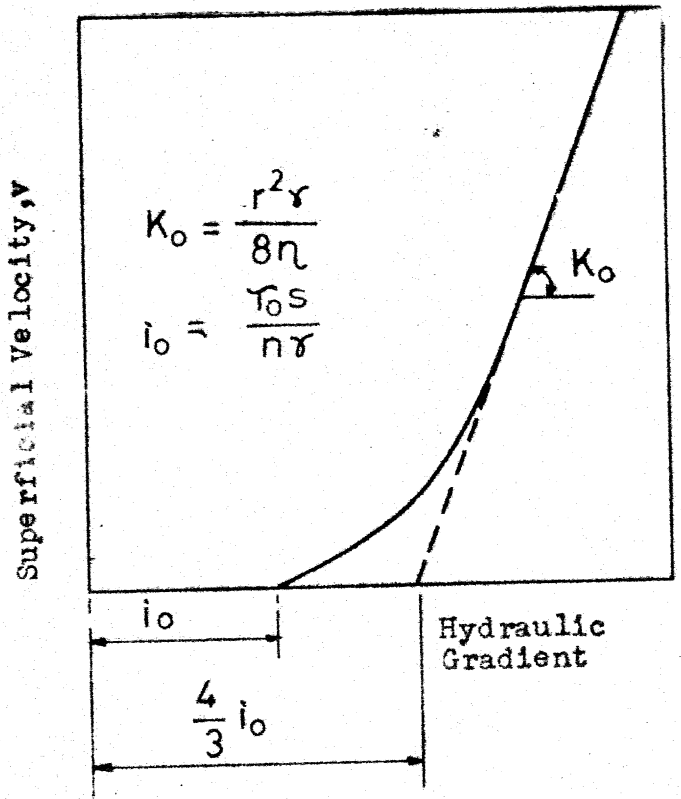

Fig.23: Velocity Gradient Relationship as proposed by Nerpin and Tchudnovskij (1967)

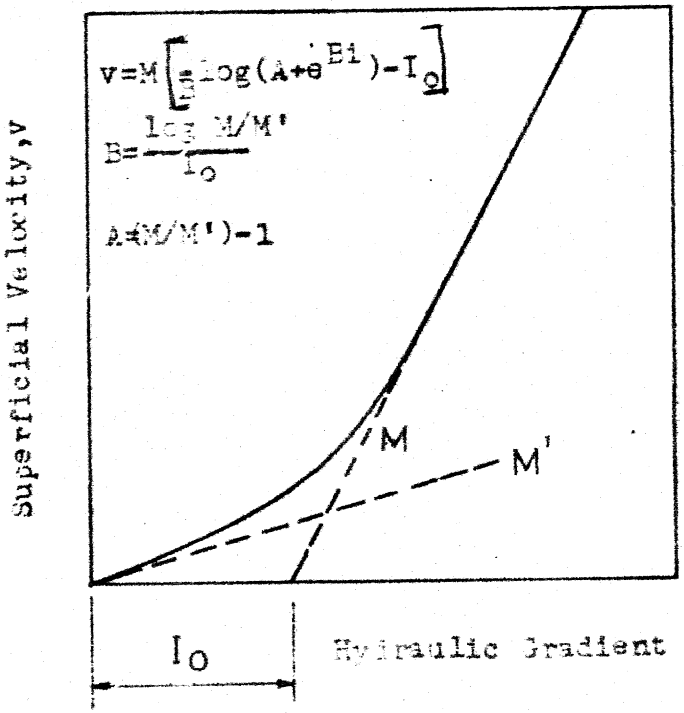

Fig.22: Velocity Gradient Relationship as proposed by Kittlek, 1964

M' = Initial hydraulic conductance

I_o = Intercept of M on I axis

The parameters M, M' and I_o of equation (16) are explained in fig. 22.

Typical values of M, M' and I_o for different soil mineral-liquid systems are shown in table 5.

PART 'B'

THEORETICAL SOLUTIONS

The following theoretical solutions available

(1) Nerpin's Bingham body equation (1967)

(2) Nerpin and Deryagin's equation (1969)

(3) Kovack's equation (1967)

(4) Klausner and Kraft's equation (1966)

(1) Nerpin's Bingham body Equation:

Nerpin and Tchudnovskij (1967) postulated that soil water behaves like a Bingham body and suggested an equation identical with the flow of Bingham liquid through a system of capillary tubes which reads as

$$v = K_o I \left[\frac{1}{3} \left(\frac{i_o}{i}\right)^4 - \frac{4}{3} \left(\frac{i_o}{i}\right) + 1 \right] \quad \ldots\ldots \quad (17)$$

where $I_o = \frac{\tau_o S}{n \gamma}$ = threshold gradient

τ_o = Threshold yield stress

S = Specific surface

n = porosity

γ = Density of water

$K_o = \frac{r^2 \gamma}{8 \eta}$ = hydraulic conductivity for a Newtonian liquid

r = radius of capillary

γ = Density of liquid

η = Viscosity of liquid.

Equation (17), takes the shape as shown in fig. 23.

Bondarenko (1968) found the value of yield stress (τ_o) of the order of 10^{-2} to 10^{-3} dynes/cm^2 for liquids with hydrogen bonds e.g. H_2O, C_2H_5OH, CH_2OH etc.

(2) Nerpin and Deriyagin's Equation:

Nerpin and Deriyagin (1969) derived a flow equation from thermodynamic principle as

$$\theta = \frac{\alpha}{\eta S^2} \delta^3 \text{ grad } \theta + \epsilon \beta \delta \text{ grad } \gamma \quad \ldots \quad (18)$$

where θ = moisture potential

η = viscosity

TABLE 5

PARAMETERS M, M' and I_o FOR DIFF. CLAY MINERALS

(After Kutilek 1965)

Cation Exchangeable Mineral	Liquid	I_o	$Mx10^{-3}$ cm/hr	$M'x10^{-3}$ cm/hr
H-Kaolinite	H_2O	160	23.7	1.5
	0.01 N HCl	35	30.0	19.3
	0.001 N HCl	105	24.6	8,3
Na Kaolinite	H_2O	395	8.1	0.8
	0.1 N NaCl	0	22.2	22.2
	0.01 N NaCl	0	19.5	19.5
	0.01 N Na_2SO_4	202	15.5	3.3
Ca Kaolinite	H_2O	113	14.8	1.5
	0.1 N $CaCl_2$	0	24.9	24.9
	0.01 N $CaCl_2$	0	18.6	18.6
	0.1 N $Ca(NO_3)_2$	20	16.4	0.2
	0.01 N $Ca(NO_3)_2$	113	14.8	1.5
H-Montmorillonite	H_2O	171	1.60	0.30
	0.01 N HCl	110	1.93	0.83
	0.001 N HCl	138	1.45	0.37
Na Montmorillonite	H_2O	340	0.35	0.07
	1 N NaCl	97	31.2	5.3
	0.1 N NaCl	255	12.7	1.13
	0.01 NaCl	325	8.4	0.10
Ca Montmorillonite	H_2O	295	4.20	0.12
	1 N $CaCl_2$	90	111	20
	0.1 N $CaCl_2$	120	108	9.3
	0.01 N $CaCl_2$	210	66	4.3
H-Illite	H_2O	260	18.2	1.1
	0.1 N HCl	140	31.4	4.2
	0.01 N HCl	160	24.5	1.5
	0.001 N HCl	260	88	1.1
Na-Illite	H_2O	185	0.86	0.29
	1 N NaCl	62	3.6	0.64
	0,1 N NaCl	85	1.21	0.38
	0.01 N NaCl	110	0.93	0.33
	0.1 N Na_2SO_4	100	1.02	0.38
Ca-Illite	H_2O	230	13.2	1.5
	1 N $CaCl_2$	150	22.5	4.2
	0.1 N $CaCl_2$	185	15.4	2.2
	0.01 N $CaCl_2$	210	13.8	1.5

S = Specific kinetic energy

δ = Active porosity

α = A numerical coefficient

ε = Coefficient of convolution of the pores

ψ = This is any one of the following three quantities

(i) Temperature

(ii) Electric field potential

(iii) Concentration of dissolved substances

β = Corresponding coefficient of thermo-osmosis or capillary osmosis

After making the following substitutions

$$\frac{\alpha \delta^3}{\eta S^2} = K$$

$$\text{grad } \theta = i$$

$$- \varepsilon \beta \eta S^2 / \alpha \delta^2 \text{ grad } \psi = i_o$$

equation (18) gets converted to

$$q = K(i - i_o) \quad \ldots\ldots \quad (18a)$$

(3) KOVAC's EQUATION.

Based on capillary tube model and with liquid obeying the relation

$$\tau = \tau_o + \eta \frac{dv}{dn} \quad \ldots\ldots (19)$$

where τ_o = Threshold shear stress

η = Viscosity of fluid, 'n' symbolises the direction, at right angles to the direction of movement

Kovac (1967) derived the following velocity - gradient relationship:

$$\frac{v}{v_D} = \left(1 - \frac{i_o}{i}\right)^2 - \frac{2}{3}\frac{i_o}{i}\left[\left(1 - \frac{i_o}{i}\right)^{3/2} \tan^{-1}\sqrt{1 - \frac{i_o}{i}} - \log\frac{i_o}{i} - \left(1 - \frac{i_o}{i}\right)\right] \quad \ldots\ldots (20)$$

where v_D = Darcy velocity for Newtonian fluid

$$= \frac{r_o^2 \gamma}{8\eta} i$$

From his experimental results, Kovacs approximated equation (20) as

$$v = 0.714\, K_D \left(\frac{i - i_o}{i_o}\right) \quad \ldots\ldots (21)$$

for $i < 12\, i_o$

where K_D = Darcy's permeability coefficient

$$= \frac{\gamma r_o^2}{8\eta}$$

Eqn. (20) and (21) are plotted in fig. 24 and 25.

(4) Klausner and Kraft's Equation:

Based on capillary tube model Klausner and Kraft (1965a, 1965b, 1966a and 1966b) theoretically explained the

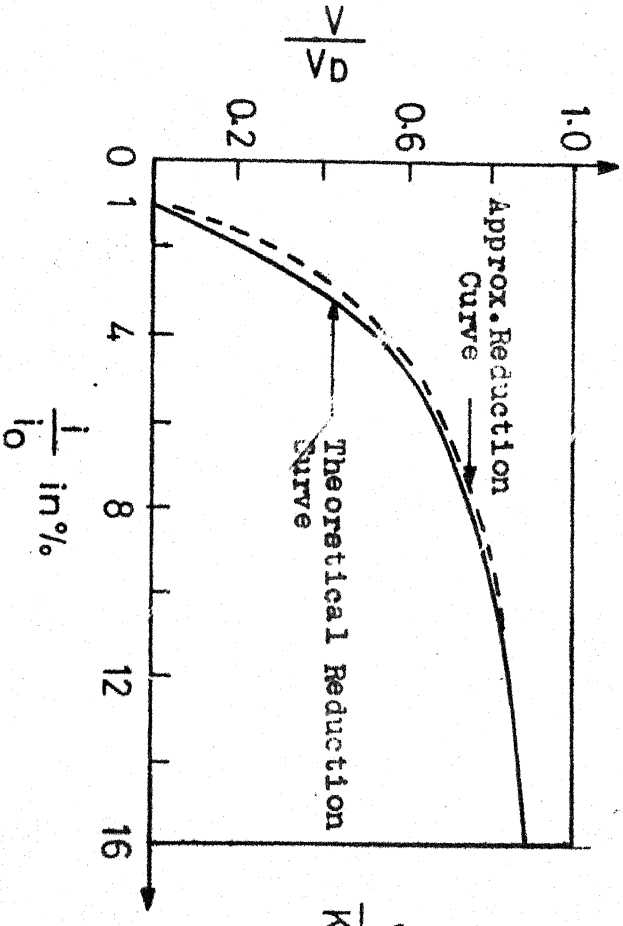

Fig.24: Relation between V/V_D and i/i_o (After Kovacs, 1967)

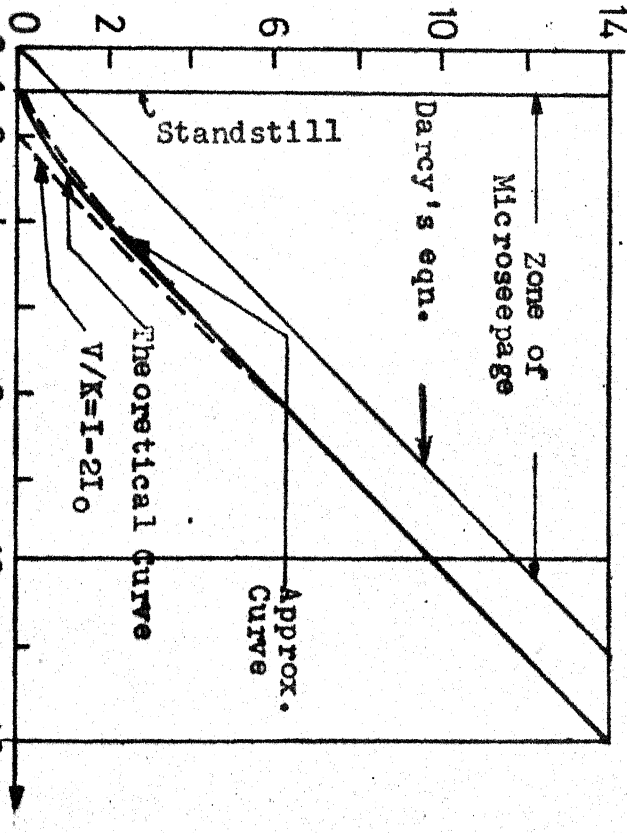

Fig.25: Relationship between V/K_D and i/i_o (After Kovacs, 1967)

non Darcy behaviour of soil water flow assuming wall forces arising out of active clay surfaces. They considered a force F acting normal to the wall as shown in fig. 26. The force F is the average electrical field arising from the unbalanced charge on the crystalline wall. This force 'F' is the same electrical force that gives rise to Chapman-Gouy potential at a crystalline interface. The force F is assumed to influence the fluid by bringing into existence a force $\bar{f}$ of magnitude ($C/\bar{F}/$, C is a const. of proportionality) acting along the capillary axis (see fig. 27) and resisting the motion. For a linear increase in $\bar{f}$ with a discontinuous jump near the wall, for the system as shown in fig. 27, Klausner and Kraft had set up equillibrium momentum equation for a Newtonian fluid and then solved for discharge Q for different pressure gradient (ΔJ) and the ultimate solution reads as

$$- Q(\Delta j, R) = \frac{a^4}{8} \Delta J - \frac{1}{2}\left[a^3 W(a, R) - \int_0^a r^3 f(r, R)\, dr \right]$$

$$= \frac{a^4}{8} \Delta j - R^*(\Delta j, R) \qquad \ldots (22)$$

where η = Viscosity of the fluid

a = a(Δj, R) and is defined by the radius 'r' upto which flow zone extends and this is a solution of equation

$$a\left(\frac{\Delta j}{2}\right) = W(a, R) \quad \text{where}$$

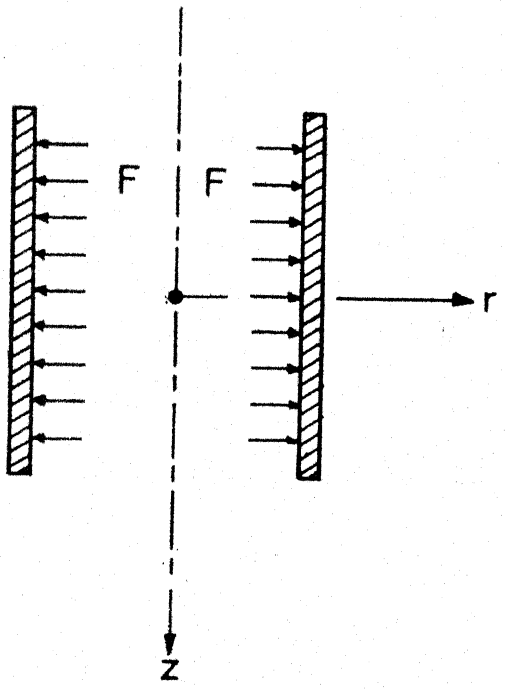

Direction of Flow

Fig.26: Wall force as assumed by Klausner and Kraft (1966 b)

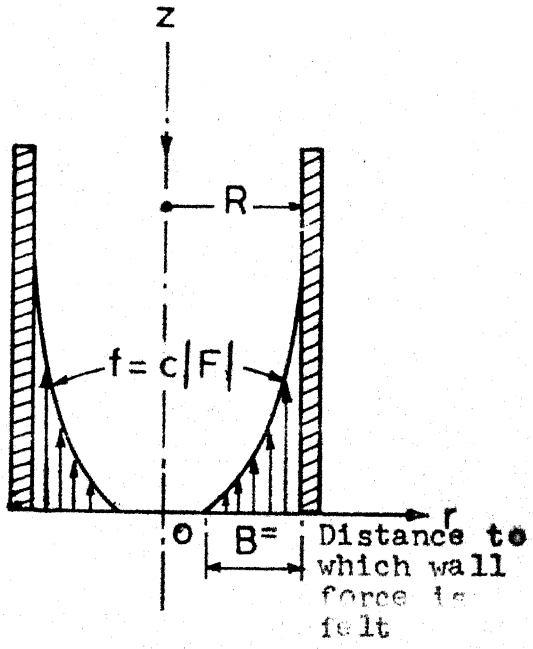

Fig.27: Force opposing the fluid motion as visualised by Klausner and Kraft (1966b)

$$W(r, R) = \frac{1}{r} \int_{o}^{r} r\, f(r, R)\, dr$$

Eqn. (22) is shown in fig. 28.

Equation (22) as seen from the plots qualitatively explains the observed non Darcy velocity-gradient relationship - but one of the main drawbacks of the theory is that, it does not consider the variable viscosity, density and non Newtonian behaviour of the pore fluid whose existence is more or less certain due to the very nature of clay-water environment. So an approach similar to Klausner and Kraft considering the soil-water interaction and rheological parameters of pore fluids holds a promising future.

PART C

SOLUTIONS BASED ON NON-NEWTONIAN FLUID FLOW

Kutilek (1969), Govier and Aziz (1972) and others have suggested a few velocity-gradient (v-i) relationships based on non Newtonian fluid flow. Each non Newtonian fluid is characterised by a distinct shear stress (τ) - velocity gradient ($\frac{du}{dr}$) relationship. Ten v-i relationships can be suggested based on ten different non Newtonian fluids characterised by respective constitutive equations as completely described in Table 5A. This table also gives velocity distribution and discharge through a capillary tube for some of the cases. If

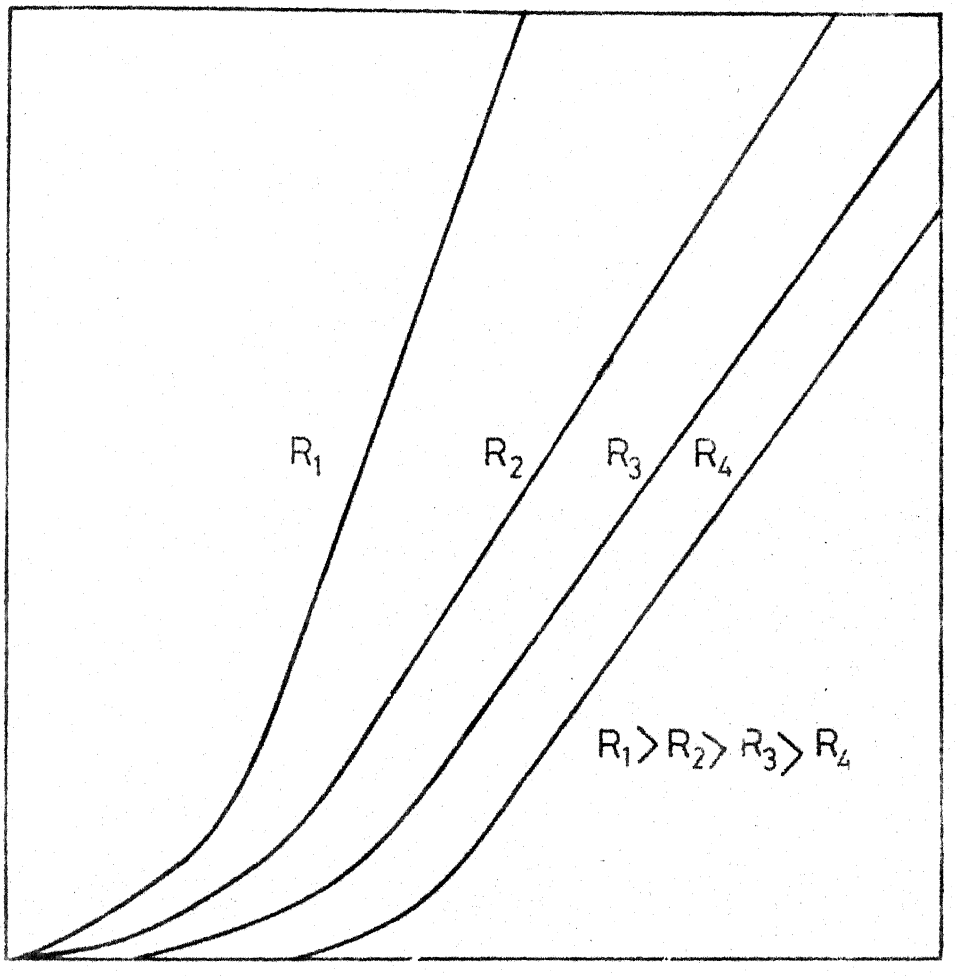

Fig.28: Shape of Discharge Pressure Gradient curve as found by Klausner and Kraft (1966b)

TABLE - 5A

SUMMARY OF v-i RELATIONSHIPS FOR VARIOUS FLUIDS

VISCOUS FLUIDS

NON-NEWTONIAN FLUIDS

PSEUDO PLASTIC FLUIDS

	CONSTITUTIVE EQUATION	VELOCITY DISTRIBUTION IN CIRCULAR PIPE	DISCHARGE IN CIRCULAR PIPE	VELOCITY - GRADIENT RELATIONSHIP IN CIRCULAR PIPE	REFERENCE
NEWTONIAN FLUID	$\tau = \mu\dot{s}$	$u = i\frac{\gamma_w R^2}{4\mu}\left(1-\frac{x^2}{R^2}\right)$	$Q = \frac{\gamma_w R^4}{8\mu} i a$	$v = \frac{\gamma_w R^2}{8\mu} i$	Govier & Aziz (1972)
DILATANT FLUID	$\tau = m\dot{s}^n$ $n>1$	$u = \left[\left(\frac{i\gamma_w}{2m}\right)^{\frac{1}{n}} \cdot \frac{n}{1+n}\right]\left(R^{\frac{1+n}{n}} - x^{\frac{1+n}{n}}\right)$	$Q = \pi R^{\frac{3+n}{n}}\left[\left(\frac{\gamma_w}{2m}\right)^{\frac{1}{n}} \cdot \frac{n}{1+3n}\right] i^{1/n}$	$v = \left[\left(\frac{\gamma_w}{2m}\right)^{\frac{1}{n}} \cdot \frac{n}{1+3n} \cdot R^{\frac{1+n}{n}}\right] i^{1/n}$	Buckingham (1921)
BINGHAM FLUID	$\tau - \tau_y = \eta\dot{s}$	$u = \frac{1}{\eta}\left[\frac{i\gamma_w}{4}(R^2-x^2) - \tau_y(R-x)\right]$	$Q = \left[\pi R^4 \frac{\gamma_w}{8\eta}\right] i\left\{1 - \frac{4}{3}\left(\frac{i_0}{i}\right) + \frac{1}{3}\left(\frac{i_0}{i}\right)^4\right\}$	$v = \frac{\gamma_w R^2}{8\eta} i\left[1 - \frac{4}{3}\left(\frac{i_0}{i}\right) + \frac{1}{3}\left(\frac{i_0}{i}\right)^4\right]$	Govier and Aziz (1972) [First part only]
YIELD PSEUDO-PLASTIC FLUID	$\tau - \tau_y = \eta\dot{s}^n$	$u = \frac{\left(\frac{1}{\eta}\right)^{\frac{1}{n}}}{\left(\frac{i\gamma_w}{2}\right)} \cdot \frac{n}{1+n}\left[\left(\frac{i\gamma_w R}{2} - \tau_y\right)^{\frac{1+n}{n}} - \left(\frac{i\gamma_w x}{2} - \tau_y\right)^{\frac{1+n}{n}}\right]$		$v = \left(\frac{\gamma_w}{2\eta}\right)^{\frac{1}{n}} \cdot R^{\frac{1+n}{n}} \cdot i^{\frac{1}{n}}\left[\frac{\left(1-\frac{i_0}{i}\right)^2}{\frac{1+3n}{n}} + \frac{2\frac{i_0}{i}\left(1-\frac{i_0}{i}\right)}{\frac{1+2n}{n}} + \frac{\left(\frac{i_0}{i}\right)^2}{\frac{1+n}{n}}\right]$	
POWER LAW FLUID	$\tau = m\dot{s}^n$ $n<1$	SAME AS DILATANT FLUID		$v = \frac{M}{i} - \frac{N}{i^2} - \frac{1}{2}\left(e^{bi} - e^{-bi}\right) + \frac{O}{i^3}\left(\frac{e^{bi}-e^{-bi}}{2} - 1\right)$ $M = \frac{2\varepsilon}{\gamma_w}\frac{A'}{B'}$; $N = \frac{4s}{\gamma_w^2}\frac{A'}{(B')^2}$; $O = \frac{4s^2}{\gamma_w^3\varepsilon}\cdot\frac{A'}{(B')^3}$; $b = \frac{\gamma_w\varepsilon}{s}B'$	Kutilek (1969)
EYRING'S FLUID	$\tau = \frac{1}{B'}\sinh^{-1}\left(\frac{\dot{s}}{A'}\right)$				
POWELL - EYRING FLUID	$\tau = \mu_\infty\dot{s} + \frac{1}{B'}\sinh^{-1}\left(\frac{\dot{s}}{A'}\right)$			$v = A'R\left[\frac{\Gamma_w}{3} - \frac{1}{3\Gamma_w^2}\left\{\frac{1}{4}\Gamma_w^4\omega^3 + \omega^2\left[\Gamma_w^3\sinh^{-1}\Gamma_w - \Gamma_w^2\sqrt{1+\Gamma_w^2} + \frac{2}{3}\left(1+\Gamma_w^2\right)^{3/2} - \frac{2}{3}\right] + \frac{3}{4}\omega\left[\left(2\Gamma_w^2+1\right)\times\left(\sinh^{-1}\Gamma_w\right)^2 - 2\Gamma_w\sqrt{1+\Gamma_w^2}\sinh^{-1}\Gamma_w + \Gamma_w^2\right] + \Gamma_w\left(\sinh^{-1}\Gamma_w\right)^3 - 3\sqrt{1+\Gamma_w^2}\left(\sinh^{-1}\Gamma_w\right)^2 + 6\left[\Gamma_w\sinh^{-1}\Gamma_w - \sqrt{1+\Gamma_w^2}+1\right]\right\}\right]$	Christianson Ryan and Stevens (1956)
ELLIS FLUID	$\dot{s} = (\phi_0 + \phi_1\tau^{\alpha+1})\tau$	$u = \phi_0\left(\frac{i\gamma_w}{4}\right)\left(R^2-x^2\right) + \left(\frac{\phi_1}{\alpha+3}\right)\left(\frac{i\gamma_w}{2}\right)^\alpha\left(R^{\alpha+3} - x^{\alpha+3}\right)$	$Q = \pi R^3\left[\frac{\phi_0}{4}\left(\frac{i\gamma_w R}{2}\right) + \left(\frac{\phi_1}{\alpha+3}\right)\left(\frac{i\gamma_w R}{2}\right)^\alpha\right]$	$v = R\left[\frac{\phi_0}{4}\left(\frac{i\gamma_w R}{2}\right) + \left(\frac{\phi_1}{\alpha+3}\right)\left(\frac{i\gamma_w R}{2}\right)^\alpha\right]$	Skelland (1967)
METER FLUID	$\tau = \mu_\infty\dot{s}$ where $\mu_\infty = \mu_\infty + \frac{\mu_0 - \mu_\infty}{1+\left(\frac{\tau}{\tau_m}\right)^{\alpha+1}}$	$u = \frac{\tau_w R}{2\mu_\infty}\left\{\left[1-\left(\frac{x}{R}\right)^2\right] + \frac{2}{\alpha+1}\left(\frac{\tau_w}{\tau_m}\right)^{\alpha-1}\left[1-\left(\frac{x}{R}\right)^{\alpha+1}\right]\right\} - \left(\frac{\mu_\infty}{\mu_0}\right)\left(\frac{\tau_w}{\tau_m}\right)^{\alpha-1}\left[\left(\frac{2}{\alpha+1}\right)\left(1-x^{*\alpha+1}\right) + \frac{1}{\alpha}\left(\frac{\tau_w}{\tau_m}\right)^{\alpha-1}\left(1-x^{*2\alpha}\right)\right] + O\left[\left(\frac{\mu_\infty}{\mu_0}\right)^2\right]$	$Q = \frac{\pi R^3\tau_w}{4\mu_\infty}\left[1 + \frac{4}{\alpha+3}\left(\frac{\tau_w}{\tau_m}\right)^{\alpha-1}\right] - \left(\frac{\mu_\infty}{\mu_0}\right)\left(\frac{\tau_w}{\tau_m}\right)^{\alpha-1}\left[\frac{4}{\alpha+3} + \frac{2}{\alpha+1}\left(\frac{\tau_w}{\tau_m}\right)^{\alpha+1}\right] + O\left[\left(\frac{\mu_\infty}{\mu_0}\right)^2\right]$	$v = \frac{\tau_w R}{4\mu_0}\left[1 + \frac{4}{\alpha+3}\left(\frac{\tau_w}{\tau_m}\right)^{\alpha-1}\right] + \left(\frac{\mu_\infty}{\mu_0}\right)\left(\frac{\tau_w}{\tau_m}\right)^{\alpha-1}\left[\frac{4}{\alpha+3} + \frac{2}{\alpha+1}\left(\frac{\tau_w}{\tau_m}\right)^{\alpha-1}\right] + O\left[\left(\frac{\mu_\infty}{\mu_0}\right)^2\right]$	Meter and Bird (1964)
REINER'S FLUID	$\dot{s} = \left[\left(\frac{1}{\mu_\infty} - \frac{1}{\mu_0}\right)e^{-\frac{\tau^2}{\tau_m^2}} + \frac{1}{\mu_0}\right]\tau$			$v = Mi + \frac{N'}{i^2}e^{-b'i^2} - \frac{O'}{i^4}$, $M' = \frac{\mu_0\varepsilon^3\gamma_w}{2s^3}$, $N' = \frac{\lambda^2 s^3(\mu_0-\mu_\infty)(4+\nu)}{4\varepsilon^3\gamma_w^2}$, $b' = \frac{\varepsilon^2\gamma_w^2}{s^2}$, $O' = \frac{\lambda^2 s^5(\mu_0-\mu_\infty)}{\varepsilon^5\gamma_w^3}$	Kutilek (1969)
REINER-PHILIPOFF'S FLUID	$\dot{s} = \frac{\tau}{\mu_\infty + \frac{\mu_0-\mu_\infty}{1+\left(\frac{\tau}{\tau_m}\right)^2}}$			$v = \frac{M''}{i}\left[F_1(i) + F_2(i)\log 2F_3(i) - N''\right] + O''i$, $M'' = \frac{(\mu_0-\mu_\infty)s^2\gamma_w^2}{2\varepsilon\lambda^2\mu_0}$, $N'' = \frac{2\varepsilon^2}{s^2}$, $O'' = \frac{\varepsilon^3\gamma_w}{2\mu_\infty s^2}$, $F_1(i) = \frac{2\varepsilon^2}{s^2}\log\frac{\mu_0\gamma_w i\lambda}{s^2}$, $F_2(i) = \frac{2\varepsilon^2}{s^2} + \frac{2\mu_\infty\gamma_w^2}{\mu_0\lambda^2\gamma_w^2}$	Kutilek (1969)

SYMBOLS USED

$A', B', \alpha, \tau_s, \phi_0, \phi_1$ μ_∞ = characteristic Constants

e = Exponential

i = Hyd. grad.

i_0 = Threshold gradient

m = Consistency of Fluid

n = + ive no.

Q = Discharge Rate

x = Variable Co-ordinate

$x^* = \frac{x}{R}$

R = Radius of Tube

s = Specific Surface

$\dot{s} = -\frac{dv}{dx}$

$T_w = B'\tau_w = \omega\Gamma_\omega^3\sinh^{-1}\Gamma_w$

v = Avg vel.

$\omega = A'B'\mu_\infty$

Subscript 'w' refers to capillary wall.

μ = Viscosity

μ_a = Apparent Viscosity $= \frac{\tau}{\dot{s}}$ (Bofn)

μ_0 = Viscosity when $\dot{s}=0$

μ_∞ = Viscosity when $\dot{s}\to\infty$

γ_w = Density

η = Rigidity

τ_m = Shear Stress at $\mu_a = \frac{\mu_0+\mu_\infty}{2}$

τ_y = yield shear stress

τ_w = Shear stress at the wall

ε = porosity

O = of the order

desired, for soils which can be modelled as a bunch of parallel capillary tubes, the tube radius R can be equated to the soil porosity ε and its specific surface S by the relation $R = \frac{2\varepsilon}{S}$ (Kutilek 1969). For the sake of general interest, a typical derivation of a v-i relationship for pseudo-plastic fluid is given here. v-i relationship for other fluids can be derived similarly. Table 5A gives only the final result.

A TYPICAL DERIVATION:

Pseudo Plastic Fluid:

The constitutive eqn. is

$$\tau = m \dot{S}^n = m\left(-\frac{du}{dr}\right)^n$$

Again $\tau = -\frac{r}{2}\frac{dP}{dL}$, $\frac{dP}{dL}$ being the press. drop in a length of dL.

Combining the above two equations, we have

$$-\frac{du}{dr} = \left(\frac{1}{2m}\frac{dP}{dL}\right)^{1/n} r^{1/n}$$

Integrating this equation and substituting u = 0 at r = R, we have

$$u = \left[\left(-\frac{1}{2m}\frac{dP}{dL}\right)^{1/n}\frac{n}{1+n}\right]\left[R^{\frac{1+n}{n}} - r^{\frac{1+n}{n}}\right]$$

Again $Q = 2 \int_0^R u\, r\, dr$

$\therefore \quad Q = \pi \left(-\frac{1}{2m}\frac{dP}{dL}\right)^{1/n} \frac{n}{1+3n} R^{\frac{1+3n}{n}}$

$\therefore$ The average velocity (v) is given by

$$v = \frac{Q}{\pi R^2} = \left(-\frac{1}{2m}\frac{dP}{dL}\right)^{1/n} \left(\frac{n}{1+3n}\right) R^{\frac{1+n}{n}}$$

Putting $\frac{dP}{dL} = \gamma_w \frac{dh}{dL} = -i\gamma_w$, we have

$$v = \left[\left(\frac{\gamma_w}{2m}\right)^{1/n} \frac{n}{1+3n} R^{\frac{1+n}{n}}\right] i^{1/n}$$

which is the reqd. relations.

PART 'D'

EXPERIMENTALLY OBSERVED TYPES OF NONDARCY VELOCITY GRADIENT CURVES

Kutilek (1969) and Olsen (1965) made a survey of experimentally observed velocity-gradient curves by various authors. The net results are summarised in figs. from (29 to 35). Each fig. gives the shape of v-i curves observed along with the names of authors, type of soil and moisture condition. Deviations met by various authors at low gradients are only considered here.

Chapter 4

REVIEW OF EXPERIMENTAL DATA

This review is done under the following heads.

A. Non Darcy flow data for clays and clay minerals

B. Non Darcy flow data for sands and other inert materials

C. Non Darcy results attributed to causes other than the surface phenomena

D. Summary of published data and analysis of deviations from Darcy behaviour.

Results are reported chronologically as far as possible.

A. NON DARCY FLOW DATA FOR CLAYS AND CLAY MINERALS

One of the earliest non Darcy flow rate-gradient data for clay is due to Stearns (1927) as quoted by Swartzendruber (1962b). Stearns provided data on clay content ($<5\mu$) along with the velocity gradient data and Swartzendruber (1962b) fitted equation 1a to the above data

$$q = C_1 i + C_2 \quad \ldots\ldots (1a)$$

where q = Flow rate

i = Hydraulic gradient

C_1 and C_2 are constants.

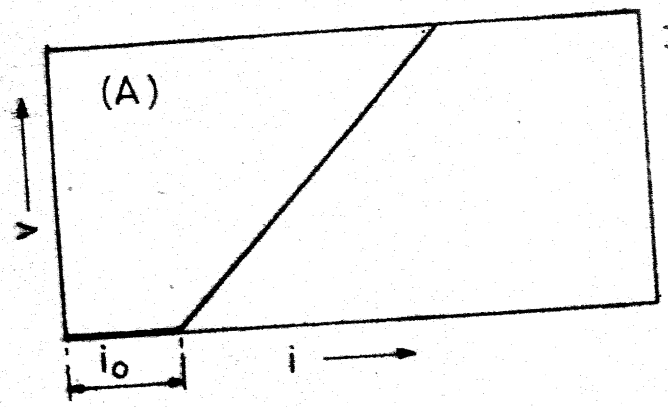

Fig.29 : Summary of Velocity-Gradient Tests

Authors	Type of soil tested	Moisture Condition
1. King (1898)	Sand and Sand-stone	Saturated
2. Izbash (1931)	Gravel	-Do.-
3. Puzyrevskaya (1931)	Clay	-Do.-
4. Miller and Low (1963)	Bentonite Paste	-Do.-
5. Li (1963)	Clay	-Do.-
6. Rawlins and Gardner (1963)	Silty clay Loam	Un-saturated

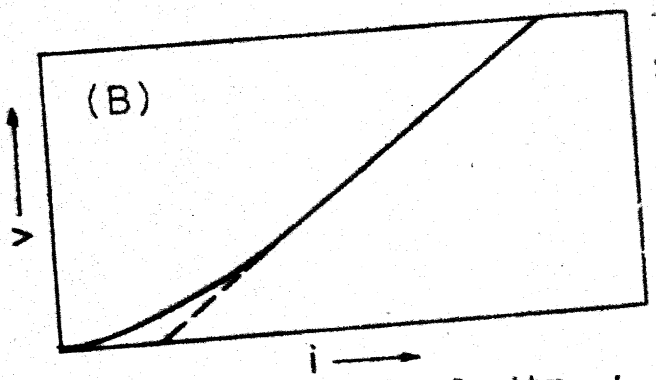

Fig.30: Summary of Velocity Gradient Tests

1. Izbash (1931)	Gravel	Saturated
2. Vom Engelhardt & Tunn (1955)	Clay	-Do.-
3. Lutz & Kemper (1959)	Bentonite, Halloysite & Clay Paste	-Do.-
4. Hansbo (1960)	Clay	-Do.-
5. Slepicka (1961)	Sand-stone	-Do.-
6. Rawlins and Gardner (1963)	Silty Clay Loam	Un-saturated

(Contd.to next page)

Authors	Type of Soil Tested	Moisture Condition
7. Davidson et.el. (1963)	Silty loam	Unsaturated
8. Hades (1964)	Loes, clay	Do
9. Dudgeon(1966)	Sand	Saturated
10. Thames (1966)	Sandy loam and silty loam	Unsaturated
11. Olsen and Swartzendruber (1968)	Mixtures of sand, silica flow and kaolinite	Unsaturated

FIG. 30 (Contd.)

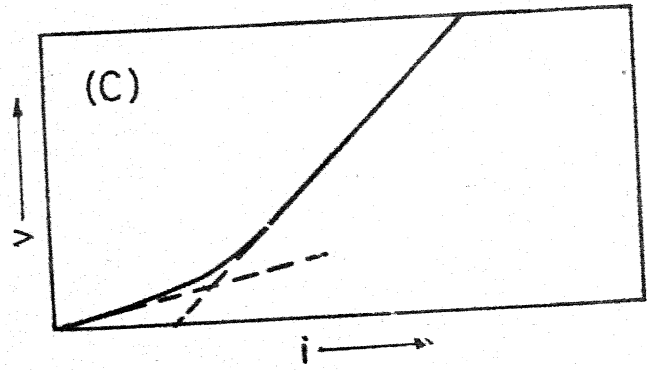

Fig.31: Summary of Velocity Gradient Tests

Authors	Type of soil tested	Moisture condition
1. Slepicka (1961)	Sand-stones	Saturated
2. Miller & Low (1963)	Bentonite Paste	-Do.-
3. Hadas (1964)	Loess, clay	Un-saturated
4. Kutilek (1964 & 1967)	Kaol., Illite & Montmorillonite	Saturated
5. Tchuraev and Yashtchenko (1966)	Sand and Humic Soils	-Do.-
6. Thames (1966)	Sandy loam & Silty loam	Un-saturated

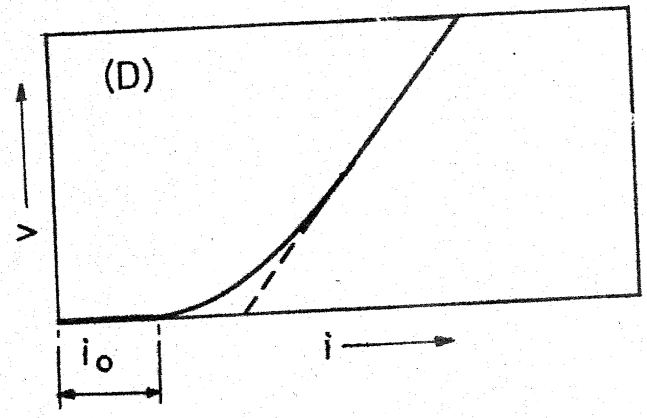

Fig.32: Summary of Velocity Gradient Tests

1. Von Engelhardt & Tunn (1955)	Sand-stone	Saturated
2. Davidson, et.el (1963)	Silty loam	Un-saturated
3. Valdrovitch & Tchuraev (1964)	Peat	Saturated
4. Kutilek (1964 &'67)	Kaol., Illite & Montmorillonite	-Do. -
5. Thames (1966)	Silty loam	Un-saturated
6. Nerpin & Tchudnovskij (1967)	Clays	Saturated
7. Kovacs (1967)	Kaol., Illite & Montmorillonite	-Do.-

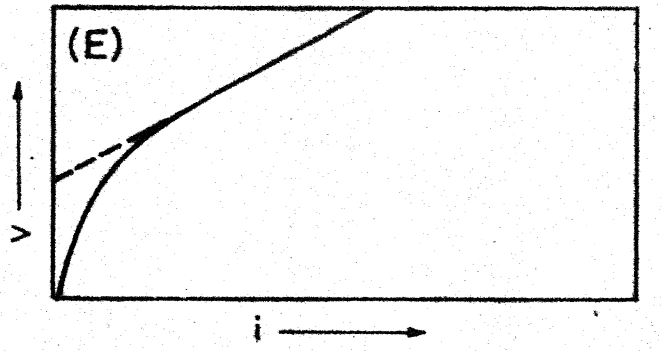

Fig.33: Summary of Velocity Gradient Tests

Authors	Type of soil tested	Moisture Condition
1. Olsen & Swartzendruber (1968)	Mixtures of Sand, silica, flour & Kaol.	Un-saturated
2. Russell (1968)	-Do.- with Bentonite	Saturated

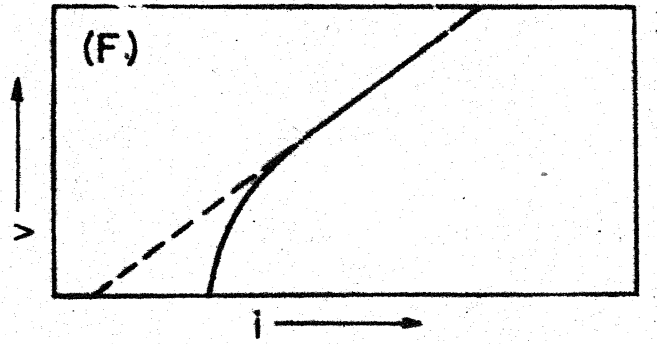

Fig.34: Summary of Velocity Gradient Tests

1. Miller & Low (1963)	Bentonite Paste	Saturated

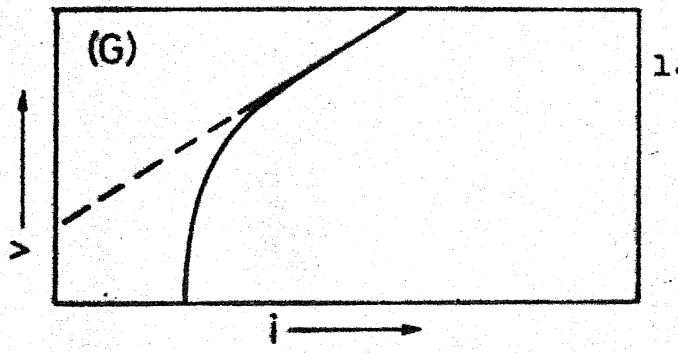

Fig.35: Summary of Velocity Gradient Tests

1. Lutz and Kemper (1959)	Bentonite	Saturated

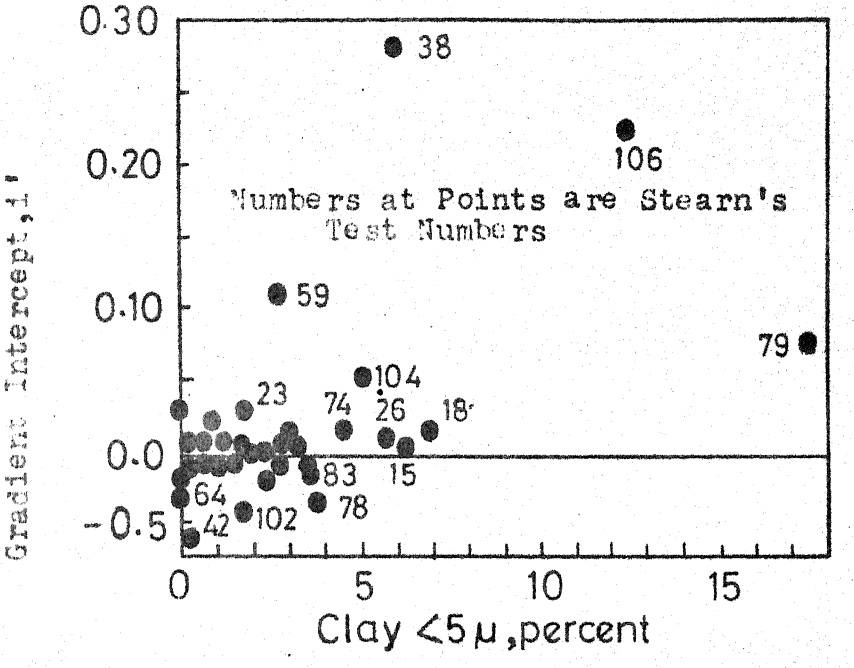

Fig.36: Gradient intercept i' vs. Content of <5μ clay using Stearn's (1927) data (After Swartzendruber, 1962b)

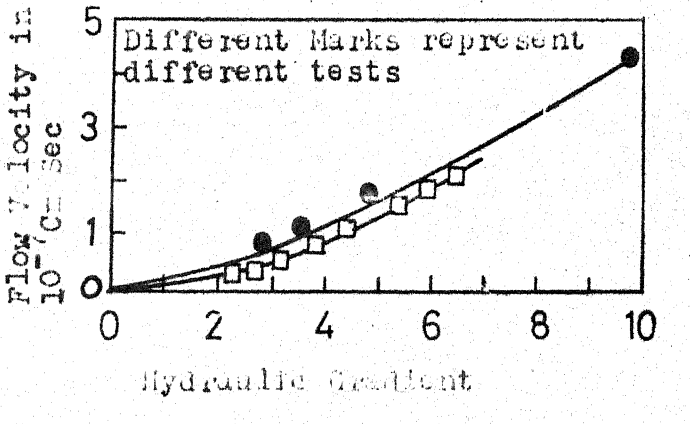

Fig.37: Results of permeability tests on muddy clay from Vasby performed by Silfverberg in 1949. Sample consolidated under a pressure of 0.3 Kg/Cm². Curves drawn by Hansbo, 1960 (After Hansbo, 1960)

by the method of least squares. From equation (1a), the gradient intercept (i') for q = 0 is obtained by the equation

$$i' = \frac{C_2}{C_1} \quad \ldots\ldots \quad (2a)$$

and i' can be considered as a measure of deviations from Darcy's law. Swartzendruber calculated the i' values from Stearns' data and plotted them against percentage of clay ($<5\mu$) by weight as shown in fig. 36.

For the samples of low clay contents, the calculated points are bounded by i' = $\pm$ 0.06 signifying thereby the obeyance of Darcy's law within reasonable experimental error. The remaining i' values outside the selected error interval of $\pm$ 0.06 are positive, and have clay contents above 4 percent Swartzendruber concludes that fig. 36 gives a strong indication that deviations from Darcy's law are associated with clay content which is a crude measure of surface active material.

Silfverberg (1949) as quoted by Hansbo (1960) conducted some velocity-gradient tests on "muddy clay" at low gradients and his experimental results show a nonlinear relationship. However, no conclusions can be made regarding the existence of threshold gradient as shown in fig. 37.

Lutz and Kemper (1959) studied the effect of water film (bound) on the intrinsic permeability of different clay

layer systems. The materials tested were Ma, Ca and H saturated Bentonite, Halloysite, Woyming Bentonite and Bladen clay. The percolating solutions used were; for Na-clays, NaCl; for K clays, KCl_3; for Ca clays, $CaCl_2$ and for H clays, HCl. The normalities of the solutions were varied. The experimental results are shown in Tables 6, 6A and 7. The experimental results indicate the increase in intrinsic permeability with increasing pressure which is completely out of accord with Darcy's law. This was particularly true for Na-clays, in which the diffuse layer of cations and the water structure extended to a distance greater than the radius of the pores between particles; this was attributed to a breakdown of the water structure. In Ca-clays with a restricted diffuse layer and water structure, increasing the pressure head particularly had no effect on permeability.

From experimental investigation on Sweedish clays, Hansbo (1960) confirmed the nonlinearity in the velocity gradient relationship at low gradients. However, no threshold gradient was found and this nonlinearity was attributed to the interaction between skeleten grains and pore water. The results are shown in Figs. 38, 39 and 40.

Karadi and Nagy (1961) hypothesised that the lower validity limit of Darcy law and the v-i relationship in the low gradient zone is controlled by rheological properties of bounded water sarrounding the soil particles. They further

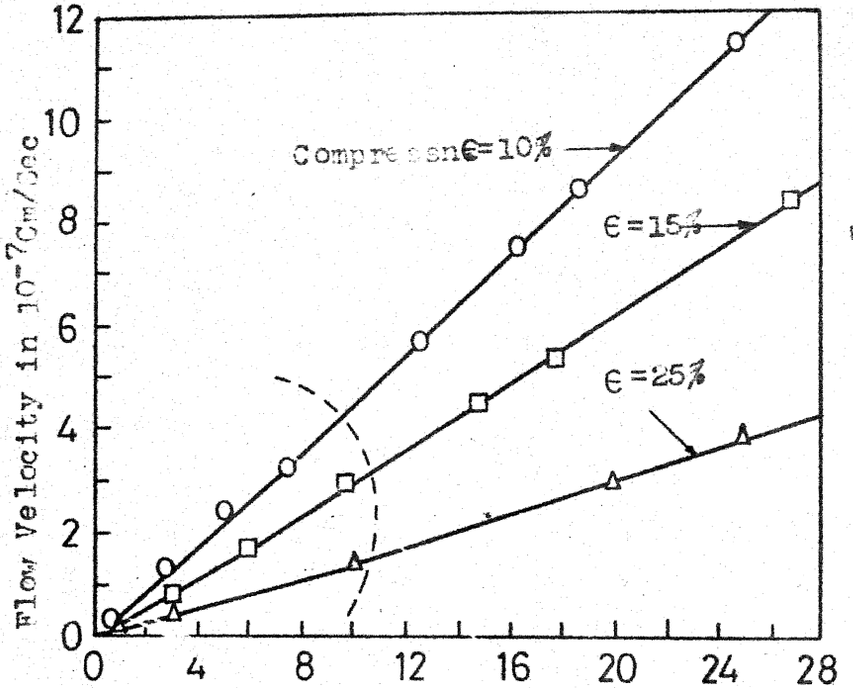

Fig.38: Results of Permeability Tests on Sweedish clay,5 M below G.L.

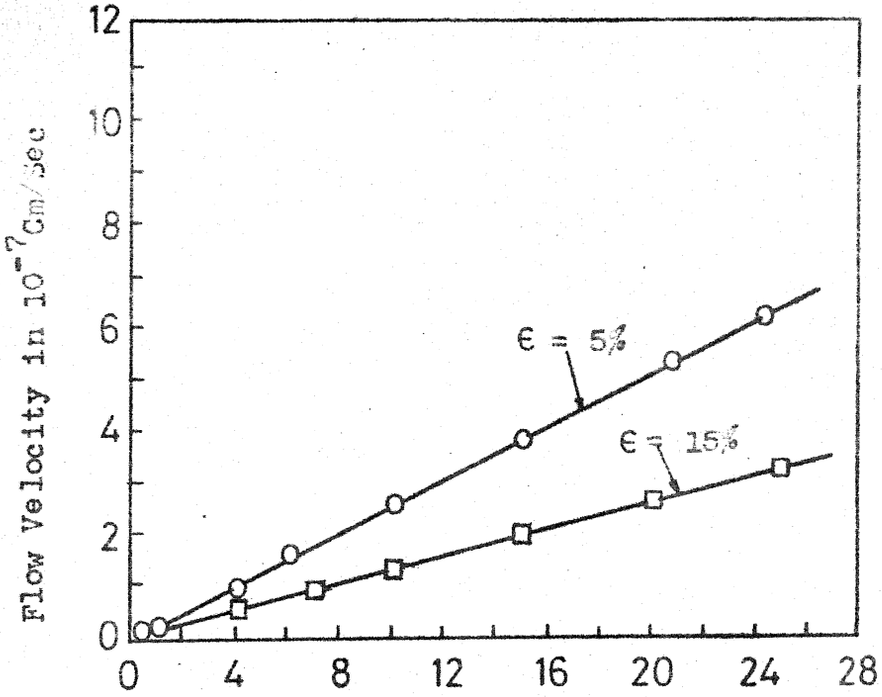

Fig.39: Permeability Test Results on Swedish clay,2 M below G.L.

AFTER HANSBO (1960)

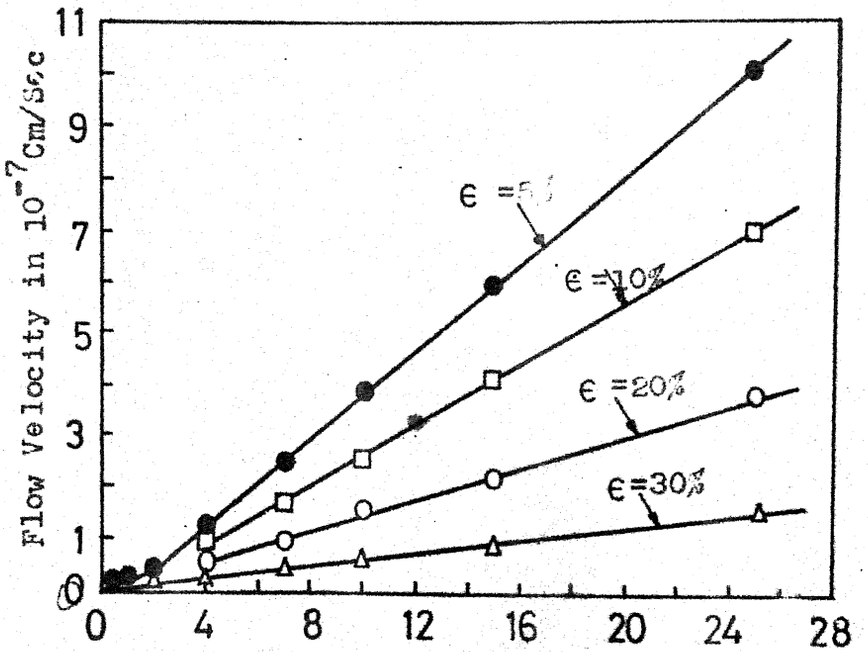

Fig.40: Permeability Test results on Swedish clay,6 M below G.L.

TABLE 6 & 6A

(After Lutz and Kemper 1959)

Effects of pressure, adsorbed cations and electrolyte concentration on the intrinsic permeability of clays.

System	P cms of Hg	Percolating Solutions: Water $\frac{\Delta Q}{\Delta t}x10^{-3}$ cc/sec	Water $K'=\frac{\Delta Q/t}{\Delta p}$ $^2(x10^{-5})$	Salt or Acid* $\frac{\Delta Q}{\Delta t}x10^{-3}$ cc/sec	Salt or Acid* $K'=\frac{\Delta Q/t}{\Delta p}$ $^2(x10^{-5})$	Salt or Acid* $\frac{\Delta Q}{\Delta t}x10^{-3}$ cc/sec	Salt or Acid* $K'=\frac{\Delta Q/t}{\Delta p}$ $^2(x10^{-5})$
					(0.005N)		(0.5N)
Na-Sat. Utah bentonite	10	0.037	3.18	0.092	7.81	0.41	35.30
	20	0.089	3.82	0.230	9.90	0.90	38.78
	30	0.165	4.76	0.395	11.30	1.43	41.00
	40	0.241	5.18	0.610	13.10	1.99	42.70
	50	0.335	5.75	0.850	14.63	2.60	44.80
	60	0.460	6.60	1.140	16.36	3.27	46.90
	70	0.610	7.50	1.470	18.05	3.95	48.50
					(0.005N)		(0.5N)
Ca-Sat. Utah bentonite	10	0.66	87.0	1.32	166.0	2.50	329
	20	1.32	87.0	2.45	153.8	4.50	296
	30	1.90	83.3	3.58	150.0	6.50	286
	40	2.50	82.0	4.65	146.3	8.50	280
	50	3.12	82.0	5.65	141.7	10.5	276
	60	3.67	80.5	6.63	138.6	12.3	270
	70	4.33	87.5	7.55	135.4	14.0	264
					(0.005N)		
H-Sat. Utah bentonite	10	0.72	92.2	0.82	100.8		
	20	1.44	92.2	1.67	102.2		
	30	2.16	92.2	2.41	98.6		
	40	2.93	93.8	3.22	98.8		
	50	3.72	95.2	4.05	99.3		
	60	4.57	97.5	4.93	101.0		
	70	5.40	98.6	5.84	102.0		
					(0.005N)		(0.5N)
Na-Sat. halloy site	10	0.68	83.5	0.90	113.0	2.45	322.2
	20	1.45	89.0	2.0	125.6	5.0	329.0
	30	2.25	92.0	3.10	129.7	7.45	326.7
	40	3.14	96.5	4.20	131.5	10.10	332.5
	50	4.05	99.5	5.28	132.6	12.95	340.0
	60	5.05	103.3	6.32	132.2	15.79	346.0
	70	6.05	106.1	7.50	134.6	19.10	359.0

Continued...

Table 6 & 6A continued.

					(0.005N)		
	10	1.40	168.7	1.54	193.4		
	20	2.85	171.7	3.10	194.5		
Ca-Sat.	30	4.30	172.7	4.64	194.0		
halloy-	40	5.75	173.3	6.25	196.3		
site	50	7.20	173.6	7.80	196.0		
	60	8.65	173.7	9.30	194.7		
	70	10.10	174.0	10.90	195.7		
					(0.005N)		(0.05N)
	10	0.60	86.6	0.78	98.0	1.97	125.0
	20	1.44	90.4	1.58	99.2	1.96	126.3
H-sat.	30	2.24	93.7	2.34	98.0	2.94	126.3
halloy-	40	3.04	94.1	3.07	95.1	3.90	125.8
site	50	3.75	94.4	3.92	98.4	4.88	126.0
	60	4.55	95.4	4.73	99.0	5.86	126.0
	70	5.42	97.1	5.64	101.0	6.84	126.0

TABLE 6A

SYSTEM	P cms Hg	Percolating solution: Water $\frac{\Delta Q}{\Delta t}\times10^{-5}$ cc/sec	Water $K'=\frac{\Delta Q/t}{\Delta p}\times(10^{-5})^2$	Salt or Acid* $\frac{\Delta Q}{\Delta t}\times10^{-3}$ cc/sec	Salt or Acid* $K'=\frac{\Delta Q/t}{\Delta p}\times(10^{-5})^2$	Salt or Acid* $\frac{\Delta Q}{\Delta t}\times10^{-5}$ cc/sec	Salt or Acid* $K'=\frac{\Delta Q/t}{\Delta p}\times(10^{-5})^2$
					(0.005N)		(0.5N)
	10	0.56	0.69	1.13	1.39	4.2	5.90
	20	1.26	0.77	2.48	1.52	9.6	6.75
Na-Sat.	30	2.09	0.85	3.90	1.60	15.6	7.32
Bladen	40	3.01	0.93	5.35	1.64	21.3	7.50
clay	50	4.13	1.01	6.90	1.69	27.2	7.66
	60	5.35	1.09	8.50	1.74	33.7	7.90
	70	6.60	1.16	9.90	1.74	39.7	7.97
					(0.005N)		(0.05N)
	10	10.1	13.03	10.4	12.76	17.7	22.21
	20	20.0	12.96	20.8	12.76	35.6	22.35
Ca-Sat	30	29.8	12.80	31.2	12.76	53.5	22.40
Bladen	40	39.7	12.63	41.7	12.78	71.5	22.45
clay	50	48.9	12.60	52.0	12.76	89.0	22.37
	60	58.1	12.50	62.3	12.76	106.2	22.25
	70	66.9	12.30	72.6	12.73	123.8	22.20
					(0.005N)		(0.05N)
	10	9.0	10.60	11.5	13.88	12.2	14.97
	20	18.0	10.60	21.8	13.14	23.4	14.38
H-Sat.	30	26.8	10.51	31.2	12.53	33.5	13.62
Bladen	40	35.5	10.45	40.5	12.20	44.4	13.65
clay	50	44.0	10.27	49.6	11.96	53.4	13.13
	60	52.4	10.27	59.0	11.87	63.6	13.03
	70	60.5	10.17	68.5	11.79	73.6	12.81
					(0.005N)		
	10	0.27	0.31	0.34	0.40		
	20	0.51	0.31	0.67	0.39		
Ca-Sat.	30	0.76	0.31	1.01	0.40		
Wyoming	40	1.05	0.32	1.34	0.40		
bento-	50	1.32	0.32	1.69	0.40		
nite	60	1.60	0.32	2.08	0.41		
	70	1.89	0.33	2.53	0.43		
					(0.005N)		(0.05N)
	10	0.33	0.41	1.15	1.45	14.7	18.97
	20	0.72	0.44	2.35	1.47	32.7	21.10
H-Sat.	30	1.16	0.47	3.65	1.53	53.6	23.67
Wyoming	40	1.73	0.53	5.10	1.60	74.5	24.00
bento-	50	2.40	0.59	6.80	1.71	97.5	25.10
nite	60	3.25	0.67	8.55	1.79	123.0	26.43
	70	4.21	0.74	10.54	1.89	147.0	27.07

*The percolating solutions used were; for Na clays, NaCl; for K clays; KCl; for Ca clays, $CaCl_2$; for H clays, HCl. The normality used is given at the top each section.

TABLE 7

(After Lutz and Kemper (1959))

Summary of the Permeability averages given in table 6 and 6A

SYSTEM	Average permeabilities for percolating solutions and adsorbed cations indicated*										
	Water			0.005N Salt or Acid			0.05N Salt or Acid			0.5N Salt	
	Na	Ca	H	Na	Ca	H	Na	Ca	H	Na	Ca
Woyming Bentonite	-	0.32	0.55	-	0.40	1.63	-	-	23.79	-	-
Bladen Clay	0.93	12.68	10.42	1.62	12.76	12.48	7.29	22.32	13.66	336.5	
Utah Bentonite	5.26	83.53	94.53	13.02	147.40	100.48	-	-	-	42.57	285.9
Halloysite	95.70	172.53	93.10	128.47	194.90	98.39	-	-	125.91	336.50	-

*All values in ^{2} to be multiplied by 10^{-5}. See footnote, table 3, for percolating solutions used.

T A B U L K A 11

Pozorovane a pocitane hodnoty rychlosti filtracniho proudeni vody v pri hydraulickem spadu I

(After Kutilek 1967)

mereno		H kaolinit 20°c pocitano		mereno		H kaolinit 30°c pocitano	
v	I	v	I	v	I	v	I
cm.h-1		cm.h-1		cm.h-1		cm.h-1	
0.06	6	0,46	52	0.08	6	0.60	50
0.23	26	1,07	101	0.29	26	1.26	98
0.56	60	1.70	150	0.70	60	2.08	148
0.94	94	2.46	200	1.18	94	3.90	233
1.41	128	4.28	300	1.83	128	5.10	300
2.35	196	8.89	505	2.90	196	10.27	500
3.37	264			4.35	264		
4.85	332			5.79	332		
6.33	400			7.52	400		
7.86	468			9.31	468		
9.35	536			11.38	536		
		Na kaolinit 20°c				Na kaolinit 30°c	
0.07	26	0.12	51	0.09	28	0.14	50
0.14	60	0.26	99	0.24	60	0.36	100
0.27	94	0.48	151	0.35	94	0.61	150
0.40	128	0.73	201	0.58	128	0.94	200
0.63	196	1.39	300	0.77	196	1.76	300
1.10	264	3.44	502	1.31	264	4.21	500
1.62	332			1.99	332		
2.27	400			2.78	400		
3.12	468			3.75	468		
3.81	536			4.72	536		

Note: Results of Kutilek (1967) as presented in pages 75 to 76a are given in the original language of the paper(Czech.) as no authentic translator was available.

Pokracovani tabulky 11.

mereno		pocitano		mereno		pocitano	
v	I	v	I	v	I	v	I
Ca kaolinit 20°C				Ca kaolinit 30°c			
0.03	9	0.25	50	0.04	9	0.30	50
0.15	37	0.58	101	0.22	37	0.68	100
0.46	86	0.96	150	0.59	86	1.16	150
0.83	134	1.49	200	1.07	134	1.75	201
1.25	183	2.76	307	1.63	183	3.21	301
2.41	280	5.80	495	2.86	280	7.40	502
3.70	377			4.69	377		
5.53	474			6.87	474		
7.06	571			9.00	571		
H montmorillonit 20°c				H montmorillonit 30°c			
0.0078	107	0.00286	50	0.0091	107	0.003	43
0.0158	162	0.0071	101	0.017	162	0.0068	86
0.0225	220	0.0125	151	0.0248	220	0.0118	130
0.0315	277	0.0185	204	0.0340	277	0.0170	170
0.0387	334	0.0336	304	0.0438	334	0.0311	260
0.0472	390	0.0679	504	0.0550	390	0.0626	430
0.057	447			0.0668	447		
0.0692	515			0.0793	515		
Na montmorillonit 20°c				Na montmorillonit 30°c			
0.00088	160	0.000064	50	0.0023	160	0.00045	49
0.0027	245	0.00033	100	0.0052	245	0.00105	98
0.0061	330	0.00083	152	0.0109	330	0.00196	148
0.0122	415	0.0015	202	0.0175	415	0.0034	195
0.0201	500	0.0047	297	0.0258	500	0.0082	293
0.0283	585	0.0199	499	0.0373	585	0.0262	489
0.0378	670	0.0305	604	0.0503	670	0.0378	586

Pokracovani tabulky 11 (contd...)

mereno		pocitano		mereno		pocitano	
v	I	v	I	v	I	v	I
Ca montmorillonit 20°C				Ca montmorillonite 30°C			
0.0138	128	0.00506	56	0.0166	128	0.0056	50
0.0242	196	0.0117	114	0.0270	196	0.0122	100
0.0364	264	0.0201	174	0.0415	264	0.0199	151
0.0488	332	0.0279	222	0.0525	332	0.0288	201
0.0623	400	0.0488	332	0.0697	400	0.0486	301
0.0775	468	0.101	560	0.0862	468	0.0963	502
0.0960	536			0.108	536		
H illit 20° C				H illit 30° C			
0.0118	107	0.0049	51	0.0146	107	0.0055	51
0.0205	163	0.011	101	0.0228	163	0.0133	104
0.0274	220	0.0178	151	0.032	220	0.0203	150
0.0378	227	0.0262	208	0.0433	277	0.0289	201
0.0516	333	0.043	296	0.0546	333	0.0492	300
0.067	390	0.0935	504	0.0725	390	0.104	508
0.0802	447			0.090	447		
Na illit 20°C				Na illit 30°C			
0.0056	160	0.0021	72	0.0071	160	0.0019	50
0.0094	245	0.00326	103	0.012	245	0.00408	100
0.0148	330	0.00504	154	0.0173	330	0.0067	155
0.0199	415	0.00745	206	0.0239	415	0.00946	203
0.027	500	0.0131	309	0.0316	500	0.0164	310
0.0336	585	0.028	515	0.0398	585	0.0324	502
0.044	670			0.0518	670		
Ca illit 20°C				Ca illit 30°C			
0.00605	116	0.0038	73	0.0081	116	0.0031	51
0.0112	178	0.0057	105	0.0135	178	0.0075	104
0.0154	240	0.0093	157	0.0176	240	0.0114	150
0.021	302	0.0135	209	0.0274	302	0.0163	201
0.0281	363	0.024	314	0.0338	363	0.0277	300
0.036	425	0.0515	323	0.0402	425	0.0585	508
0.0438	487			0.056	487		

TABULKA 12

CALCULATION OF M, M' AND I_o

Vyhodnoceni filtracnich krivek: Pocatecni hydraulicka vodivost

M' hydraulicka vodivost M a I_o

(After Kutilek 1967)

Jilovy mineral	kaolinit			montmorillonit			illit		
Vymenny Kation	H	Na	Ca	H	Na	Ca	H	Na	Ca
				1. serie					
$M.10^{-3}$ cm.h^{-1}	23,7	8.1	14.8	1.60	0,35	4.2	18.2	0.86	13.2
$M'.10^{-3}$ cm.h^{-1}	1,5	0.8	1.5	0.13	0.07	0.12	1.1	0.29	1.5
M/M'	15,8	11.4	9.9	12.3	5	35	16.5	3	8.8
I_o	160	395	113	171	340	295	185	185	230
				2. serie T 20°C					
$M.10^{-3}$ cm.h^{-1}	27.4	15,1	25,3	0,18	0,107	0,26	0.37	0.105	0.19
$M'.10^{-3}$ cm.h^{-1}	8.7	2,1	4.3	0.05	0.002	0.08	0.09	0.025	0.045
M/M'	3.15	7.19	5.88	3.6	53.5	3.25	4.1	4.2	4.2
I_o	200	310	283	130	319	178	310	295	300
				2. serie T 30°C					
$M.10^{-3}$ cm.h^{-1}	31.5	18.0	29.7	0.20	0.130	0.28	0.39	0.12	0.22
$M'.10^{-3}$ cm.h^{-1}	11.0	2.8	5.4	0.06	0.006	0.10	0.105	0.035	0.06
M/M'	2.86	6.43	5.5	3.33	21.65	2.8	3.71	3.43	3.67
I_o	195	300	285	120	300	172	300	295	300
$M_{20}M_{30}$	0.87	0.84	0.85	0.90	0.82	0.93	0.95	0.87	0.86
M'_{20}/M'_{30}	0.79	0.75	0.795	0.83	0.33	0.80	0.86	0.72	0.83
$(M/M'_{20}/M/M'_{30}$	1.10	1.12	1.07	1.08	2.46	1.16	1.10	1.22	1.15
I_{o20}/I_{o30}	1,03	1,03	1,01	1.08	1.06	1.04	1.03	1.00	1.00
M'_{20}/M'_{30} zkmerenych dat	0.79	0.58	0.75	0.85	0.38	0.83	0.81	0.79	0.80

Ist Serie : I increased from 0
2nd serie : I (hydr. gradient) decreased from initial highest value to zero.

state that if the entire flow cross-section is occupied by bonded water, seepage may not start untill an initial gradient is reached. The value of the initial gradient depends on the water content of the soil. After the initiation of movement, the seeping fluid behaves like a fluid whose behaviour is between that of Bingham body and the generalised Newtonian fluid. With increasing water content, the properties resembling those of Bingham body disappear and the movement takes place in a fashion characteristic for the generalised Newtonian fluids. In support of this hypothesis, Karadi and Nagy (1961) conducted some velocity-gradient tests on clay samples of different water content and the results are reproduced in Fig. 41. Experimental results indicate that up to certain water content, seepage does not occur unless the hydraulic gradient exceeds the initial value i_o or i_k. Beyond this value, the relationship between seepage velocity and the hydraulic gradient is described by a curve which joints the Darcy line at a certain limit gradient (i_h).

Initial or threshold gradient is found to increase appreciably with reduction in water content and the summary of the results are shown in Table 8.

Swartzendruber (1962a and b) replotted some of the data of earlier workers e.g. Von Engelhardt and Tunn (1955), Hansbo (1960) and Lutz and Kemper (1959) and fitted them in equations 14 and 15 as shown in Figs. 17, 18, 19 and 21.

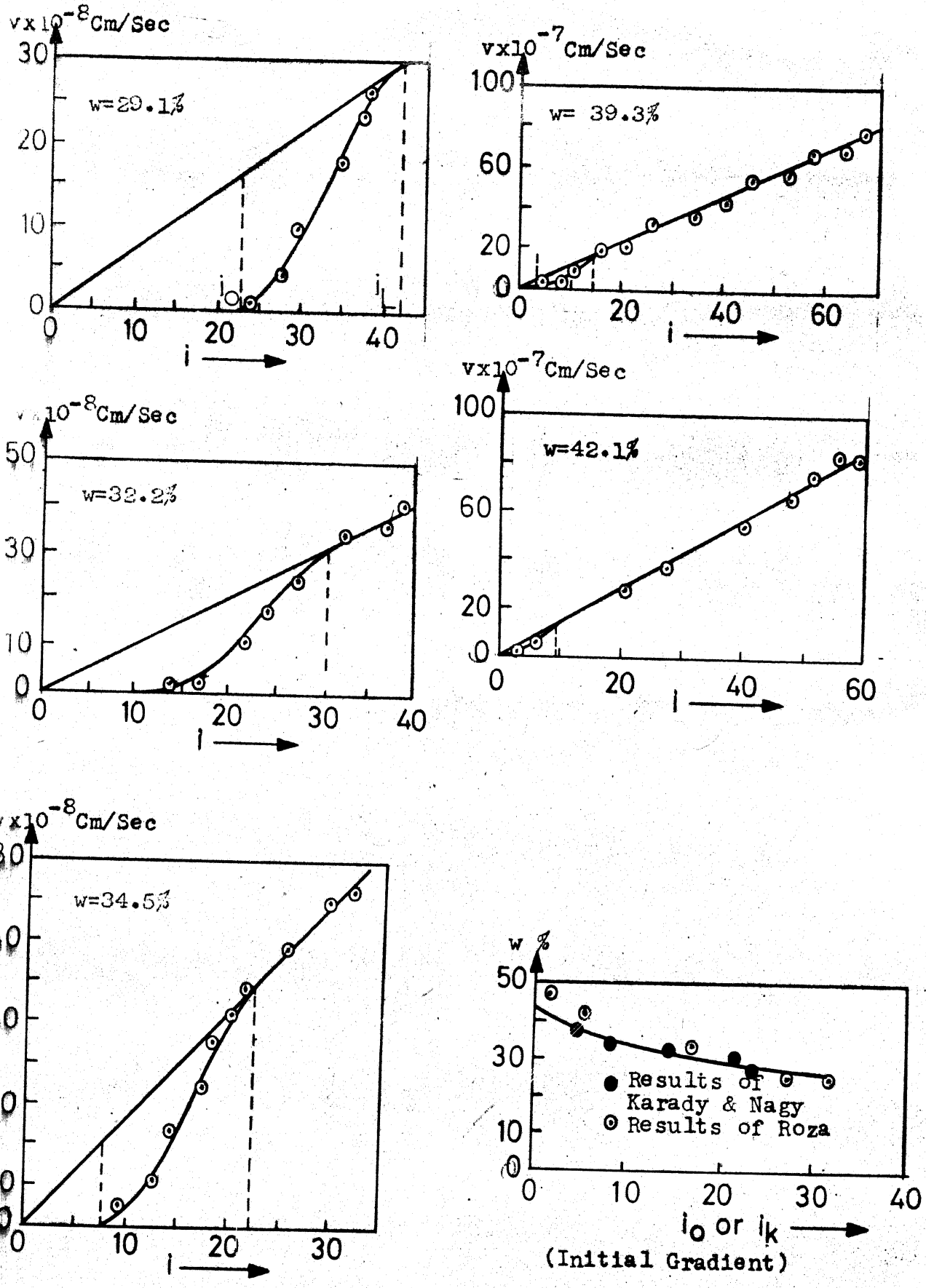

Fig41: Vel.-Grad.-Water Content & Initial Grad.Relationship
(After Karady & Nagy,1961)

Table 8

Summary of Karadi and Nagy's Result (After Karadi and Nagy 1961)

Experiment number	Water content w%	Permeability coefficient (K cm/sec.)	Initial gradient (i_o or i_k)	Limit gradient i_h OR i_o
1	29.1	0.72×10^{-8}	22.8	42
2	32.2	1.03×10^{-8}	12.8	31
3	34.5	5.32×10^{-8}	7.3	22.2
4	39.3	11.20×10^{-8}	3.1	14.8
5	42.1	15.20×10^{-8}	0	8.6

The experimental results of Li (1963) for Houston clay (clay content 72% and initial void ratio of 0.85) as shown in Fig 42 indicate a threshold gradient of around 50 and essentially a linear velocity-gradient curve after that.

Miller and Low (1963) conducted several tests on Na and Lithium clay pastes. Their experimental graphs are reproduced and are shown in Figs. 43 to 46. As seen from these figures, threshold gradient for Na-clay paste and Li-clay paste is established and its magnitude being dependent on clay concentration in the paste. The nonlinearity of the flow rate-gradient relationship is not very conspicous and inconclusive. Miller and Low state that for most materials

exhibiting a yield value or threshold gradient, the flow rate-gradient relationship is initially curvilinear (Powell and Eyring 1944). This curvature is attributed to any one of the following causes.

(1) Reversible re-orientation of particles with the increase in hydraulic gradient

(2) If there is a range of pore sizes, the yield value decreases in successively smaller pores as the hydraulic gradient increases.

and (3) Structural breakdown of water under stress begins near the center of the flow channel, where the water is farthest from the clay surfaces and then progresses towards these surfaces as the gradient increases i.e., effective flow area gradually increases with gradient.

The lack of curvature in the experimental data is explained by Miller and Low as due to (1) the particles being so close together that they could not [illegible] orient along the streamlines or (2) the limited interstitial volume precluded a wide range of yield values for the pore water or (3) there was little variation in the structural rigidity of the water. To clarify the last point, Miller and Low state that the structural rigidity of the water decreases with distance from the particle surfaces. When the water films on these surfaces are thin, there is less distance over which the decrease can occur than

when they are thick. Hence, there is a smaller total variation in structural rigidity of the water in the former case than in the latter. The water films in the concentrated clays were thin relative to those in the less concentrated clays.

Miller and Low (1963) also points out that water structure in clay resists disruption, but once the structure has been disrupted by flow, it does not immediately reform even though the disruptive force is removed.

To clear up the problem of filtration in the direct vicinity of the origin and to check the most suitable equation, Kutilek (1964) conducted model filtration experiments with minerologically homogeneous and homoionic (H, Na and Ca derivatives) clay fractions and the materials used were Kaolinite, Montmorillonite and Illite. Kutilek chose these materials because of the maximum development of the surface phenomena in these materials, the shape of curvature in the velocity-gradient relationship and all the factors influencing filtration can be more exactly determined. Distilled water and the solutions of HCl, NaCl, Na_2SO_4, $CaCl_2$, $Ca(NO_3)_2$ in different concentrations were used as the permeating fluid. The hydraulic gradient ranged from 0 to 500-600. The general nature of the experimental results as obtained by Kutilek (1964) is reproduced in fig. 47. For distilled water, velocity-gradient relation always showed a nonlinearity

at low gradients whereas other solutions with high normalities showed essentially a linear plot. For low normality solutions slight curvature was noted. The experimental results were fitted to equation (16)

$$v = M\left[\frac{1}{B}\log\left(A + e^{Bi}\right) - I_o\right] \quad \ldots\ldots \quad (16)$$

where

$$B = \frac{\log M/M'}{I_o}$$

$$A = (M/M' - 1)$$

The parameters M, M' and I_o are calculated from the fitted curves and are shown in Table 5. All the experimental curves were observed to pass through the origin and hence no threshold gradient was in sight.

Kutilek (1966) further conducted velocity-gradient tests with these clay minerals which were saturated with quinolinium, pyridinium and calcium. The experimental results are once again fitted into eqn. (16). The nonlinearity is explained in terms of non Newtonian behaviour of soil water. (Tables 9 and 10 and Fig 48).

Kutilek (1967) investigated the effect of temperature on the velocity-gradient relationship using eqn. (16). Complete set of this data is presented in Tables 11 and 12. A partial plot of these data is made and is shown in Fig 49.

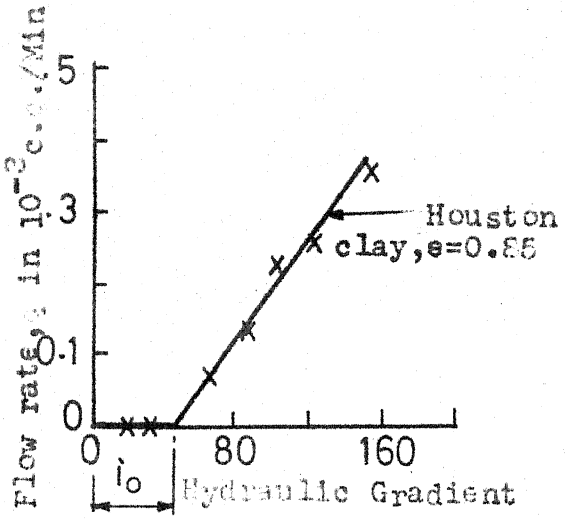

Fig.42: Experimental q vs. i relation (After Li, 1963)

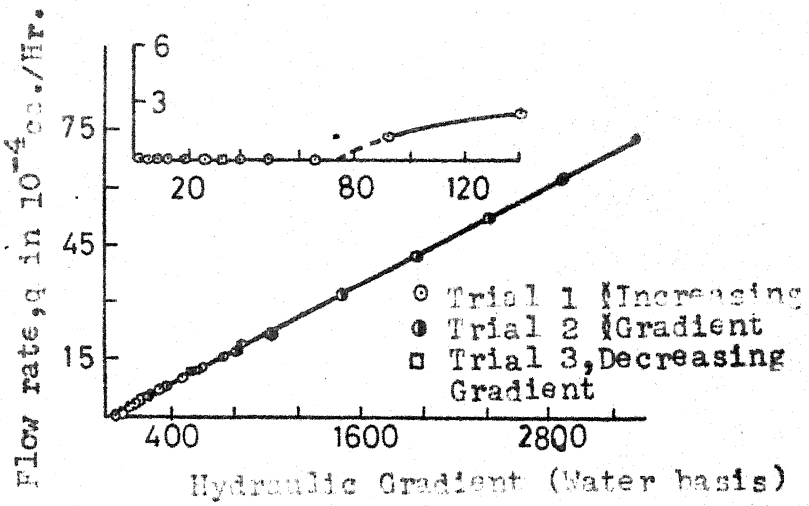

Fig.43: q vs. i relation for 55.5% Na-clay paste (After Miller & Low, 1963)

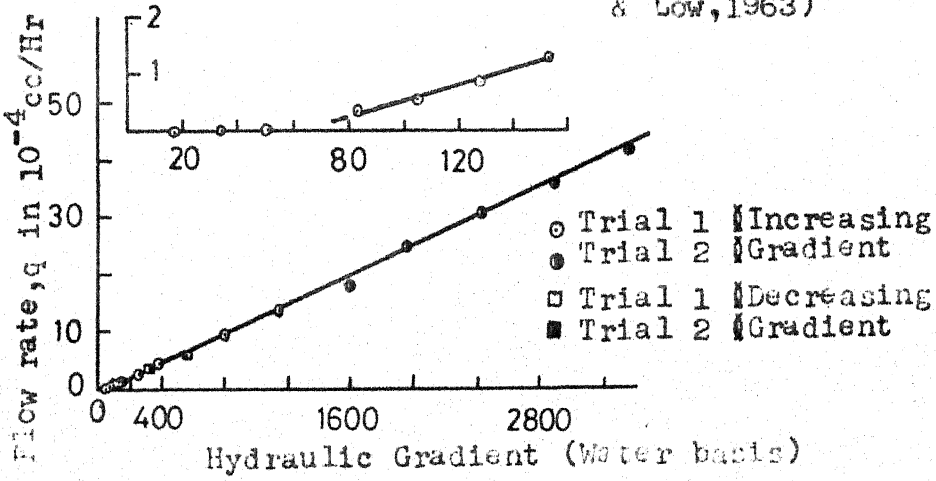

Fig.44: q vs. i relation for 45.9% Li-clay paste (After Miller & Low, 1963)

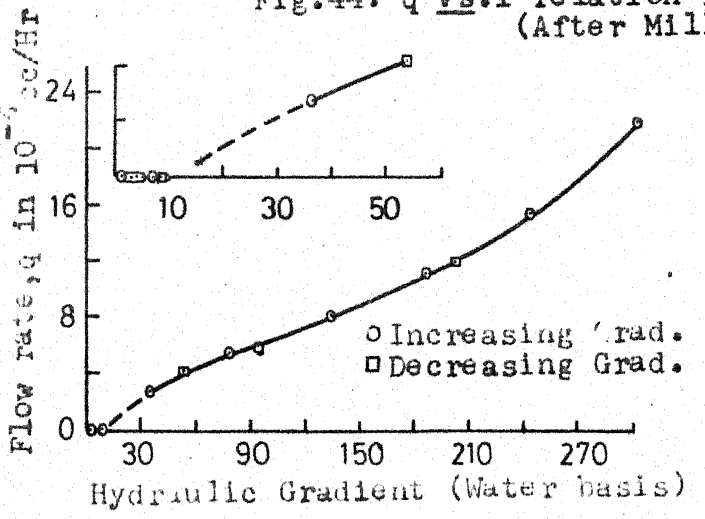

Fig.45: q vs. i relation for 32.2% Na-clay paste (After Miller & Low, 1963)

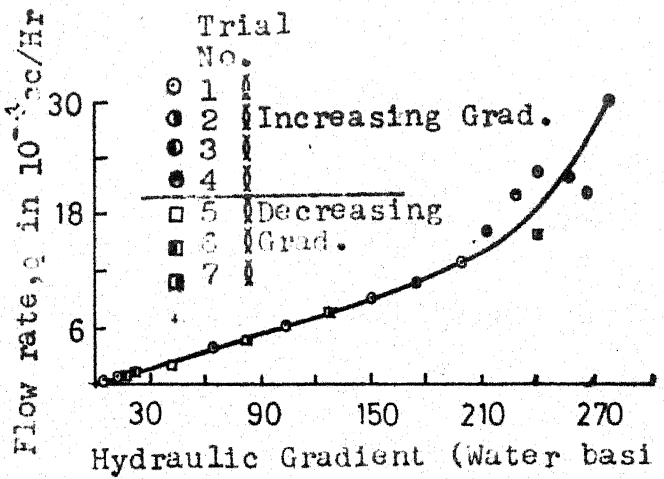

Fig.46: q vs. i relation for 27 Li-clay paste (After Miller & Low, 1963)

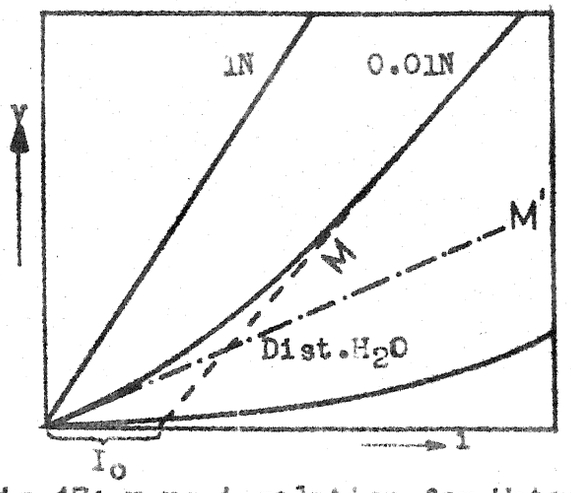

Fig.47: v vs.i relation for Water & solns.of diff. concentrations. M/M' and I_o are the characteristics of non-Newtonian behaviour of soil water (After Kutilek,1964)

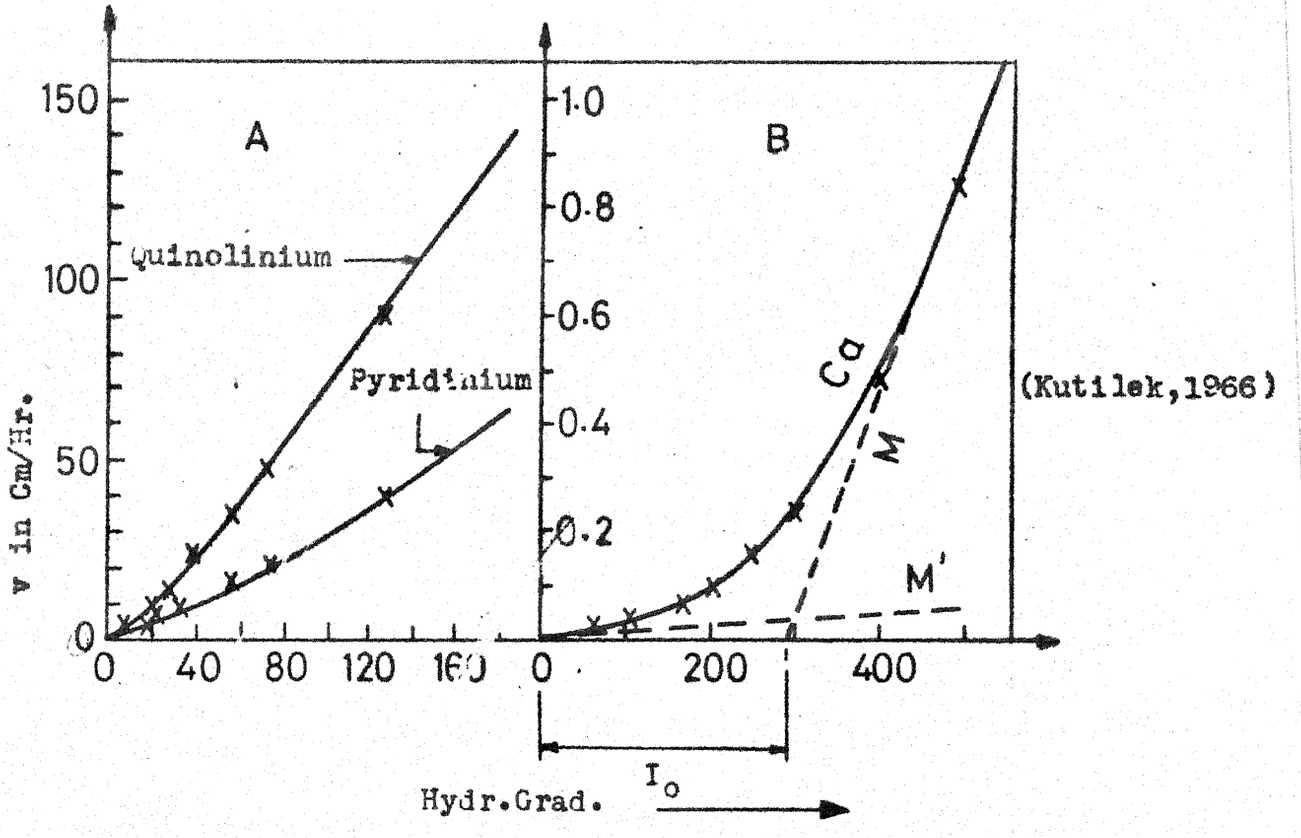

Fig.48: Fit of Experimental data using equation 16
A : Quinolinium-Montmorillonite, Pyridinium-Montmorillonite and Dist.water
B : Ca-Montmorillonite and Dist.water

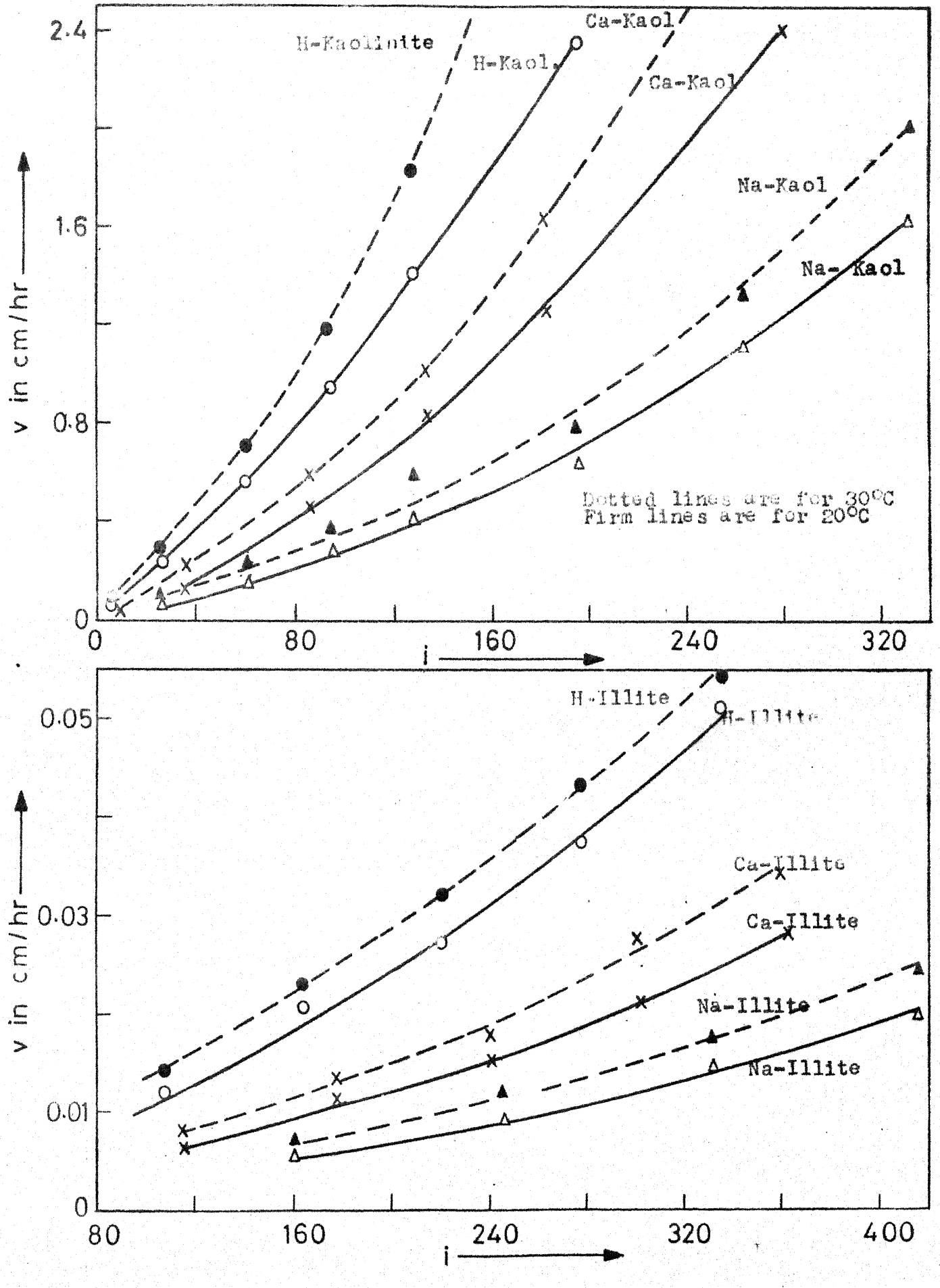

Fig 49 : Effect of Temp. on v-i relation (After Kutilek,1969)

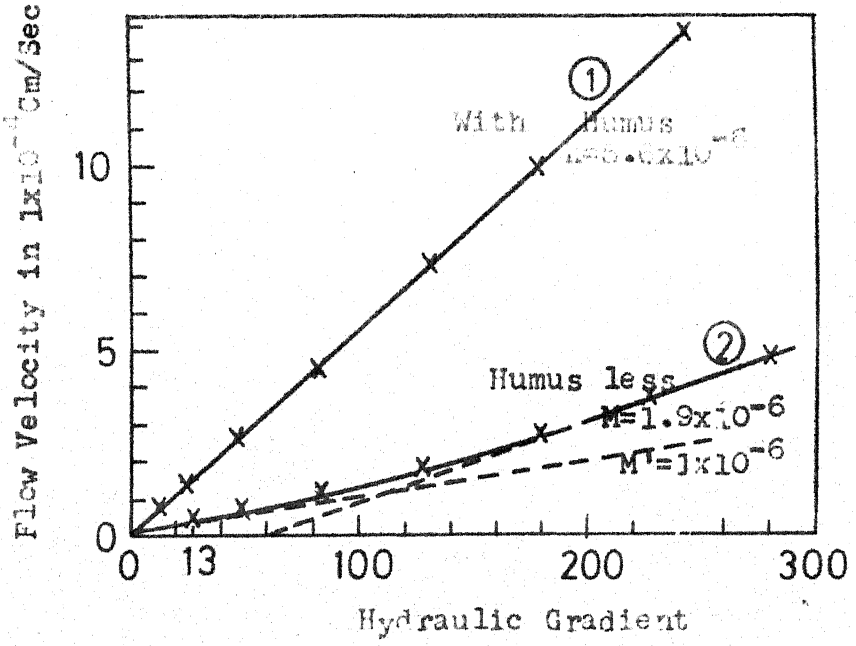

Fig.50 : Flow Velocity v. Hydraulic Gradient of original [illegible] and humusless ranszim (A-horizon)

(After Kutilek, 1971)

The data shows that at all temperatures; the velocity-gradient response is nonlinear for allmost all the samples but the more conspicous ones are with Na and Ca base. For all temperatures, the existence of threshold gradient appears to be certain for Montmorillonite and Illite but for kaolinite, it is difficult to draw any conclusion.

Kondon (1967) concluded that initial or threshold gradient increases with decreasing porosity, with increasing specific surface and with decreasing hydraulic radius ($= \frac{\text{porosity}}{\text{sp. surface}}$) and he explained these results on the basis of rheological properties of water in thin slits and narrow capillaries.

Churayev and Gorokhov (1970) demonstrated that for unsaturated soils also water conductivity must be a function of not only moisture content but also of the pressure gradient (i,e velocity-gradient relationship is nonlinear). They explained this effect as due to visco-elastic properties of adsorbed water that separates the capillary wedges.

Kutilek (1971) studied the effect of humus upon velocity-gradient relationship. He found he humusless Rendzina (loamy clay) showed nonlinearity at low gradients but the existence of threshold gradient was not assured. But Kutilek observed a linear curve for Rendzina with humus. Kutilek explained the results in terms of non Newtonian water

TABLE 9

Values of flow velocity V measured at hyd. grad. I .

(After Kutilek 1966)

Ca		Quinolinium		Pyridinium	
I	v	I	v	I	v
		cm/hour			
		Kaolinite			
		8	0.38	8	0.36
23	0.04	18	0.92	18	0.90
53	0.11	23	1.49	23	1.50
131	0.56	28	1.57	28	1.97
210	0.65	56	3.63	34	2.33
310	2.72	73	5.02	73	5.55
420	4.55	95	6.92	129	9.20
495	5.70	129	10.18	184	14.20
		180	15.25	240	18.0
				350	26.6

Montmorillonite

63	0.018	8	2.8	8	1.5
111	0.032	18	9.2	18	3.6
170	0.058	28	13.2	23	5.8
506	0.090	40	25.0	28	6.9
257	0.152	56	36.3	33	8.4
302	0.234	73	47.5	56	15.4
400	0.485	129	90	73	21.6
485	0.84			128	38.8
592	1.28				

Illite

60	0.122	8	0.41
136	0.364	18	1.00
201	0.687	23	1.38
240	0.98	28	1.62
316	1.33	40	2.44
360	1.95	56	3.35
		73	4.35
		95	6.40
		139	9.52

TABLE 10

Flow parameters M (hydraulic conductance), M' (initial hydraulic conductance), and I_o (intercept of M on I axis)

(After Kutilek 1966)

Slay Mineral Cation	I_o	M	M'	M/M'
		in cm/hour x 10^{-3}		
Kaolinite				
Ca	113	14.8	1.5	9.9
Quinolinium	32	103	50	2.06
Pyridinium	4	79	45	1.76
Montmorillonite				
Ca	295	4.2	0.12	35
Quinolinium	14	810	300	2.7
Pyridinium	7	320	160	2.0
Illite				
Ca	230	13.2	1.5	8.8
Quinolinium	32	90	50	1.8

in the humusless soil and he claims that humus prevents water from gaining such a type of structure which makes the soil water to behave as non Newtonian. The experimental results are reproduced in Fig. 50.

B. EXPERIMENTAL NON DARCY DATA FOR SAND AND OTHER INERT MATERIALS

Compared to the appreciable amount of data available for non Darcy velocity-gradient relationships (at low gradients) for clays and clay minerals, there is only limited data in the literature for sands and other inert materials.

One of the earliest thorough investigations with wide range of materials including sand is due to Slepicka (1961). He conducted velocity gradient tests over a large range of gradients and the general relationship obtained is shown in Fig. 13 and the fitted equation is of the form

$$v = K_f i^f \quad \ldots . \quad (13a)$$

Slepicka found the value of f as 1.3 to 2.3 in the prelinear regime depending on the value of K in the Darcian (i.e. linear) regime. The experimental variation of f in the prelinear regime and i_c (critical gradient as explained in fig. 13) with Darcian K is reproduced in Figs. 14 and 15.

Dudgeon (1966) conducted tests on (a) River Gravel, (b) Crushed Blue Metal and (c) Glass Marbles for various grain sizes

and porosities. In the low gradient zone, his fitted equation is of the form, $v = ki^n$, in which n varies from 1.12 to 1.27 (Figs. 51, 52 and 53).

Miller, Overman and King (1970) observed non linear velocity-gradient relationship for fine and medium pyrex sintered glass frits. Phenol, added to the water destroyed curvilinearity and re-established Darcy flow.

The nonlinearity observed in sand and other inert material by various authors as described above is attributed mainly to the phenomenon of streaming potentials and electrokinetic effect but they are inconclusive.

C. NON DARCY RESULTS ATTRIBUTED TO CAUSES OTHER THAN THE SURFACE PHENOMENA

Olsen (1960) showed the abnormality of flow behaviour in clay by comparing his experimental results with the Kozeny's equation (1927) which is based on Darcy's law. (Figs. 54 through 57). The deviation from Darcy's law, i.e. the parallel tube model is explained by Domain Structure Hypothesis as explained earlier.

Martin (1960) attributed the nonlinear velocity-gradient relationship, as obtained by Von Engelhardt and Tunn (1955) to the clay fabric changes. Olsen (1965) holds the contamination

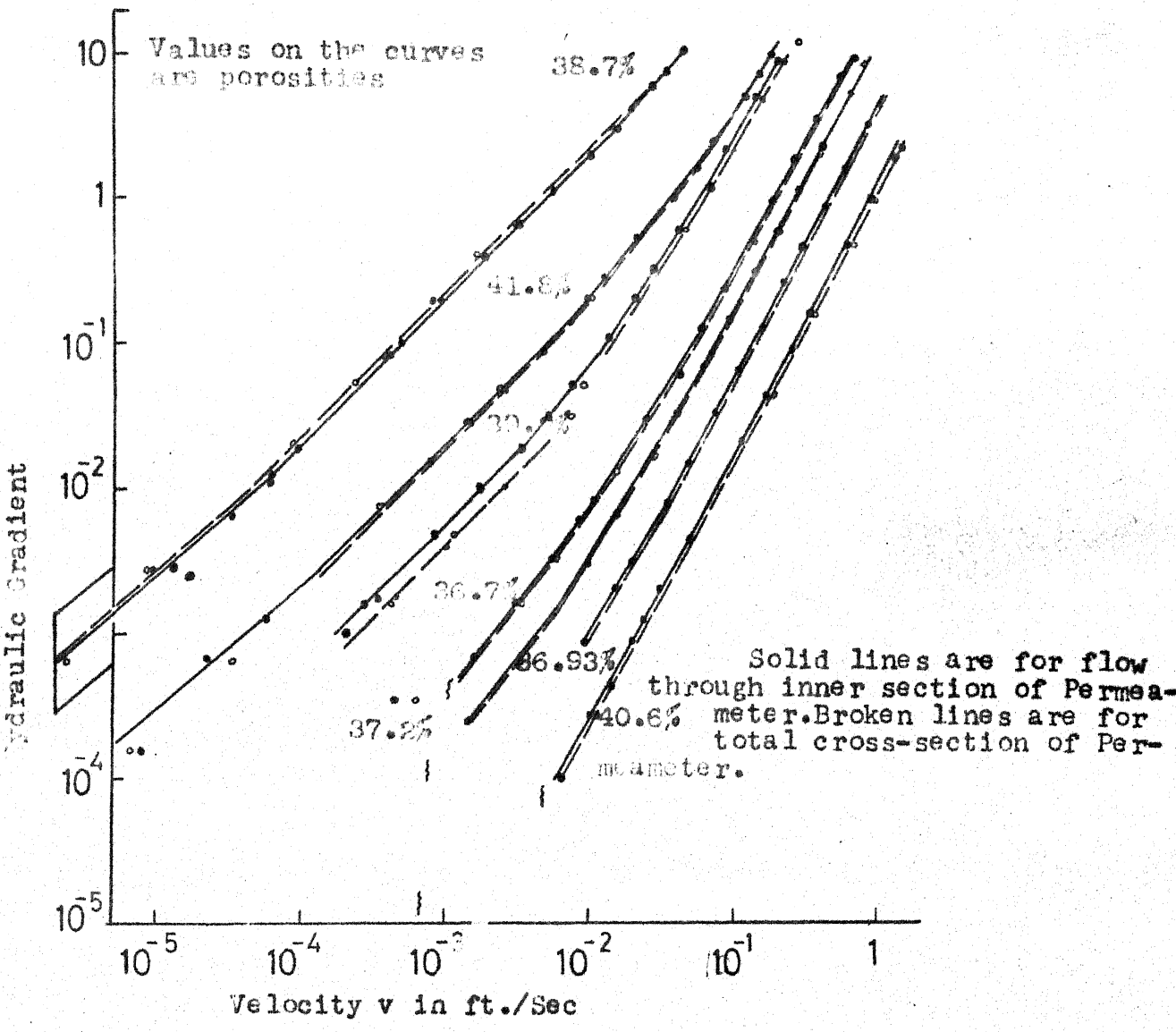

Fig.51: v-i Relation for river gravels
(after Dudgeon,1966)

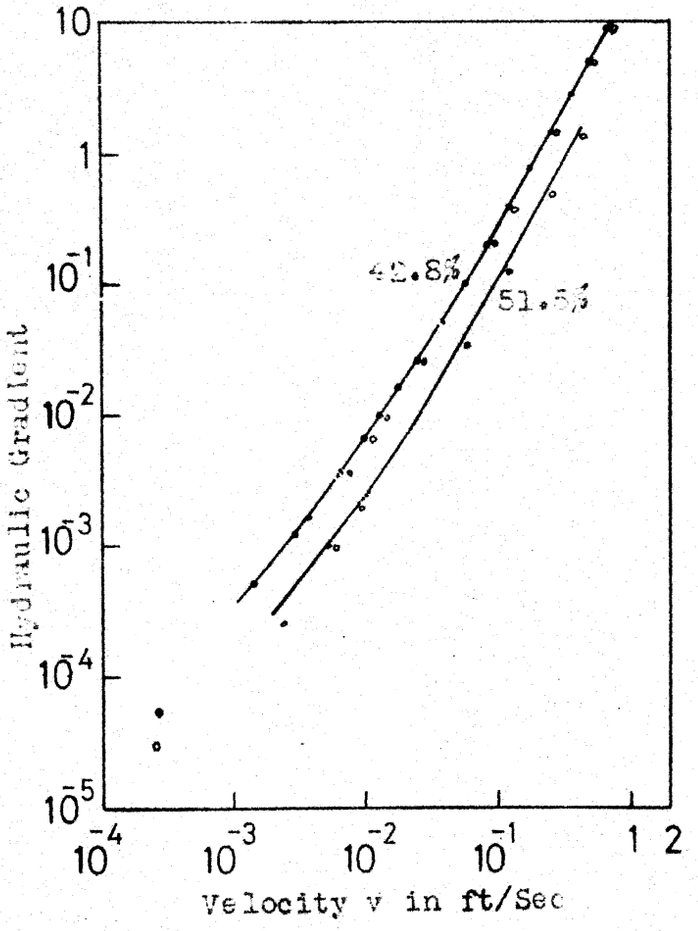

Fig.52: v-i Relation for 3/4 inch blue metal for diff.porosities

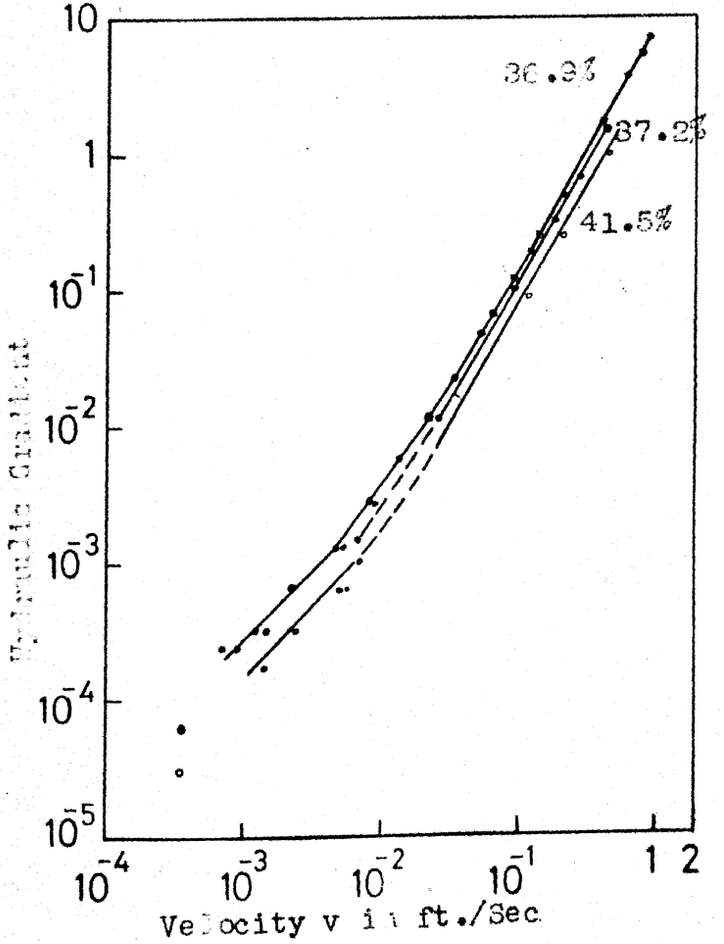

Fig.53: v-i Relation for 16 mm glass marbles for diff.porosities

(After Dudgeon,1966)

of capillary tube as responsible factor for various non Darcy data of different authors.

From the tests on compacted silty clay, Mitchell and Younger (1967) observed a nonlinear velocity-gradient relationship upto certain gradient for both increasing and decreasing gradients with a hysterisis loop as shown in Fig. 58. The nonlinear behaviour is attributed to the particle migration rather than abnormal water properties due to surface phenomenon.

Bondarenko (1968) postulated that the liquids with hydrogen bonding show nonlinear velocity-gradient relationship. He showed (Fig. 59) that liquids with hydrogen bonding e.g. H_2O, C_2H_5OH, CH_2OH and a mixture of CH_3CO, CH_3 and $CHCl_3$ behave like a Bingham liquid characterised by a plastic viscosity and yield stress τ_o of the order of 10^{-2} to 10^{-3} dynes/cm^2 and hence correspondingly these liquids show a threshold gradient before any movement starts and once the motion is initiated, the velocity-gradient relationship is linear. But the liquids with no hydrogen bonding e.g. CCl_4, CH_3COCH_3 and $CHCl_3$ show a purely Darcian behaviour (a straight line passing through the origin).

Childs and Tsimus (1971) contradicted Bondarenko's result and produced experimental results with glass spheres fully obeying Darcy's law and no threshold gradient.

Novak (1972) obtained non linear velocity-gradient relationship for Bentonite and Kaolinite with a hysterisis loop

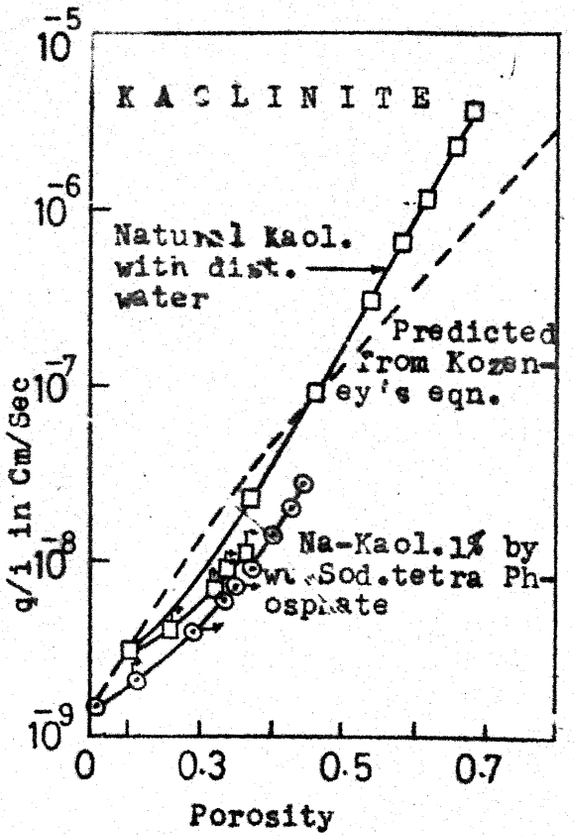

Fig.54: Hydraulic Flow rates vs. Porosity (After Olsen,1960)

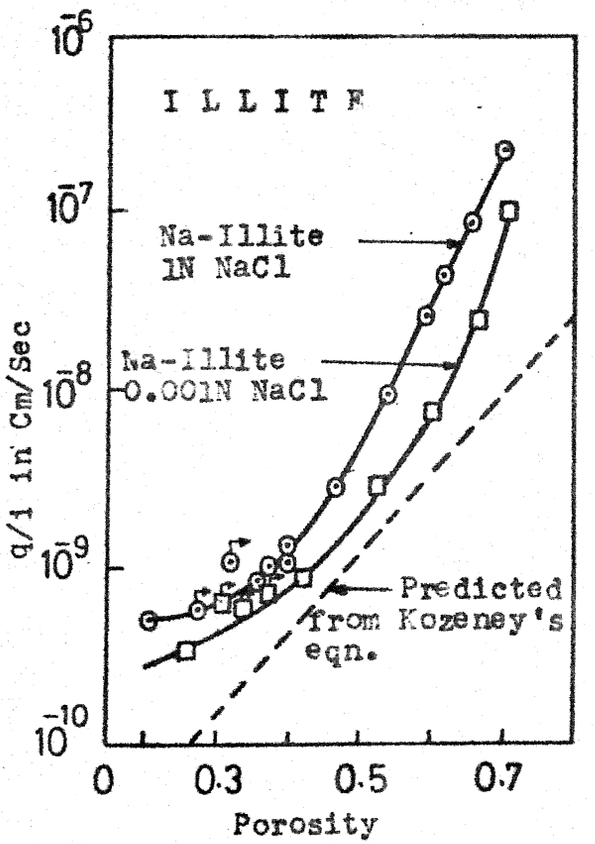

Fig.55: Hydraulic Flow rates vs.Porosity (After Olsen,1960)

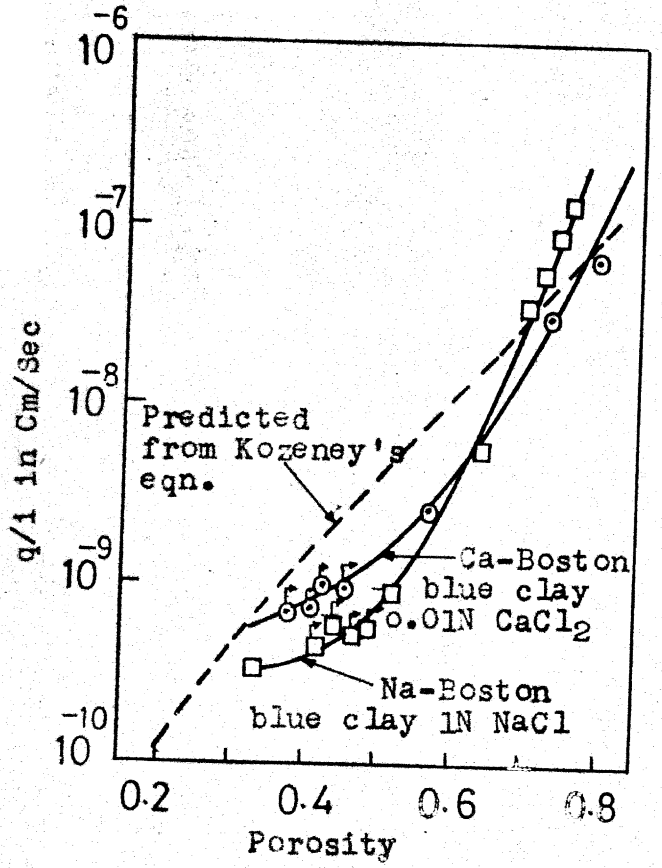

Fig.56: Hydraulic Flow rates vs.Porosity for Boston blue clay (After Olsen,1960)

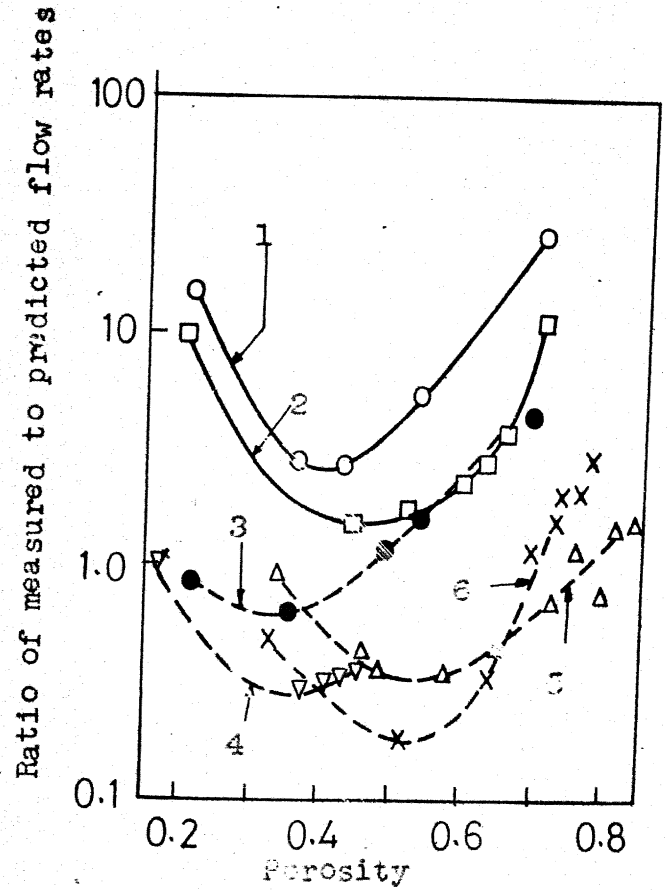

Fig.57: Discrepencies betn. measured and predicted flow rates data from Compression cycle (Olsen,1960)

1.: Na-Illite,1N NaCl

2.: Na-Illite,o.001N NaCl

3.: Nat.Kaol.with Dist.water

4.: Na-Kaol.1% by wei[illegible] Na-tetra phosphat[illegible]

5.: [illegible]-Boston blue clay [illegible] NaCl

6.: Ca-Boston blue cla[illegible],o.01N $CaCl_2$

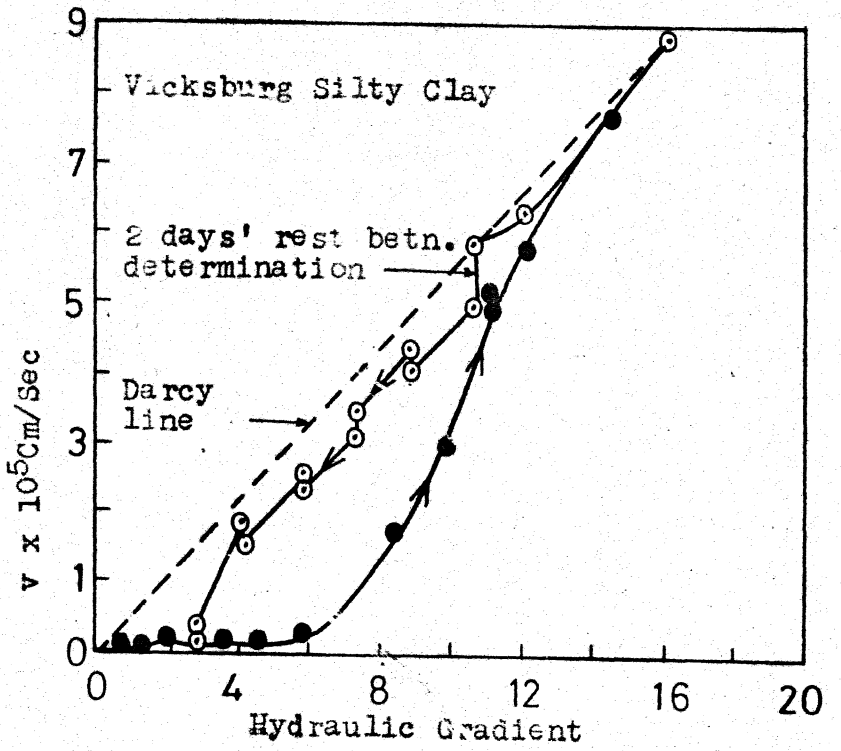

Fig.58: v-i Relationship for compacted silty clay (for successive increasing and decreasing grad.) (After Mitchell & Younger, 1967)

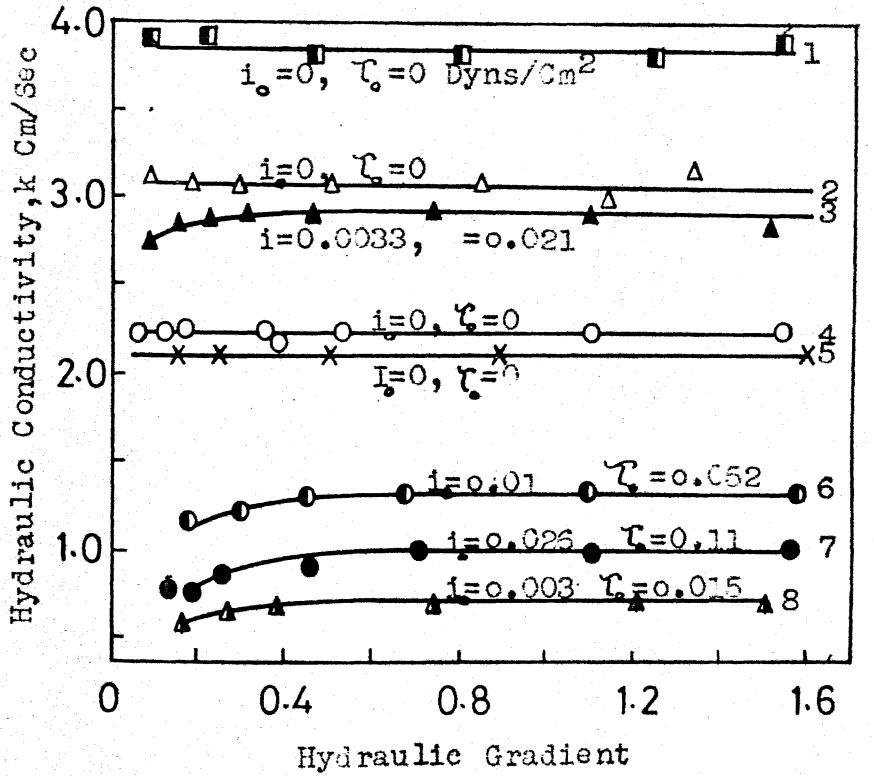

Fig.59: Relation between k & i. The nos. of the curves indicate diff. liquids (After Bondarenko, 1968)

1 : Acetone 2 : Chloform 3 : Mixture of Acetone & Chloroform 4: Chlorinated hydrocarbon 5. Toluene 6: Water 7: Ethyl alcohol 8: Mixture of Acetone & H_2O

Radius of quartz capillary, r = 0.011 Cm
Temp. t= 21°C

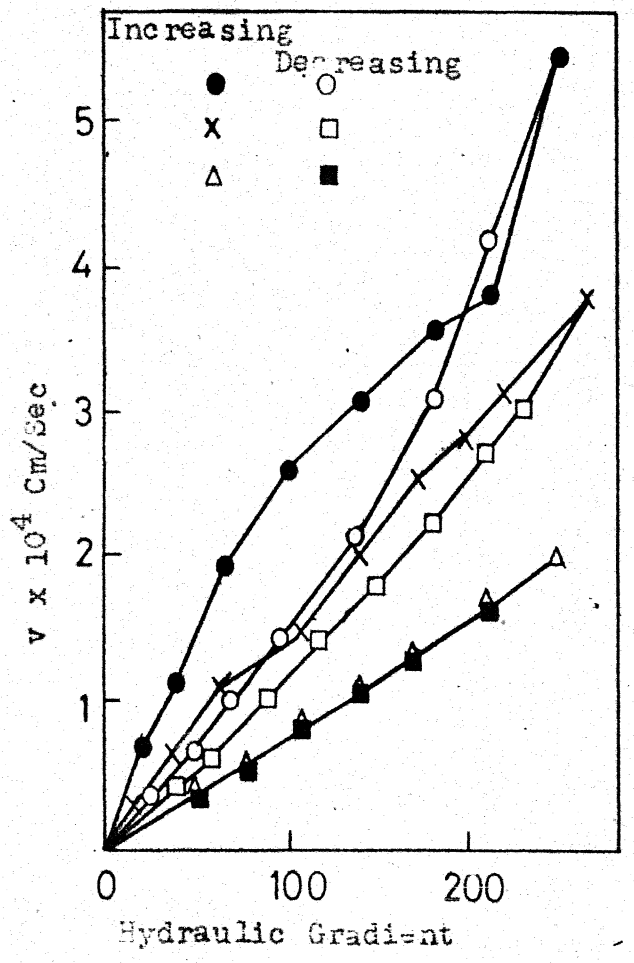

Fig.60: Relation between v & i for Kaolinite (After Novak,1972)

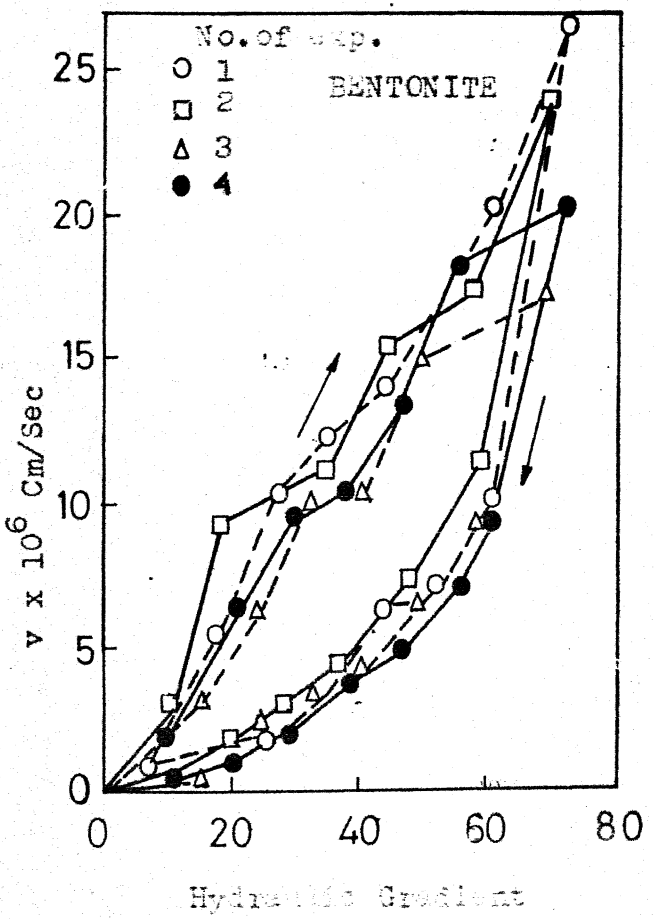

Fig.61: Relation between v & i for Bentonite (After Novak,1972)

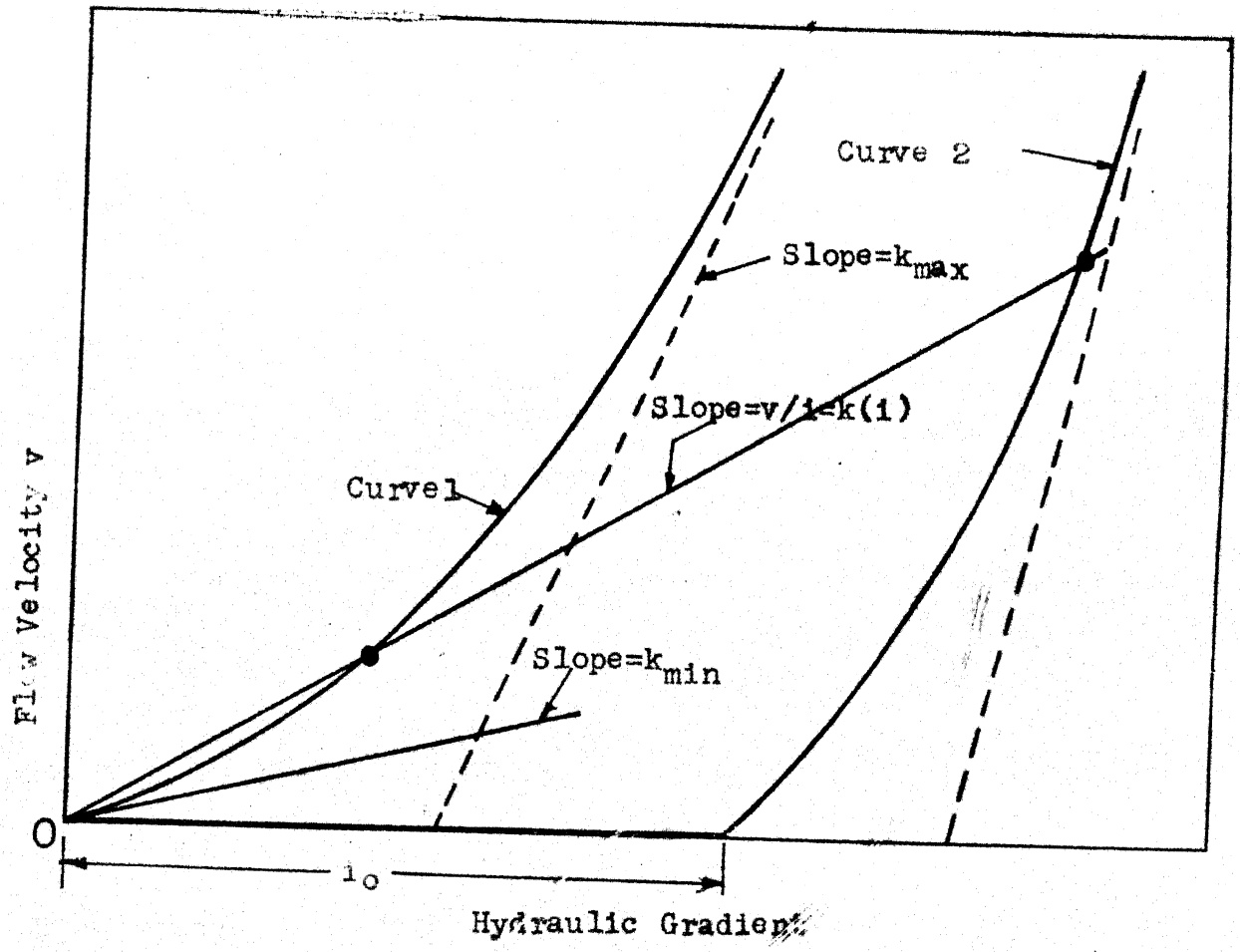

Fig.62 : Velocity-Gradient Relationships for non-Darcy behaviour, without threshold gradient (Curve 1) and with threshold gradient (curve 2)
(After Swartzendruber,1966)

(Figs. 60 and 61). Novak attributed this to the particle migration and volume change during gradient application.

D. SUMMARY OF PUBLISHED DATA AND ANALYSIS OF DEVIATIONS FROM DARCY BEHAVIOUR

In an excellent review Kutilek (1969) listed the possible errors which might have caused the reported deviations of the published non Darcy data. The list of errors, as suggested by him is shown in Table 13.

Olsen (1965) observed that slight contamination of the capillary tube in the measuring device might produce considerable spurious data and in this light he calculated the possible error in some of the published data. A complete analysis of the reported deviations is made and is shown in Table 14. This table is prepared out of Kutilek's (1969) and Olsen's (1965) observations but most recent data are included by the authors.

Swartzendruber (1968) fitted some of the experimental results available into the existing two empirical equations proposed by Kutilek and Swartzendruber and compared the non Darcy effect by the ratio K_{max}/K_{min}. The slopes K_{max} and K_{min} and explained in Fig. 62. The calculated results are reproduced in Table 15.

TABLE 13

LIST OF EXPERIMENTAL ERRORS WHICH MIGHT CAUSE THE REPORTED DEVIATIONS IN THE PUBLISHED NON DARCY DATA.

POSSIBLE SOURCE OF ERRORS:

(a) Open sample, swell with time and hence porosity changes with gradient application

(b) Closed sample, swelling under constant volume causes gradual decrease of effective porosity with time and gradient application

(c) Air trapped in the soil

(d) Bacterial growth during prolonged test

(e) Addition of phenol and similar solutions to remove bacteria might change the "quasi-crystalline" structure of soil water

(f) Cantamination of the wall of the capillary tube and other measuring devices

(g) Unsaturated soils-geometry of the flow path changes with saturation and hence gradient application.

TABLE 14
NON DARCY FLOW - A PERSPECTIVE

Sr. No.	Investigator	Sample Characteristics	No.of Tests Performed.	Condition of Flow	Observed Deviations: Type	Observed Deviations: Magnitude As Estimated by Olsen(1965)	Possible Source of Error as Suggested by Kutilek (1969)	Possible Spurious Deviations Due to Wall Contamination As Estimated by Olsen(1965) i_e=possible error in gradient	Type of Deviations Met
1.	King(1898, acc. to Swartzendruber 1962 b)	Sand and Sandstones		Sat.	A		?		
2.	Izbash(1931)	Gravel		Sat.	A , B		?		
3.	Puzyrevskaya (1931) Acc. to Polubarinovakochina, 1952)	Clay		Sat.	A		?		
4.	Von Engelhardt and Tunn(1955)	Sandstone with Clay fraction less than 5 %	14	Sat.	B,E (?)	$0 < i_o < 500$		$0 < i_e < 1$	
5.	Lutz and Kemper(1959)	Unconfined Samples of Bentonite, Halloysite and Bladen clay Pastes	30	Sat.	B , N E(?)	$-50 < i_o < 200$	a, b(?)	$0 < i_e < 2$	
6.	Hansbo(1960)	Natural Clays and confined sample	10	Sat.	B	$0 < i_o < 2.2$	f	$0 < i_e < 2.5$	
7.	Slepicka(1961)	Sandstones		Sat.	B , C		d , c(?)		
8.	Miller and Low (1963)	i) Bentonite Pastes		Sat.	M , A		f		
		ii) Confined Samples of Li and Na Mont.	6	Sat.	A, M, N, D	$0 < i_t < 70$		$0 < i_e < 10$	
9.	Li(1963)	Clay		Sat.	A		f		
10.	Rawlins and Gardner(1963)	Silty Clay Loam		Un.Sat.	A, B		g		
11.	Davidson et.el. (1963)	Silty Loam		Un sat.	B, E		g		
12.	Hadas(1964)	Loess Clay		Un sat.	B-C				
13.	Volarovitch and Tchuraev (1964)	Peat		Sat.	E				
14.	Kutilek (1964,1967)	Kaolinite, Illite, Mont.		Sat.	C,E(?)		a		
15.	Thames(1966)	Sandy Loam Silty Loam		Un sat.	B,C,E		g		
16.	Dudgeon(1966)	Sand and Gravel		Sat.	B(?)		?		
17.	Mitchell and Younger(1967)	Compacted Silty Clay		Sat.	C		a		
18.	Nerpin, Chudnovskij(1967)	A review, Clays		Sat.	E		?		
19.	Olsen, Swartzendruber(1968)	Mixtures of Sand Silica flour and Kaolinite		Un sat.	L, B		e		
20.	Russell(1968)	Mixtures ditto and Bentonite		Sat.	L,F,R		b		
21.	Gairon(1968)	Bentonite Paste		Sat.	L,F				
22.	Kutilek(1971)	Loamy Clay		Sat.	B(?)		a		
23.	Novak(1972)	Benbonite and kaolinite		Sat.	B(?)		a		

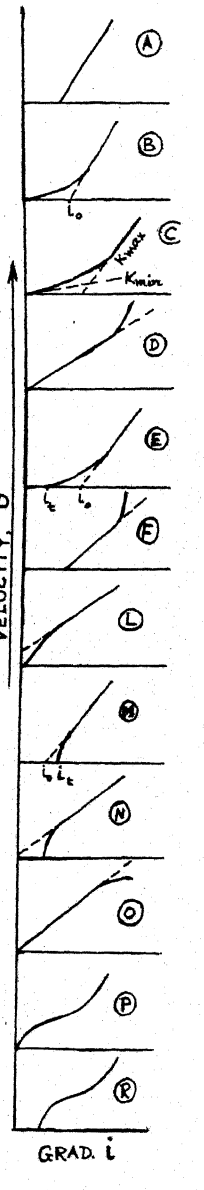

Table 15: Conductivity ratio and maximum hydraulic conductivity for water and various solutions of electrolyte.
(After Swartzendruber, 1966)

Investigators and porous materials	Electrolyte Conc.	Meas. K_{max}, 10^{-2} cm./hr.	(K_{max}/K_{min}), K_{max} and K_{min} are explained in fig.					
			Directly measured*			From fitted equation**		
			Smallest	Largest	Mean	Smallest	Largest	Mean
Von Engelhardt and Tunn (1955), clay-bearing sandstones.	0.00 N	84.00	1.4	5.1	2.5	3.5	16.7	9.0
	0.88 N	80.00	1.7	2.7	2.3	3.2	37.0	16.8
	1.83 N	105.00						
Lutz and Kemper (1959), clays	0.000 N	0.18	1.4	1.6	1.5	2.2	2.4	2.3
	0.005 N	0.21						
	0.050 N	0.24						
	0.500 N	0.51	1.1	2.4	1.6	1.3	22.2	7.1
Kutilek(1965)	0.000 N	0.52	1.0	2.3	1.4	1.0	13.0	3.9
			1.0	1.3	1.2	1.0	1.8	1.4
Clays	0.001 N	0.96	1.1	1.4	1.3	1.3	2.8	2.2
	0.010 N	1.52	1.3	11.1	3.8	1.8	35.0	9.0
	0.100 N	2.33	2.2	3.6	2.9	1.6	4.0	2.8
	1.000 N	3.06	1.0	12.7	3.6	1.0	84.0	14.0
			1.0	5.0	2.5	1.0	11.6	5.5
Paez(1962)	0.01 N	25.00	1.7	4.6	3.0	4.9	10.0	5.3
Hadas(1964)	2.00 ppm	140.00	1.2	2.6	1.7	1.4	10.0	5.3
			1.2	2.4	1.9	1.4	10.0	5.9

* From largest and smallest gradients actually employed experimentally.

** Equation(2a) for Kutilek's(13) data, equation(1a) for all others.

$$v = B\left[i - J\left(1-e\right)^{-Ci}\right]$$

at largei, $v = B(i-j)$ .....(1 a)

B, J, & C are constants

$$v = E\left[\log\left(A+e^{+\,i\,M/E}\right) - \log(A+1)\right]$$ .....(2

at largei, $v = Mi - E \log(A+1)$

A, E, & M are constants

APPENDIX B

(To be read with Vol. I, Chapter 2, Section B)

CAPILLARY MODEL FOR SURFACE ACTIVE SOILS

Velocity distribution :

For the free water zone, integration of equation (2.47) yields

$$\phi_F = -\frac{\lambda^2}{4} + c_2 \tag{2.67}$$

where

c_2 = constant of integration

For the bound water zone, integration of equation (2.59) yields

$$\phi_B = -\varepsilon^{A\lambda_o}\left[\frac{I_2(\lambda)}{2} + \frac{i_w}{i} I_1(\lambda_o) I_4(\lambda) - \frac{i_w}{i} I_3(\lambda)\right] + c_3 \tag{2.68}$$

where

c_3 = constant of integration

$$I_2(\lambda) = \int \lambda \varepsilon^{-A\lambda} d\lambda = -\frac{1 + A\lambda}{A^2} \varepsilon^{-A\lambda} \tag{2.69}$$

$$I_3(\lambda) = \int \frac{I_1(\lambda)}{\lambda \varepsilon^{A\lambda}} d\lambda = \frac{1}{BG^2}\left[(G\lambda - 1)\varepsilon^{G\lambda}\right] - \frac{P_1}{G} \varepsilon^{G\lambda} + P_2 \log \lambda$$

$$+ P_2\left[\sum_{n=1}^{\infty} \frac{(G\lambda)^n}{n\lfloor n}\right] \tag{2.70}$$

$$G = B - A \tag{2.71}$$

$$P_1 = \frac{2}{B^2} + \frac{\lambda_o}{B} \tag{2.72}$$

$$P_2 = \frac{2}{B^3} + \frac{\lambda_o}{B^2} \tag{2.73}$$

$I_1(\lambda)$ and $I_1(\lambda_o)$ are defined earlier in equations (2.52) and (2.54)

$$\text{and } I_4(\lambda) = \int \frac{\varepsilon^{-A\lambda}}{\lambda}\, d\lambda = \log \lambda + \sum_{n=1}^{\infty} (-1)^n \frac{(A\lambda)^n}{n \lfloor n} \tag{2.74}$$

By equations (2.39) and (2.68), one gets

$$C_3 = \varepsilon^{A\lambda_o} \left[\frac{I_2(\lambda_s)}{2} + \frac{i_w}{i_o} I_1(\lambda_o)\, I_4(\lambda_s) - \frac{i_w}{i_o} I_3(\lambda_s) \right] \tag{2.75}$$

where

$$I_2(\lambda_s) = \text{value of } I_2(\lambda) \text{ at } \lambda = \lambda_s \tag{2.76}$$

$$I_3(\lambda_s) = \text{value of } I_3(\lambda) \text{ at } \lambda = \lambda_s \tag{2.77}$$

$$I_4(\lambda_s) = \text{value of } I_4(\lambda) \text{ at } \lambda = \lambda_s \tag{2.78}$$

By equations (2.41) and (2.68)

$$C_2 = C_3 + \frac{\lambda_o^2}{4} - \varepsilon^{A\lambda_o} \left[\frac{I_2(\lambda_o)}{2} + \frac{i_w}{i} I_1(\lambda_o)\, I_4(\lambda_o) - \frac{i_w}{i} I_3(\lambda_o) \right] \tag{2.79}$$

where

$$I_2(\lambda_o) = \text{value of } I_2(\lambda) \text{ at } \lambda = \lambda_o \tag{2.80}$$

$$I_3(\lambda_o) = \text{value of } I_2(\lambda) \text{ at } \lambda = \lambda_o \tag{2.81}$$

$$I_4(\lambda_o) = \text{value of } I_3(\lambda) \text{ at } \lambda = \lambda_o \tag{2.82}$$

Equations (2.67) and (2.68) along with equations (2.75) and (2.79) complete the solution for velocity distribution.

Average velocities

Average velocity over the entire cross section of the capillary is obtained from eqn. (2.83)

$$u_{av} = \frac{1}{\pi R^2} \left[\int_0^{r_o} u_F \, 2\pi r \, dr + \int_{r_o}^{r_s} u_B \, 2\pi r \, dr \right] \qquad (2.83)$$

Equation (2.83) can also be written as

$$\phi_{av} = 2 \left[\int_0^{\lambda_o} \phi_F \lambda \, d\lambda + \int_{\lambda_o}^{\lambda_s} \phi_B \lambda \, d\lambda \right] \qquad (2.84)$$

where

$$\phi_{av} = \frac{u_{av}}{i \frac{\gamma_o R^2}{\mu_o}} \qquad (2.85)$$

Substituting expressions for ϕ_F and ϕ_B from equations (2.67) and (2.68) in eqn. (2.83) and integrating one gets,

$$\phi_{av} = 2 \left[-\frac{\lambda_o^4}{16} + \frac{c_2}{2} \lambda_o^2 + \frac{c_3}{2} (\lambda_s^2 - \lambda_o^2) \right.$$

$$- \epsilon^{A\lambda_o} \left\{ \frac{1}{2} (I_5(\lambda_s) - I_5(\lambda_o)) + \frac{i_w}{i_o} I_1(\lambda_o) \right.$$

$$\left. \left. I_6(\lambda_s) - I_6(\lambda_o)) - \frac{i_w}{i_o} (I_7(\lambda_s) - I_7(\lambda_o)) \right\} \right] \qquad (2.86)$$

Equation (2.86) can be rearranged as

$$u_{av} = i \left(\frac{1}{8} \frac{\gamma_o R^2}{\mu_o} \right) \left[\left(8c_2\lambda_o^2 - \lambda_o^4 \right) + 8 \left\{ c_3(\lambda_s^2 - \lambda_o^2) - \varepsilon^{A\lambda_o}(I_5(\lambda_s) - I_5(\lambda_o)) \right\} \right]$$

$$- 2 \frac{f_w}{\gamma_o} \left(\frac{\gamma_o R^2}{\mu_o} \right) \varepsilon^{A\lambda_o} \left[I_1(\lambda_o) \{ I_6(\lambda_s) - I_6(\lambda_o) \} - \{ I_7(\lambda_s) - I_7(\lambda_o) \} \right] \qquad (2.87)$$

where

C_2 and C_3 are defined by equations (2.75) and (2.79)

λ_s is related with i by equation (2.62)

$$I_5(\lambda) = \int \lambda I_2(\lambda) \, d\lambda$$

$$= \frac{\varepsilon^{-A\lambda}}{A^4} \left[A^2 \lambda^2 + 3A\lambda + 3 \right] \qquad (2.88)$$

$I_5(\lambda_s)$ = value of $I_5(\lambda)$ at $\lambda = \lambda_s$ (2.89)

$I_5(\lambda_o)$ = value of $I_5(\lambda)$ at $\lambda = \lambda_o$ (2.90)

$$I_6(\lambda) = \int \lambda I_4(\lambda) \, d\lambda$$

$$= \frac{\lambda^2}{2} \left[\log \lambda - \frac{1}{2} \right] + \lambda^2 \sum_{n=1}^{\infty} (-1)^n \frac{(A\lambda)^n}{n(n+2)\underline{|n}} \qquad (2.91)$$

$I_6(\lambda_s)$ = value of $I_6(\lambda)$ at $\lambda = \lambda_s$ (2.92)

$I_6(\lambda_o)$ = value of $I_6(\lambda)$ at $\lambda = \lambda_o$ (2.93)

$$I_7(\lambda) = \int \lambda I_3(\lambda)\, d\lambda$$

$$= \frac{\varepsilon^{G\lambda}}{BG^4}\,(G^2\lambda^2 - 2G\lambda + 2)$$

$$- \left(\frac{1}{BG^2} + \frac{P_1}{G}\right)\left(\frac{G\lambda - 1}{G^2}\,\varepsilon^{G\lambda}\right)$$

$$+ \frac{P_2\lambda^2}{2}\left[\log\lambda - \frac{1}{2}\right]$$

$$+ P_2\lambda^2\left[\sum_{n=1}^{\infty} \frac{(G\lambda)^n}{n(n+2)\lfloor n}\right] \qquad (2.94)$$

$I_7(\lambda_s)$ = value of $I_7(\lambda)$ at $\lambda = \lambda_s$ (2.95)

& $I_7(\lambda_o)$ = value of $I_7(\lambda)$ at $\lambda = \lambda_o$ (2.96)

P_1 and P_2 are given by equations (2.72) and (2.73).

Equation (2.87) completely defines the average velocity gradient response for the system. It is evident from eqn. (2.87) that velocity gradient response remains non linear as long as $\lambda_s < 1.0$ or $i < i_L$. Once i exceeds i_L, the flow remains fully developed along the entire cros section of the capillary and the velocity gradient response takes a linear shape of the form

$$u_{av} = \frac{1}{8}\,\frac{\gamma_o R^2}{\mu_o}\, a(m, \lambda_o)[\, i - i_w\, b(m, \lambda_o)] \qquad (2.87a)$$

where a and b are functions of m and λ_o.

In the absence of the bound water zone

$$\lambda_o = \lambda_s = 1 \tag{2.97}$$

$$f_w = 0 \tag{2.98}$$

$$\text{and} \quad A = \alpha \tag{2.99}$$

$$\text{Hence} \quad I_2(\lambda_s) = 0 \tag{2.100}$$

$$C_3 = 0 \tag{2.101}$$

$$C_2 = \frac{1}{4} \tag{2.102}$$

Substitution of equations (2.97) to (2.102) in equation (2.87) results in

$$u_{av} = \left(\frac{1}{8} \frac{\gamma_o R^2}{\mu_o} \right) i \tag{2.103}$$

which is the Hagen-Poisuelle's equation.

As a particular case, when interacting force f_w is absent in the bound water zone, but the viscosity variation as per equation (2.30) exists in the system, then equation (2.87) reduces to

$$u_{av} = \left[\frac{\gamma_o R^2}{\mu_o} \{ F(m, \lambda_o) \} \right] i \tag{2.104}$$

where

$$F(m,\lambda_o) = F_1 \frac{\lambda_o^2}{2} - \frac{\lambda_o^4}{4} + \frac{F_3}{2} (1 - \lambda_o^2) + \frac{F_2}{A^2} (A^2 + 3A + 3) \varepsilon^{-A} - \frac{2}{A^4} (A^2 \lambda_o^2 + 3A\lambda_o + 3) \tag{2.105}$$

$$F_1 = \frac{2\varepsilon^{A\lambda_o}}{A^2}\left[(1+A)\,\varepsilon^{-A} - (1+A\lambda_o)\,\varepsilon^{-A\lambda_o}\right] \tag{2.106}$$

$$F_2 = \frac{2\varepsilon^{A\lambda_o}}{A^2} \tag{2.107}$$

$$F_3 = \frac{2\varepsilon^{A\lambda_o}}{A^2}\left[(1+A)\,\varepsilon^{-A}\right]$$

$$= F_2(1+A)\,\varepsilon^{-A} \tag{2.108}$$

and as found earlier

$$A = \frac{\log m}{1-\lambda_o} \tag{2.31}$$

Equation (2.104) completely defines the velocity gradient response in the capillary element with bound and free water zone having an exponential variation of viscosity within the bound water zone but without the presence of any interacting force.

If the soil is assumed to be composed of bundle of straight parallel capillaries of uniform radius R and using the concept of hydraulic radius R_H and equivalent grain diameter D_s(Taylor 1948), equation (2.104) can be written in the form

$$u_{av} = \left[\frac{1}{72}\, D_s^2\, \frac{e^3}{1+e}\, \frac{\gamma_o}{\mu_o}\, \{4F(m, \lambda_o)\}\right] i \tag{2.109}$$

where e = void ratio

The factor $\frac{1}{72}$ in eqn. (2.109) has come because of circular capillaries and hence using a general shape factor C_s for an

irregular capillary, eqn. (2.109) becomes

$$u_{av} = [\, C_s\, D_s^2\, \frac{\gamma_o}{\mu_o}\, \frac{e^3}{1+e}\, \{4F(m, \lambda_o)\}]\, i \qquad (2.110)$$

Comparing this with Darcy's law, one gets, the expression for coefficient of permeability K as

$$K = [\, C_s\, D_s^2\, \frac{\gamma_o}{\mu_o}\, \frac{e^3}{1+e}]\, \{4F(m, \lambda_o)\} \qquad (2.111)$$

Equation (2.111) gives the permeability or the hydraulic conductivity coefficient taking into consideration constant viscosity in the free water zone and exponential increase of viscosity in the bound water zone of a soil water system. But the terms in square bracket in equation (2.111) give Kozeny's hydranlic conductivity coefficient (K_{kozeny}) for a soil water system having constant viscosity throughout, therefore, equation (2.111) can be rewritten as

$$\frac{K}{K_{Kozeny}} = 4F(m, \lambda_o) \qquad (2.112)$$

The ratio $\frac{K}{K_{Kozeny}}$ may be looked on as a discrepancy ratio arising out of the existence of two distinct zones of water (free water zone and bound water zone) and the exponential increase of viscosity in the bound water zone.

As a special case, if free water zone is absent (i.e. $\lambda_o = 0$) in a clay water system, equation (2.112) reduces to

$$\left.\frac{K}{K_{Kozeny}}\right| = 4\psi(m) \qquad (2.113)$$

no free water

where

$$\psi(m) = F(m,\lambda_o)\Big|_{\lambda_o = 0} \qquad (2.114)$$

The function $\psi(m)$ is obtained by putting $\lambda_o = 0$ in the expression for $F(m, \lambda_o)$ (equation (2.105)).

Equations (2.112) and (2.111) clearly bring out the effect of changed viscosity of the bound water on the permeability coefficient K and they are plotted in figs. 2.7 and 2.8. Fig. 2.7 shows the variation of the discrepancy ratio (ratio of actual permeability K and the permeability given by Kozeny's eqn.) with the change in the values of m and λ_o and Fig. 2.8 shows the variation of discripancy ratio with the change in m values for a system where all the water present is only bound water. As seen from the derived equations and their plots that even within the Darcian linear zone of velocity-gradient response, the hydraulic conductivity characteristics for surface active soils, among other things are also a functions of m and λ_o. The actual permeability is found to be very much sensitive to λ_o but some what less sensitive to the m values. In the absence of bound water ($\lambda_o = 1$) (as may be expected for sand and other inert material) the discrepancy ratio becomes 1.0 as

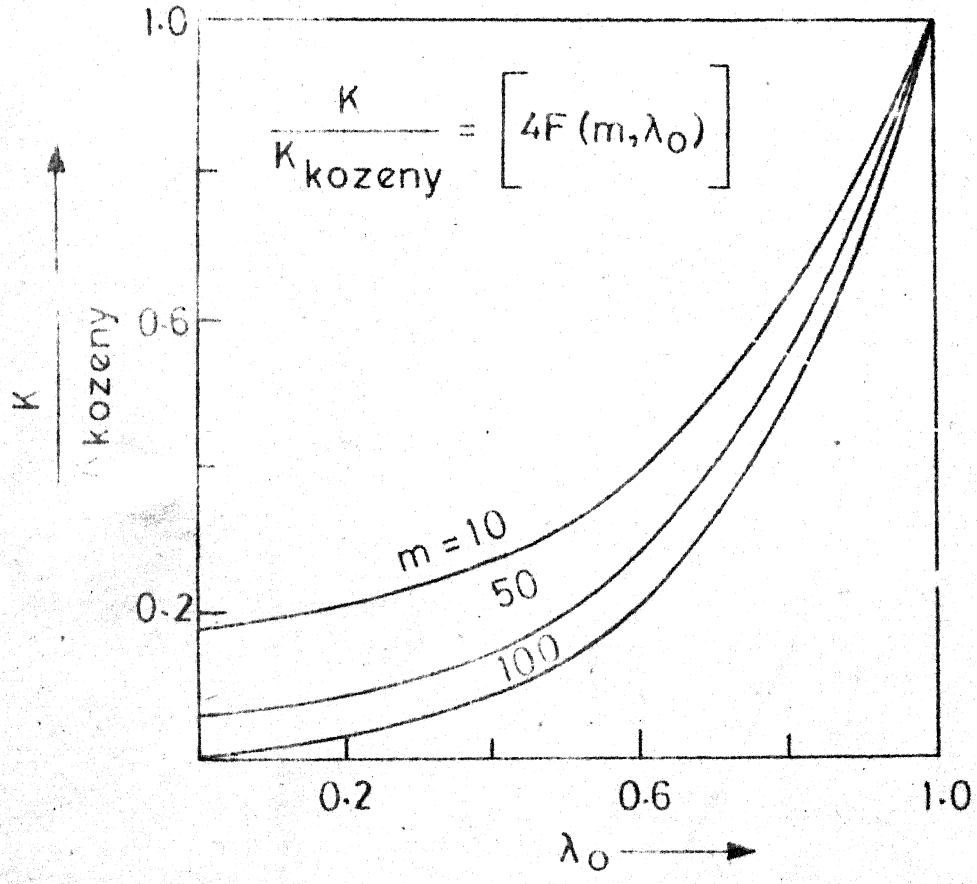

FIG. 2·7 VARIATION OF DISCREPANCY RATIO WITH m & λ_o IN THE ABSENCE OF INTERACTING FORCE.

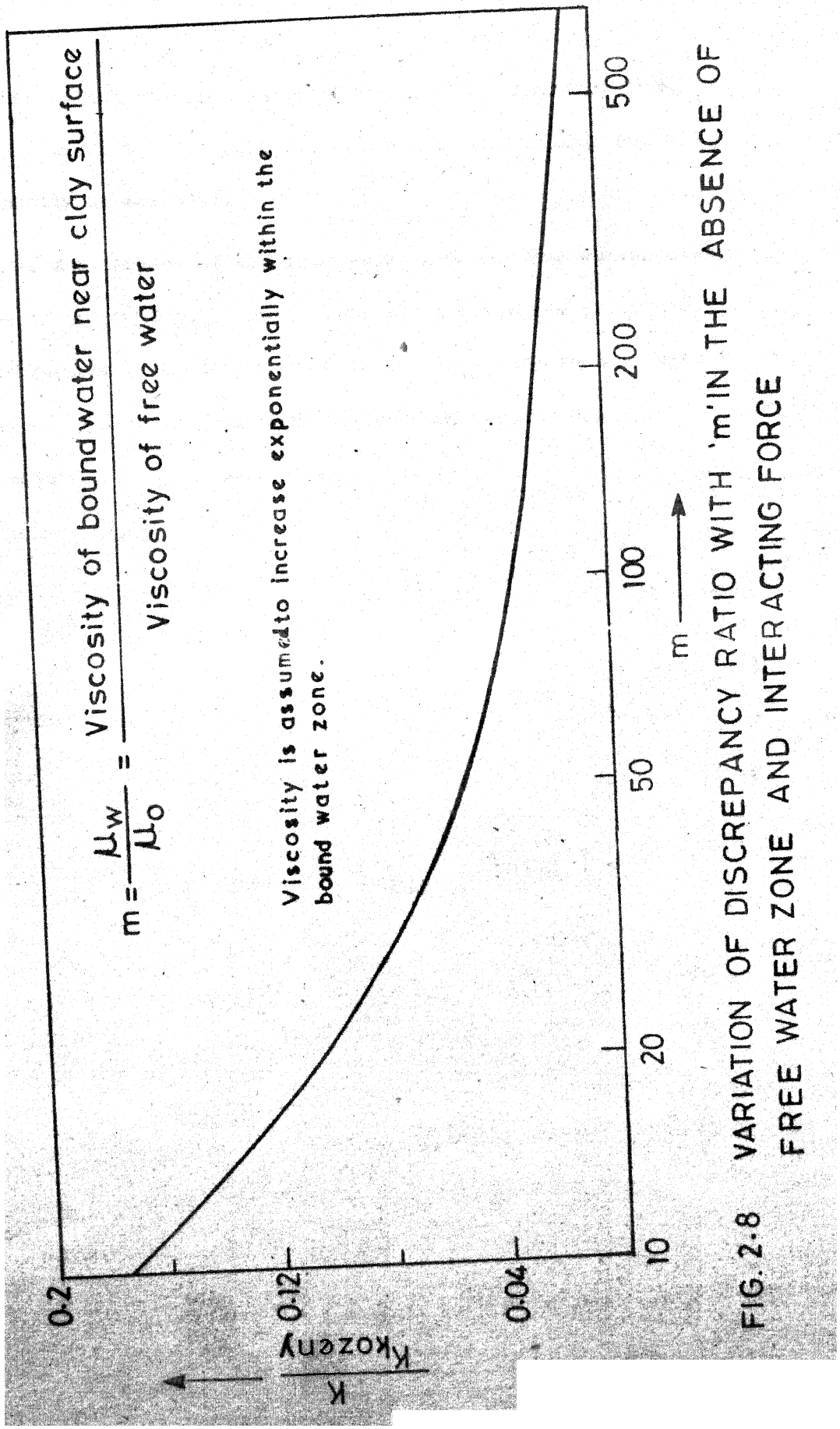

FIG. 2.8 VARIATION OF DISCREPANCY RATIO WITH 'm' IN THE ABSENCE OF FREE WATER ZONE AND INTERACTING FORCE

expected. The practical range of 'm' and λ_o may vary from 1 to 500 and 1 to 0 respectively depending on the clay content and porosity of the soil.

In the absence of any free water zone (as may be expected in case of comparitively dense clays of high surface activity), the discrepancy ratio is observed to decrease very rapidly upto 'm' values of 50 and the rate of decrease becomes smaller there after.

APPENDIX - C

WATER MOVEMENT IN CAPILLARY ZONE

Movement of saturation line in the capillary zone is of interest in earth dams and other similar structures. Assuming the flow to be one dimensional (either horizontal or vertical), a theoretical expression for the movement of the saturation line as a function of time would be of great help to the field and design engineers for estimating the time dependent strength and stability of the capillary zone. When the flow is assumed to be Darcian, expressions for both horizontal and vertical capillary rises are available (Taylor, 1948). Here, an extension of the same for the non Darcy flow defined by equation (C.1) is made and presented. Expressions for both the rate of horizontal and vertical

$$v = Mi^n \qquad (C.1)$$

Capillary saturation are forwarded.

RATE OF HORIZONTAL CAPILLARY SATURATION

To assure a truly one dimensional flow, a system as shown in fig. C.1 is considered. The system, as shown, is used many times for the capillarity - permeability test (Taylor 1948). Here, the soil sample has been brought to state of dry powder and then packed into a glass tube having a screen over one end and a vented stopper at the other end. The tube is then immersed in shallow depth of water in a horizontal position and the water proceeds into the interior of the soil by capillary action. The distance of saturation

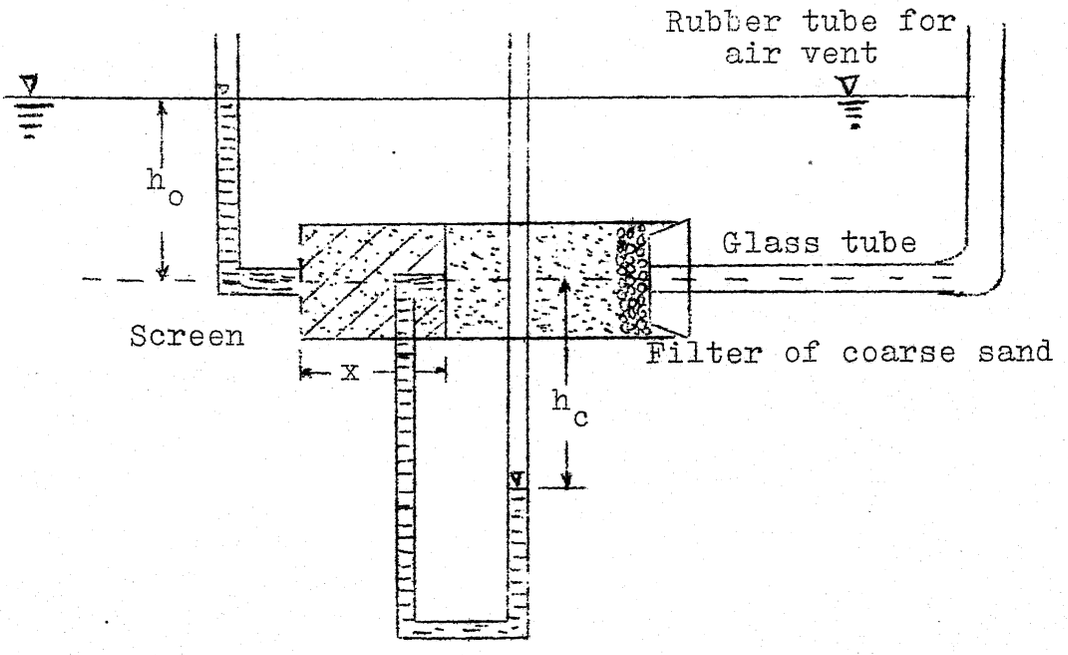

Fig. C1: SET UP FOR HORIZONTAL CAPILLARY SATURATION

x as a function of time is to be found out for a non Darcy flow law of the type as given in equation (C.1).

For the system as shown in fig. C.1 and considering the flow as given in equation C.1, equation C.2 can be written as

$$S\, n_e\, v_s = M \left(\frac{h_c + h_o}{x}\right)^n \qquad (C.2)$$

where

S = degree of saturation

n_e = porosity

v_s = Seepage velocity

h_c = Capillary head which is constant for a given soil at a given void ratio

h_o = As shown in fig. C.1

Eqn. (C.2) can further be written as

$$Sn_e \frac{dx}{dt} = M\left(\frac{h_c + h_o}{x}\right)^n \qquad (C.3)$$

Separating the variables and integrating, one gets

$$\frac{x^{n+1}}{n+1} = \frac{MH^n}{Sn_e}\, t + C_1 \qquad (C.4)$$

where C_1 is the constant of integration.

The initial condition is given by equation (C.5)

$$t = 0,\ x = 0 \qquad (C.5)$$

By equation (C.4) and (C.5)

$$C_1 = 0$$

Hence, equation (C.4) can be written as

$$\tau_H = \frac{X^{n+1}}{n+1} \qquad (C.6)$$

where τ_H = Time factor = $\frac{Mt}{H\, Sn_e}$ (C.7)

and $X = \frac{x}{H}$ (C.8)

$H = h_o + h_c$ (C.9)

Equation (C.6) gives the desired relation between time and distance of capillary saturation in a non dimensional form. For Darcy flow ($n = 1$), equation (C.7) reduces to the known parabolic relation between X and τ_H as given by Taylor (1948). For various values of 'n' equation (C.6) is plotted for X ranging from 0 to 1 and is shown in fig. C.2. For a laboratory set up and for a normal size of the sample, the value of X will hardly exceed unity. It is concluded from equation C.6 and its plot that compared to Darcy flow, non-Darcy flow leads to slower rates of capillary saturations if $n < 1$, and vice versa.

RATE OF VERTICAL CAPILLARY SATURATION

For this case, the system along with heads acting on it is schematically presented in fig. C.3.

At any instant of time, if z is the height of saturation line, then by the flow law assumed (eqn. C.1)

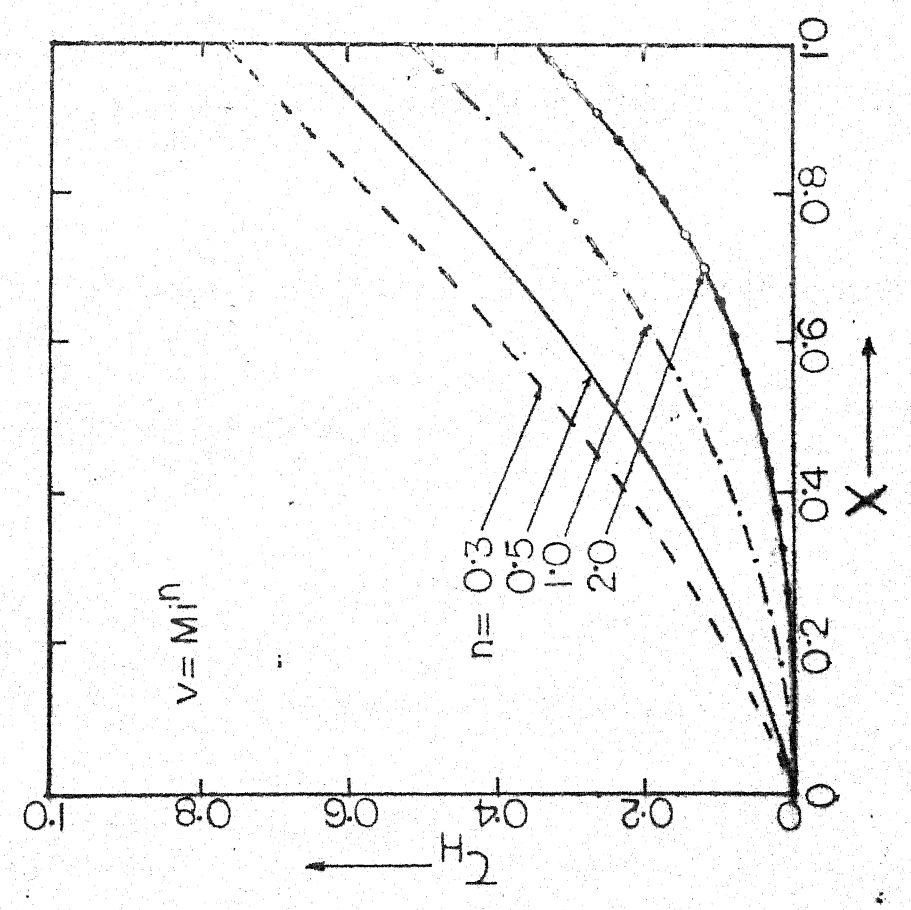

FIG. C.2: τ_H vs. X FOR HORIZONTAL CAPILLARY RISE

$$Sn_e \frac{dz}{dt} = M\left(\frac{h_c - z}{z}\right)^n \qquad (C.10)$$

The above equation can be non dimensionalised as

$$\frac{dZ}{d\tau_v} = \left(\frac{1-Z}{Z}\right)^n \qquad (C.11)$$

where

$$Z = \frac{z}{h_c} \qquad (C.12)$$

$$\tau_v = \frac{Mt}{h_c\, Sn_e} \qquad (C.13)$$

As seen from fig. C.3 the value of Z will not exceed unity in this case. Separating the variables from eqn.(C.11)and integrating and using the initial condition $\tau_v = 0$, $Z = 0$, one gets

$$\tau_v = Z^{n+1}\left[\frac{1}{n+1} + \frac{n}{n+2} Z + \frac{n(n+1)}{(n+3)\underline{|2}} Z^2 + \frac{n(n+1)(n+2)}{(n+4)\underline{|3}} Z^3 + \frac{n(n+1)(n+2)(n+3)}{(n+5)\underline{|4}} Z^4 + \ldots\ldots\right] \qquad (C.14)$$

For non Darcy flow equation (C.14) is the required relation between time and capillary saturation height in non dimensional form. Equation (C.14) is plotted for various values of non Darcy exponent 'n' and shown in fig. C.4. When n = 1, equation (C.14) can be written as

$$\tau_v = \left[Z + \frac{Z^2}{2} + \frac{Z^3}{3} + \frac{Z^4}{4} + \ldots.\right] - Z$$

or

$$\tau_v = -Z - \log(1-Z) \qquad (C.15)$$

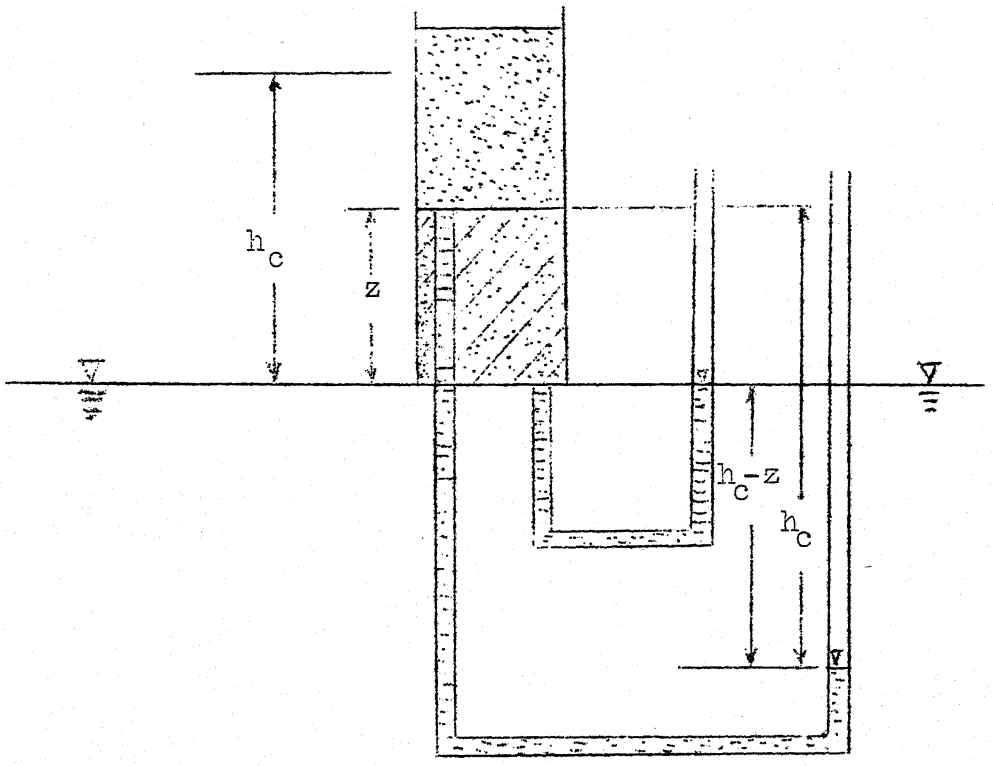

FIG.C3: DEFINITION SKETCH FOR VERTICAL CAPILLARY SATURATION

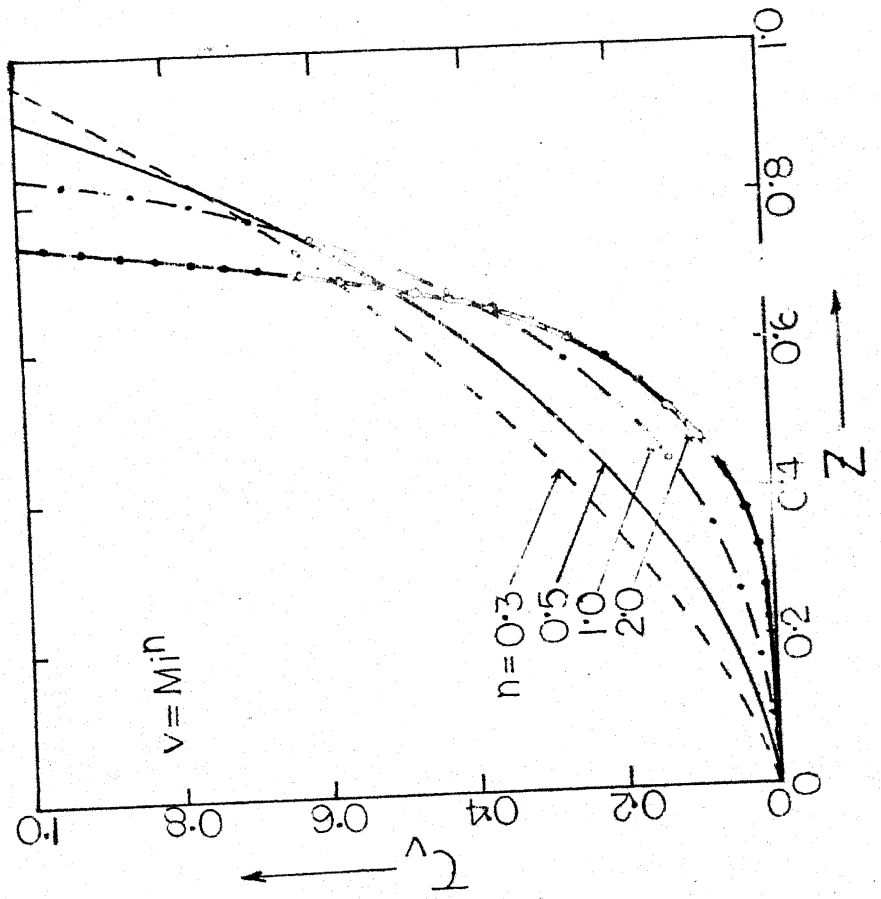

FIG. C.4: τ_v vs. Z FOR VERTICAL CAPILLARY RISE

which is the well known solution for Darcy flow (Taylor 1948). Equations (C.14) and (C.15) and their plot (fig. C.4) suggest that for $n < 1$, compared to Darcy flow, non Darcy flow predicts slower rate of capillary saturation at early times and faster rates of capillary saturation at later times. The trend for $n > 1$ is just the opposite.